

THESIS

WATER RESOURCES ON OUTER-LYING ISLANDS IN MICRONESIA

Submitted by

Alise Marie Beikmann

Department of Civil and Environmental Engineering

In partial fulfillment of the requirements

For the Degree of Master of Science

Colorado State University

Fort Collins, Colorado

Spring 2016

Master's Committee:

Advisor: Ryan Bailey

Robert Ettema

Neil Grigg

Michael Ronayne

Copyright by Alise Marie Beikmann 2016

All Rights Reserved

ABSTRACT

WATER RESOURCES ON OUTER-LYING ISLANDS IN MICRONESIA

Pacific islands are long-settled by mankind, dating back several hundreds to thousands of years ago since discovery by islanders traveling by boat. Amongst these islands are atoll islands, which are small coral islands that lie at a low elevation and are usually part of a ring-like coral reef formation. Past and present islanders collect water from rainwater catchments and groundwater wells, with rainwater used primarily for drinking water and groundwater used as a supplement for wash water. Unfortunately, this region can experience severe drought, over-wash events during strong tropical storms, and typhoons, all of which threaten the freshwater supply for these islands. Due to rising concerns over climate change, there is interest in studying the water security of these especially vulnerable land forms. This thesis evaluates the reliability of the water supplies on four atoll islands in Yap, Micronesia by modeling the reliability of the two main sources. To first analyze rainwater catchment performance, Ifalik Island is evaluated using data collected on the island in 2015 by a collaborative research field team and a water balance model. Second, the results are used to develop design curves as a tool for rainwater catchment design and improvement. The fresh groundwater source is also modeled for each of the four islands to test the effects of varying climate conditions on the shallow, freshwater lens.

Rainwater catchment systems on Ifalik Island are evaluated for their performance using a mass balance model that quantifies water storage through time. Performance is quantified primarily by *reliability*, which is a term to represent the percentage of days a rainwater catchment supplies sufficient water to the users. Based on the data from the Ifalik field survey,

the average household rainwater catchment system on Ifalik uses a 16.5 square meter guttered roof with a 2,000 liter storage tank and serves seven individuals at 12 liters per capita per day. As a result of a rainwater catchment system sensitivity analyses based on the average rainwater catchment conditions, the most important factors in performance are effective roof area size, water demand, and gutter-downspout efficiency. Further analyses using the mass balance model found that the performance of each individual catchment is sufficient to provide water to the community during conditions similar to the severe drought year of 1997-1998, as well as projected rainfall conditions for the next 30 years. Therefore, analyses suggest Ifalik Island has sufficient rainwater catchment performance to provide water for the community. However, to introduce a conservative measure for water security, it is recommended that the catchment area be extended to the full size of the roof area. This would thereby increase the storage supply for the community by 25 cubic meters on the day of lowest supply under the 1997-1998 severe drought conditions.

Design curves developed from the mass balance model are created to serve as a tool for rainwater catchment expansion and design. This tool allows water users and managers to determine the size of rainwater catchment components based on a selected reliability goal of 80%, 90%, 95%, or 99%. Curves developed using the severe drought conditions provide the most conservative design requirements. Further simplified design curves are created to suggest complete networks of rainwater catchments for the three remaining islands examined in this study: Eauripik, Satawal, and Falalop (Ulithi Atoll).

A groundwater modeling approach is used to simulate saltwater movement between the thin, freshwater lens located under the surface of the islands and the surrounding seawater. SEAWAT, a computer program that models three-dimensional variable-density groundwater

flow and salt transport, is used to estimate the volume and thickness of the freshwater lens for the four islands in this study under steady, average rainfall and projected future climate conditions through year 2040. To calibrate the models, the geologic parameters in the Falalop model are calibrated according to data collected on Falalop during 1987-1988 and the calibration is extended to the remaining islands. For the island of Falalop, the calibration found that a hydraulic conductivity of 175 m day^{-1} is appropriate for the upper-lying, Holocene aquifer. Findings show that the groundwater lens for Eauripik Island is less than a meter for average rainfall conditions at steady, average rainfall conditions, and is therefore not a recommended source for drinking water. The remaining islands have a significant, maximum freshwater lens thickness under the steady, average rainfall scenario: 7.64 (Falalop), 5.6 (Ifalik), and 7.65 (Satawal).

Projected, precipitation data generated through climate models developed by NASA are used to analyze groundwater lens dynamics from 2010-2040. For these scenarios, the islands show a relatively stable lens shape under the low-level climate change scenario, however the high-level climate change scenario appears to decrease the groundwater lens stability. Findings show the groundwater lens may fluctuate over 2 meters in thickness within just 2-3 years and decadal episodes of periodic increasing and decreasing lens size indicate an oscillatory climate forcing. Falalop, Ifalik, and Satawal did not deplete the freshwater lens at any point in time during either simulation. Due to the strong groundwater responses seen from the high-level climate scenario, incorporating such a GCM into a groundwater evaluation is recommended.

Results from this thesis can be used by coral island water managers to examine the community water supply during droughts and future climate conditions. This thesis also provides

tools and approaches for improving rainwater catchment system performance by identifying influential parameters, design rainfall conditions, and reliability curves for expansion.

ACKNOWLEDGEMENTS

I would like to thank my thesis advisor Dr. Ryan Bailey of the Civil and Environmental Engineering department at Colorado State University. Dr. Bailey consistently allowed this thesis to become my own work and gave me direction when I needed it. I would also like to thank Dr. John Jenson for helping me prepare for the workshop on Pohnpei and for welcoming me to the Pacific.

I would like to thank the field team, especially Maria Kottermair and Danko Taborosi, for traveling to Ifalik Island to collect extensive hydrologic data for this study and future studies. There is a wealth of detailed hydrologic data for this remote island and it is thanks to all their hard work. On the same note, I would also like to thank the island residents of Ifalik and Eauripik for graciously inviting the visiting field team into their homes and for their assistance with the field surveys.

I would also like to thank those who assisted me with collection of literature and census data, especially Bruce Robert of the College of Micronesia – FSM, Stuart Dawrs and Allyson Ota of the University of Hawaii – Manoa, and Itorie Amond and Arnold Canete of the Statistics Bureau of FSM.

Finally, I would like to thank my fiancé, Michael DeRubeis, for encouraging me throughout my research to work hard and believe in myself. More than once his support gave me the extra push I needed to get over the next hurdle, and this accomplishment would not have been possible without him.

TABLE OF CONTENTS

ABSTRACT.....	ii
ACKNOWLEDGEMENTS.....	vi
LIST OF FIGURES	x
LIST OF APPENDICES.....	xiii
1. ATOLL ISLAND WATER RESOURCES	1
1.1 Introduction	1
1.2 What is an atoll?.....	2
1.3 Hydrogeology.....	2
1.3.1 Geology.....	2
1.3.2 Geologic properties.....	3
1.3.3 Groundwater lens.....	4
1.3.4 Recharge	5
1.4 Ecology.....	6
1.4.1 Overview of plant life	6
1.4.2 Vegetative salt tolerance	7
1.4.3 Vegetative losses.....	8
1.5 Rainwater catchment systems	8
1.6 Objectives and methods	11
2. YAP STATE ATOLL ISLANDS	13
2.1 Geographic setting.....	13
2.1.1 Eauripik Island.....	14
2.1.2 Falalop Island (Ulithi Atoll).....	15
2.1.3 Ifalik Island	16
2.1.4 Satawal Island	17
2.2 Climate	18
2.2.1 Precipitation	19
2.2.2 Sea-level.....	21
2.2.3 Typhoons.....	21
2.3 Climate change.....	24
2.3.1 ENSO events.....	24

2.3.2	Accelerated sea-level rise	24
2.3.3	Intensified typhoons	25
2.4	Demographics.....	25
2.5	Water consumption	26
3.	DATA COLLECTION	28
3.1	Field survey on Ifalik	28
3.1.1	Overview.....	28
3.1.2	Rainwater catchment inventory	29
3.1.3	Groundwater survey.....	30
3.1.4	Surveyed locations	31
3.1.5	Water quality.....	31
3.1.6	Household interviews.....	32
3.1.7	Vegetation survey	32
3.2	Rainfall conditions	33
3.2.1	Average conditions	33
3.2.2	Drought conditions.....	33
3.2.3	Future climate conditions.....	33
4.	RAINWATER COLLECTION AND STORAGE	37
4.1	Overview of methods	37
4.2	Rainwater catchment systems of Ifalik	39
4.2.1	Evaluation of Ifalik RWCS parameters	39
4.2.2	Evaluation of Ifalik RWCS community water supply	51
4.3	Design curves for rainwater catchment system design	57
4.3.1	Overview of design curves.....	57
4.3.2	Design curves for severe drought conditions.....	58
4.3.3	Design curves for future climate conditions	58
4.4	Proposed RWCS network for Eauripik, Falalop, and Satawal.....	61
5.	THREE-DIMENSIONAL GROUNDWATER LENS DYNAMICS.....	68
5.1	Introduction	68
5.2	Previous numerical modeling work.....	68
5.3	Freshwater lens dynamics	70
5.3.1	Model development	70

5.3.2	Future rainfall conditions	80
6.	CONCLUSIONS AND RECOMMENDATIONS	87
6.1	Rainfall conditions	87
6.2	Rainwater collection.....	87
6.3	Groundwater collection	88
6.4	Other applications and future research.....	88
7.	REFERENCES	89

LIST OF FIGURES

Figure 1 – Example of a windward and leeward islands on Ifalik Atoll, Yap, Micronesia (GIS data source: iREI)	3
Figure 2 – Exaggerated, vertical scale cross section through Laura, Majuro Atoll, Republic of the Marshall Islands (Presley, 2005).....	5
Figure 3 – Rainwater catchment with cistern (USAID - Washington, DC, US, 1982)	9
Figure 4 – Map of the Pacific Island nations, including the Carolinian Archipelago (U.S. Geological Survey, 1996)	13
Figure 5 – Map of the Federated States of Micronesia (FSM Government)	14
Figure 6 – Eauripik Atoll 2015 (imagery credit: iREi).....	15
Figure 7 – Eauripik Island 2015 (imagery credit: iREi)	15
Figure 8 – Falalop Island 2015 (imagery credit: iREi)	16
Figure 9 – Ifalik Atoll (NOAA, 2015)	17
Figure 10 – Ifalik Island 2015 (imagery credit: iREi)	17
Figure 11 – Satawal Island 2015 (imagery credit: iREi)	18
Figure 12 – Average daily rainfall for Yap Island (mm)	20
Figure 13 – Hand-drawn map of Ifalik Atoll, 19 th Century	23
Figure 14 – Geometry of Ifalik Atoll, 1948.....	23
Figure 15 – Photograph of a rainwater catchment storage tank on Ifalik (Photo credit: iREi, 2015)	29
Figure 16 – Photograph of a young, Ifalikian woman collecting water from a storage tank on Ifalik (Photo credit: iREi, 2015)	31
Figure 17 – Effective roof area of rainwater catchment systems on Ifalik Island, actual and potential.....	41
Figure 18 – Modeled storage volume for Scenarios 2 through 7, average rainfall conditions	45
Figure 19 – Modeled storage volume for Scenarios 8 through 13, average rainfall conditions ...	45

Figure 20 – Modeled storage volume for Scenarios 2 through 7, severe drought conditions	48
Figure 21 – Modeled storage volume for Scenarios 8 through 13, severe drought conditions	48
Figure 22 – Reliability of each RWCS on Ifalik for severe drought conditions.....	51
Figure 23 – Plots of reliability for parameter values: tank size, roof area, efficiency, and number of residents	52
Figure 24 – Ifalik community water supply under severe drought conditions, actual roof area ..	53
Figure 25 – Ifalik community water supply under severe drought conditions, potential roof area	54
Figure 26 – Ifalik community water supply under future climate conditions, actual roof area....	56
Figure 27 – Ifalik community water supply under future climate conditions, potential roof area	56
Figure 28 – Example design curve for rainwater catchment systems.....	57
Figure 29 – Design curves for the 1997-1998 severe drought, with varying number of residents per RWCS	59
Figure 30 – Design curves for the 2010-2040 period using rainfall data from GCM GISS-E2-H for RCP 2.6	60
Figure 31 – Design curves for the 2010-2040 period using rainfall data from GCM GISS-E2-H-p2 for RCP 8.5	60
Figure 32 – Reliability curve for average Yap rainfall conditions, 3 – 12 water users per catchment	62
Figure 33 – Reliability curve for 1997-1999 drought conditions, 3 – 12 water users per catchment	62
Figure 34 – Design curves for a network of rainwater catchment systems on Eauripik under average rainfall conditions (top) and severe drought conditions (bottom)	64
Figure 35 – Design curves for a network of rainwater catchment systems on Falalop under average rainfall conditions (top) and severe drought conditions (bottom)	65
Figure 36 – Design curves for a network of rainwater catchment systems on Satawal under average rainfall conditions (top) and severe drought conditions (bottom)	66
Figure 37 – Discretization for Ifalik SEAWAT Model (10 meter cell size)	71
Figure 38 – Map of calibration wells on Falalop.....	74

Figure 39 – Falalop calibrated, steady average rainfall model; A. Plan view, B. Profile view. Red indicates a chloride concentration for seawater of 35 g/kg and blue indicates a chloride concentration of 0.89 g/kg for freshwater.....	78
Figure 40 – Eauripik calibrated, steady average rainfall model; A. Plan view, B. Profile view. Red indicates a chloride concentration for seawater of 35 g/kg and blue indicates a chloride concentration of 0.89 g/kg for freshwater.....	78
Figure 41 – Ifalik calibrated, steady average rainfall model; Plan view, B. Profile view. Red indicates a chloride concentration for seawater of 35 g/kg and blue indicates a chloride concentration of 0.89 g/kg for freshwater.....	79
Figure 42 – Satawal calibrated, steady average rainfall model; A. Plan view, B. Profile view. Red indicates a chloride concentration for seawater of 35 g/kg and blue indicates a chloride concentration of 0.89 g/kg for freshwater.....	79
Figure 43 – Groundwater lens thickness (m) for RCP 2.6 Scenario (Falalop, Ifalik, and Satawal).....	81
Figure 44 – Groundwater lens thickness (m) for RCP 2.6 Scenario (Eauripik).....	82
Figure 45 – Groundwater lens volume (m ³) for RCP 2.6 Scenario (Falalop, Ifalik, and Satawal).....	82
Figure 46 – Groundwater lens volume (m ³) for RCP 2.6 Scenario (Eauripik).....	83
Figure 47 – Groundwater lens thickness (m) for RCP 8.5 Scenario (Falalop, Ifalik, and Satawal).....	84
Figure 48 – Groundwater lens thickness (m) for RCP 8.5 Scenario (Eauripik).....	84
Figure 49 – Groundwater lens volume (m ³) for RCP 8.5 Scenario (Falalop, Ifalik, and Satawal).....	85
Figure 50 – Groundwater lens volume (m ³) for RCP 8.5 Scenario (Eauripik).....	85

LIST OF APPENDICES

APPENDIX A – Rainwater catchment system data from Ifalik Island

APPENDIX B – Groundwater lens thickness plots from calibrated island models using three time step conditions

1. ATOLL ISLAND WATER RESOURCES

1.1 Introduction

Atolls are perhaps one of the most dynamic geologic formations on earth, subject to powerful forces of the ocean and the coral life force beneath them. Over 400 atolls exist in the world (Bryan, 1953) and they are continually re-shaped, rotated, and shifted by the climatic and oceanic disturbances (Kensch, Ford, & McLean, 2015). An atoll is a small, coral reef formation that is typically a ring-like composite of reef islands that surround a central lagoon (Davis, 1928) (Vacher, 1997). Pacific atolls are remote, yet as remote as they are the islands have rich vegetation characterized by dense coconut groves and swampy taro patches. Beneath the sandy surface lies a two-part geologic system composed of a newer and denser Holocene age formation above and an older Pleistocene age formation.

Rainfall is plentiful in the Pacific Basin due to the tropical climate, ranging from 3-4 meters annually (Anthony, 1997) and seasonal fluctuations occur by way of a dry season from November to June followed by a wet season from July to November, respectively. From the hydrologic standpoint, surface storage and runoff are negligible and therefore rainfall is either lost to evapotranspiration, consumed by plant and animal life, or infiltrated into the soil and collected in a shallow layer of freshwater. El Niño Southern Oscillation (ENSO) events in the tropical Pacific intensify the dry season which may lead to severe droughts (White, Falkland, & Scott, 1999), which negatively impacts the vegetation, animal life, and of course, human inhabitants. Natural groundwater storage becomes a vital resource during droughts and aquifer storage is determined by the hydrogeology.

1.2 What is an atoll?

Atolls are low-lying, small, coral reef formations that frequently a composite formation of reef islands in a ring-shape around a lagoon (Davis, 1928) (Vacher, 1997). Atoll is a collective term that typically refers to this classic definition of atolls, as well as and low-lying reef islands without a significant lagoon (Richmond, Mieremet, & Reiss, 1997). Reef islands without a significant lagoon are often included in the atoll definition, as well (Richmond, Mieremet, & Reiss, 1997). ‘Low’ is originated from early European explorers traveling by tall ships used to described the low elevation of these islands and the subsequent low visibility (Vacher, 1997). Researchers have also distinguished between low-lying and ‘elevated’ or ‘high’ atolls by identifying a maximum elevation, such as 4 or 7 meters above mean sea level (MSL) or less (Pernetta, 1992) (Richmond, Mieremet, & Reiss, 1997). Small is a term defined by the United Nations Educational, Scientific and Cultural Organization (UNESCO) for islands with an area of 2,000 km² or less, or with a width of 10 km or less (Vacher, 1997). Finally, pacific atolls are remote, or outer-lying, with the nearest neighboring land form located several hundreds of kilometers away.

1.3 Hydrogeology

1.3.1 Geology

The geology of Pacific atoll islands is formed by two distinct layers. The top layer is a layer of Holocene sands with relatively low permeability and below this lies a karst, Pleistocene reef deposit with high permeability (Anthony, 1997) (White, Falkland, & Scott, 1999). The depth of contact to the Pleistocene deposit is typically 15 – 25 meters deep (Falkland, 1994) (Anthony, 1997) and Bailey et al. found it varied from 15 to 20 meters for 5 selected atolls in FSM (Bailey, Jenson, & Taborosi, 2013). In addition, Pacific atolls frequently have a reef flat-plate near the

surface of the atoll, layered between surficial sediments and the lower Holocene sediments. This layer is a semi-permeable reef rock that confines the upper Holocene aquifer and thickens the freshwater lens (Bailey, Jenson, & Taborosi, 2013).

Coral atoll islands vary in sedimentary composition based on their location relative to the tradewinds. Windward islands are located upwind within the atoll and are therefore exposed to the northeasterly winds and associated swells that occur during storms (Spennemann, 2006). An example of windward and leeward islands on Ifalik Atoll is shown in Figure 1. Fine grained sediments are found on the lagoon side and sediments become coarser across the island to the ocean shore (Spennemann, 2006). This leads to an asymmetrical freshwater lenses that is thickest toward the lagoon side (Falkland, 1994) (Anthony, 1997).

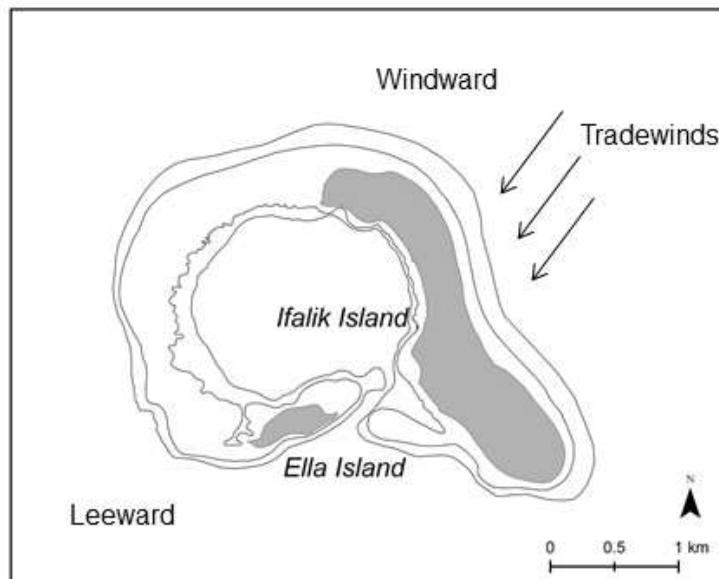


Figure 1 – Example of a windward and leeward islands on Ifalik Atoll, Yap, Micronesia (GIS data source: iREI)

1.3.2 Geologic properties

Hydraulic conductivity is one of the most important hydrogeologic parameters to consider for the Holocene aquifer and there is a broad range of values found in the literature,

with most from 0.01 m day^{-1} to over 100 m day^{-1} (Hunt & Peterson, 1980) (Ayers & Vacher, 1986) (Falkland, 1994) (Anthony, 1997) (White, Falkland, & Scott, 1999) (Bailey, Jenson, & Olsen, 2009). Hydraulic conductivity of the Holocene layer may also be truncated based on atoll position to 50 m/day for leeward islands and 400 m/day for windward islands (Bailey, Jenson, & Taborosi, 2013). Hydraulic conductivity in the Pleistocene formation is much higher than the Holocene aquifer, typically estimated to be one or two orders of magnitude greater. Typical estimates for hydraulic conductivity are between $1,000 \text{ m day}^{-1}$ and $5,000 \text{ m day}^{-1}$ (Falkland, 1994) (White, Falkland, & Scott, 1999) (Bailey, Jenson, & Olsen, 2010). Porosity is typically estimated to be 20% – 30% for the Holocene sediments (Hunt & Peterson, 1980) (Hamlin & Anthony, 1987) (Falkland, 1994) (White, Falkland, & Scott, 1999) and 30% for the Pleistocene sediments (Swartz, 1962) (Falkland, 1994), though observed values have exceeded 50% in some studies (Swartz, 1962). Specific yield, or the amount of extractable water from the pore space, is estimated by similar studies to be 100% of the porosity (Falkland, 1994) (Holding & Allen, 2015), and specific storage is typically between $1 \times 10^{-4} \text{ m}^{-1}$ and $1 \times 10^{-5} \text{ m}^{-1}$ (Batu, 1998) (Holding & Allen, 2015).

1.3.3 Groundwater lens

The dual-layer geology results in a dual-layer aquifer system (Ayers & Vacher, 1986). Groundwater lenses are thin, shallow collections of freshwater that collect within the permeable sediments of the upper, Holocene aquifer. The freshwater lens begins at the water table which is typically 0.25-0.5 meters above sea level (White, Falkland, & Scott, 1999) or 1 – 2 meters below ground surface (White & Falkland, 2010), and extends to the figurative boundary at which the water becomes saline and undrinkable (Figure 2). This boundary occurs at a chloride concentration of 0.89 g/kg , which the World Health Organization (WHO) determined to be the

point at which water becomes undrinkable. The lower Pleistocene aquifer is very permeable and typically contains pure seawater, which is characterized by a chloride concentration of 35 g/kg. Between the freshwater lens and oceanic boundary of pure seawater exists a broad interface referred to as the transition zone (Figure 2), characterized by a salinity concentration between freshwater and pure saltwater and a thickness often larger than the freshwater lens (Hunt & Peterson, 1980) (Falkland, 1994).

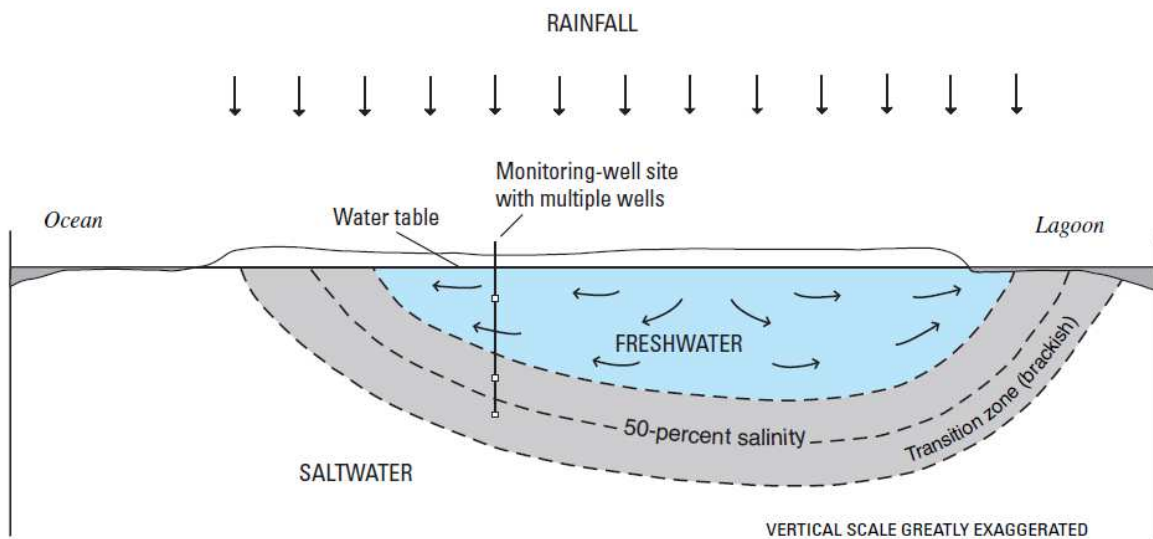


Figure 2 – Exaggerated, vertical scale cross section through Laura, Majuro Atoll, Republic of the Marshall Islands (Presley, 2005)

1.3.4 Recharge

For purposes of hydrogeology, recharge is the term that refers to the portion of water that passes through the canopy and underlying vegetation and infiltrates through the unsaturated soil zone to the groundwater aquifer. Observed precipitation is often much greater than actual recharge due losses from evapotranspiration and interception (White, 1996). Storage in the unsaturated soil zone and surface runoff, which are typically considered for estimating recharge in other geologic conditions, are commonly neglected in the case of atoll islands. Storage in the unsaturated zone is typically neglected due to the conductive nature of the surface soils and

typically seen small depths to the water table (Hunt & Peterson, 1980). Runoff is commonly neglected on atoll islands as it occurs only when soils are saturated during heavy rains or for the rare condition of compacted soils (Arnow, 1955) (Hunt & Peterson, 1980) (Hamlin & Anthony, 1987) (Falkland, 1994) (White, Falkland, & Scott, 1999).

To estimate recharge, a water mass balance model is used such as the one shown in Equation 1 (Falkland, 1994):

$$R = P - ET + dV \quad \text{Equation 1}$$

Where:

R: recharge,

P: rainfall,

ET: actual evapotranspiration (ET), vegetative and soil,

dV: change in storage within the soil zone.

As previously stated, storage in the unsaturated zone is typically neglected for broader applications therefore the dV term may be neglected. Also, as shown by this water balance model, interception by vegetation is frequently lumped in with evapotranspiration thereby making the ET term inclusive of interception and transpiration by plants, and evaporation from the soil surface. To solve for recharge, ET is often simplified to a percentage of the measured precipitation (Lloyd, et al., 1980). This recharge percentage is often approximated to 50% of precipitation as a result of several mass balance studies conducted through field surveys (Hunt & Peterson, 1980) (Hamlin & Anthony, 1987) (Anthony, 1997) (White, et al., 2007).

1.4 Ecology

1.4.1 Overview of plant life

Ecology of low, coral islands consists of three major vegetative zones: cleared coconut grove, depressed swamp, and an area of wild vegetation consisting of several species of trees and a thick understory of bushes and ferns. The latter area is sometimes referred to as ‘boondocks’ by

English speakers (Bates & Abbott, 1958). Trees are a vital resource to the islanders, providing much needed shade in the tropical heat and various materials for sustenance. Coconut trees are native to coral atolls in the Pacific (Dana, 1872) and they provide water to islanders from the coconut fruit, as well as wood and leaves for various purposes (Merlin, 2015). Over 50% of mature coconut trees have roots that run deep enough to penetrate the water table that exists 1 to 2 meters below the ground surface (Falkland, 1994). This allows coconut trees to transpire when the unsaturated zone becomes dry.

Other important trees that grow on the outer-islands include breadfruit trees, pandanus trees, fig trees, and papaya trees (Fosberg, 1969) (Merlin, 2015). Understory vegetation includes wet taro that grows central, depressed swamps, cultivated root plants grown near villages, and an array of native vines and ferns that grow in the ‘boondocks’ (Bates & Abbott, 1958) (Merlin, 2015). The prominence of certain types of vegetation depends on annual rainfall (Van der Brug, 1986), and islands with lower rainfall commonly have lower prevalence of breadfruit and taro, lower biodiversity, and less dense vegetation (Bates & Abbott, 1958).

1.4.2 Vegetative salt tolerance

Droughts and typhoon events inundate soils with saline water, which has a significant impact on the vegetation. Crops have varying levels of sensitivity to sea-spray and saltwater inundation, with plants of high tolerance including coconut trees, pandanus trees, banana trees, and swamp taro (Van der Brug, 1986), and low tolerance occurring in plants like dry taro (planted on dry land). Salinity causes a substantial reduction in taro productivity (Roy & Connell, 1991). Consequently, regrowth following a period of loss is also plant-dependent and plants that experience high losses also have the faster growth rates. For instance, dry taro, which is particularly vulnerable to drought, recovers within 18 months after return toward normal

climatic conditions, whereas the more robust wet taro takes approximately 3-4 years (Van der Brug, 1986).

1.4.3 Vegetative losses

Besides precipitation, the most important component of the water balance for determining recharge to aquifers on small coral atoll islands is evapotranspiration (Falkland, 1994) (White, 1996). As indicated in the groundwater recharge section, vegetative losses through evapotranspiration on coral atoll islands present the largest sink in the mass balance model accounting for 50% or more. It is also one of the least characterized (White, 1996). In reality, vegetative respiration is dependent on the soil conditions which fluctuate through time, especially by season. The maximum and minimum soil moisture conditions for evapotranspiration are known as the field capacity, or moisture content for maximum plant growth, and wilting point, or moisture content for which plants will begin to wilt or die. Typically for coral atoll soils near the surface, the field capacity and wilting point are 0.15 and 0.05, respectively (Falkland, 1994). For this region of coral atolls in the Pacific, monthly evapotranspiration rates are relatively constant from year-to-year (Falkland, 1994). One source estimated direct plant-root uptake from the aquifer on a per tree basis for coconut trees and found 400-750 mm per year can be transpired from coconut trees with 8 meter spacing and 100% cover (Falkland, 1994).

1.5 Rainwater catchment systems

Rainwater catchment systems have grown in popularity over the past several decades since the quality of water is better than the groundwater alternative and the costs for materials have decreased (Dillaha & Zolan, 1985) (Wallace & Bailey, 2015). The first instances of use began in the 1970s or perhaps earlier (Detay, et al., 1989). An increase in popularity occurred in

the early 1980s as the result of International Conference on Rainwater Cistern Systems held at the University Hawaii in 1982 and the College of the Virgin Islands in 1984 (Dillaha & Zolan, 1985), and an evaluation of rainwater catchment systems conducted in 1983 by the University of Guam, Water and Energy Research Institute (Detay, et al., 1989). These publications proved that rainwater collection provided higher-quality water than the alternatives which popularized the RWCS for atoll island communities. Studies have also found that RWCS are preferred due to the shorter decontamination period relative to groundwater sources (Detay, et al., 1989). Rainwater catchments require a few hours or days to clean out after a contamination event, whereas natural flushing of contaminants from groundwater requires months or years.

An effective rainwater catchment system (RWCS) collects and stores enough water to sufficiently meet the demand of the users. A standard rooftop RWCS (Figure 3) consists of a four major components: a roof which intercepts precipitation, a gutter-downspout system that captures runoff from the roof, downpipes which collect the water from the gutters, and a storage tank or cistern that stores water for use (USAID - Washington, DC, US, 1982). Several things must be considered to design, construct, and maintain a RWCS.

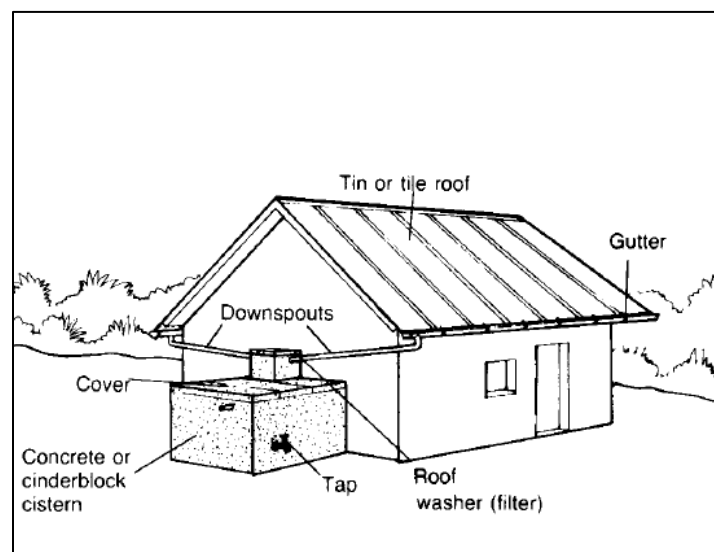


Figure 3 – Rainwater catchment with cistern (USAID - Washington, DC, US, 1982)

Stored water is dependent on roof area, therefore the effective roof area should be of sufficient size and slope. Effective roof area is the ground area covered by the roof and this can be optimized by sloping the roof shallow enough to enlarge the area and steep enough that rainfall runs off into the gutter (USAID - Washington, DC, US, 1982). The best roof materials for rainwater collection are aluminum, corrugated sheet metal, and baked tile, therefore thatched roofs commonly used on Pacific islands are typically retrofitted with an aluminum sheet overtop.

Maintenance of the RWCS is an important part of the overall performance. RWCS require periodic cleaning of the roof catchments, gutter-downspout system, and the inside of the storage tanks (Dillaha & Zolan, 1985). Animal feces, dust, and other particulate matter collect on the roofs and in the gutters which clogs the pathway to the storage tank and reduces overall performance. Screens are commonly added immediately upstream of the storage tank to improve water quality, and these need to be cleaned frequently to prevent build-up. Disinfection of the inside of storage tanks by chemical disinfectants is commonly recommended, however is rarely practiced by island residents in the Pacific (Dillaha & Zolan, 1985).

On a similar note, an important maintenance consideration for rainwater catchment systems is the foul flush, or the first run-off from the roof catchment after a rain event (USAID - Washington, DC, US, 1982). Diverting this water away helps keep high concentrations of contaminants carried by leaf litter, bird droppings, and other material from entering the storage tank. A simple way to do this is by attaching a piece to the end of the gutter or downspout at the start of a rainfall event to divert water to the adjacent ground surface. Another way that requires less work is to install a foul flush box. A foul flush box fills at the start of a rain period and rain that follows the initial flush runs over the box into a channel and the storage tank. For island

communities, this method may be a good option for larger catchments used for schools or meeting houses.

1.6 Objectives and methods

The primary objective of this thesis is to investigate the reliability of water supplies for four atoll islands in Yap, Micronesia and examine how the reliability changes during drought and future precipitation patterns. The islands studied for this thesis include Eauripik (Eauripik Atoll), Falalop (Ulithi Atoll), Ifalik (Ifalik Atoll), and Satawal (a reef island). This study also aims to give water resource managers information and comprehensive tools to improve management of rainwater and groundwater resources. Following an overview of the study region (Yap State) in Chapter 2 and a review of available data collected for analyses in Chapter 3, the methods of analysis are presented in Chapters 4 and 5 and divided into the following components:

- Conduct a literature review of published and unpublished materials that aid in evaluating water supplies of Yap outer-islands.
- Review data collected by field survey on Ifalik Island for use in analyzing water resources on Ifalik and the remaining islands of study. Data collected is pertinent to rainwater catchment infrastructure, groundwater wells, public and household storage capacity, and household water demand. The survey was carried out by a collaborative field team from the International Research and Environmental Institute (iREi) in August 2015.
- Quantify the performance of rainwater catchment systems on Ifalik through drought analysis and extend the information to recommend a network of rainwater catchment systems for the remaining islands.
- Create reliability curves based on typical rainwater catchment system component sizes to aid water managers in selecting larger components for better reliability.

- Model groundwater lens dynamics for steady, average rainfall and future climate rainfall conditions to quantify the availability of fresh groundwater and test the changes due to future rainfall patterns. This is performed for all four islands.

2. YAP STATE ATOLL ISLANDS

2.1 Geographic setting

This thesis studies outer-lying islands in Yap State of the Federated States of Micronesia (FSM), which are located in the Carolinian archipelago of the western North Pacific Ocean (Figure 4). The state is formed by a group of islands in western-most FSM, from longitude 137°E to 148°E and from latitude 7°N to 10°N (Figure 5).

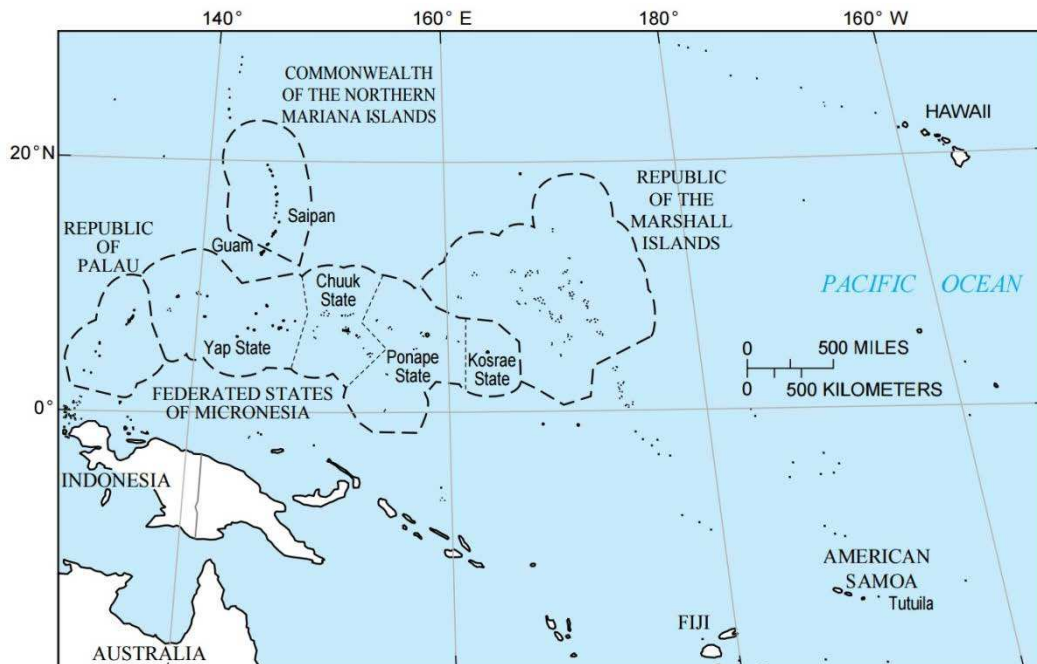


Figure 4 – Map of the Pacific Island nations, including the Carolinian Archipelago (U.S. Geological Survey, 1996)

The islands of Yap State include Yap Island, the main island of Yap State formed by a group of high volcanic islands; Fais, a high limestone island 250 km northeast of Yap Island; and 14 outer-lying atolls situated primarily between Yap and Chuuk Islands (Richmond, Mieremet, & Reiss, 1997). The islands selected for study in Yap State include: Eauripik Island, Falalop

Island (Ulithi Atoll), Ifalik Island, and Satawal Island. This section includes information pertinent to the four islands of study for modeling considerations.

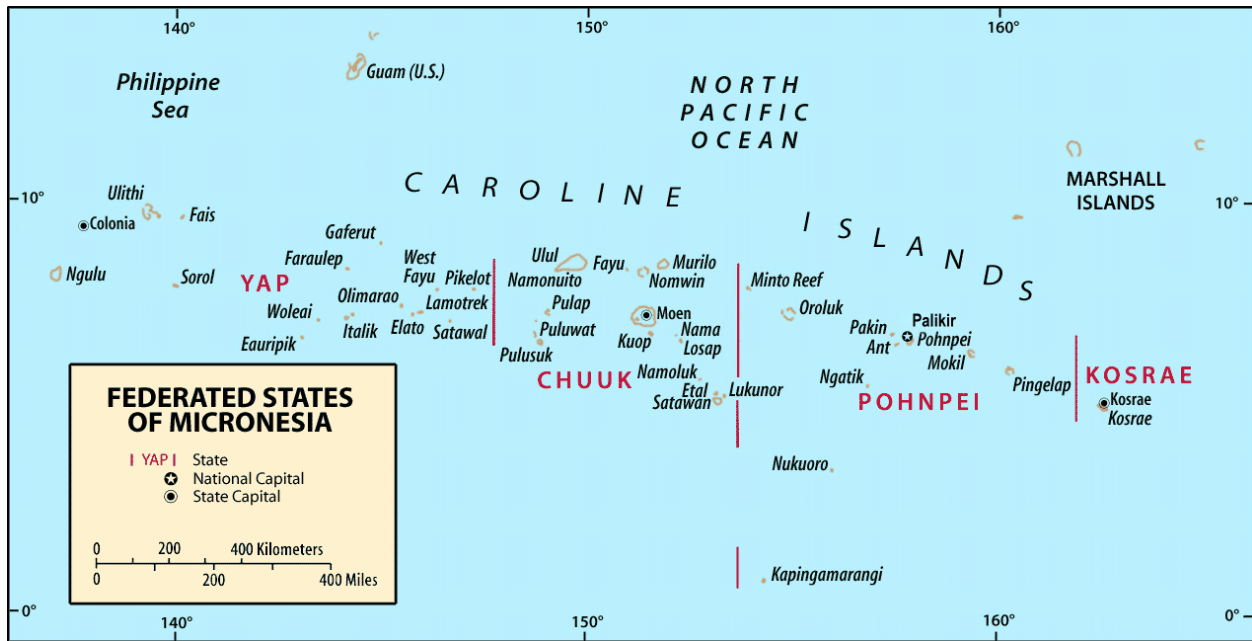


Figure 5 – Map of the Federated States of Micronesia (FSM Government)

2.1.1 Eauripik Island

Eauripik (Auripik) Atoll (Figure 6) is a low-lying coral atoll located 108 km southwest of Woleai atoll and is the southernmost atoll in Yap State (Bryan, 1953). It is also located approximately 630 km from Yap Island and 775 km from Guam. It contains three islands with the largest, Eauripik Island, as the only inhabited (Scourse & Wilkins, 2009). Land area on Eauripik Atoll is very small at 0.2 km², and it is approximately 11 km long east-to-west and 3 km wide north-to-south. Eauripik Island (Figure 7) is a windward, infinite strip island on the easternmost part of the atoll. The longest dimension has an average and maximum length of approximately 150 and 200 meters (Levin, 1976). The island has a low, swampy area in the middle that is used to cultivate swamp taro (Roy & Connell, 1991). The freshwater lens on

Eauripik is small due to the small width (Levin, 1976), and the maximum elevation on Eauripik is low, perhaps 6 meters (Levin, 1976) (Richmond, Mieremet, & Reiss, 1997).



Figure 6 – Eauripik Atoll 2015 (imagery credit: iREi)



Figure 7 – Eauripik Island 2015 (imagery credit: iREi)

2.1.2 Falalop Island (Ulithi Atoll)

Falalop (Fl'aal'ap) Island (Figure 8) is a windward island in the northeast part of Ulithi Atoll, approximately 195 km from Yap Island Airport and 665 km to Guam airport. Falalop is located 1.5 km southeast of Asor outside of the main ring of Ulithi islands. Falalop is a triangular island with the maximum width approximately equal to the length and general taper in width

throughout the full length. The approximate dimensions for the island are about 1.2 km in length and 1.1 km wide. Falalop is also the main island of Ulithi and the site of government activities, the major air strip, and much of the Ulithi population (Richmond, Mieremet, & Reiss, 1997).



Figure 8 – Falalop Island 2015 (imagery credit: iREi)

2.1.3 *Ifalik Island*

Ifalik (Ifaluk) Atoll (Figure 9) is a low-lying coral atoll located 745 kilometers southeast of Yap Islands and 690 kilometers east of Chuuk Islands. Ifalik is a circular atoll composed of two islets: Ifalik, the main island on which the Ifalik inhabitants reside, and Ella, a small, uninhabited islet west of Ifalik. Approximately 650 meters of channel separate the islets with the deepest section of atoll at the middle. Ifalik Island (Figure 10) is a semi-circular, elongate island with maximum dimensions 2.45 km north-to-south and 1.9 km east-to-west. Ella Island is 0.35 km north-to-south and 0.7 km east-to-west. Ifalik has a maximum elevation of approximately 5 meters, or 15 feet (Tracey, Abbott, & Arnow, 1961) (Richmond, Mieremet, & Reiss, 1997).



Figure 9 – Ifalik Atoll (NOAA, 2015)

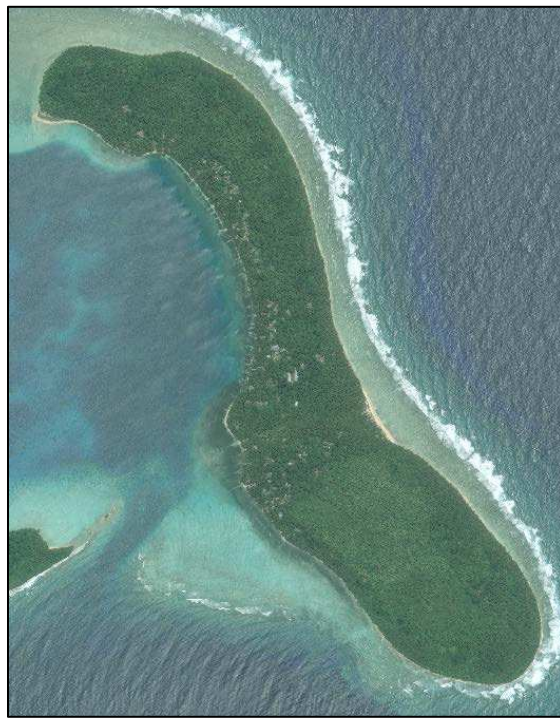


Figure 10 – Ifalik Island 2015 (imagery credit: iREi)

2.1.4 *Satawal Island*

Satawal (Satuwal) Island (Figure 11) is a reef island located in the easternmost part of Yap State, approximately 530 km from Chuuk Island and 1,010 km from Yap Island. Satawal

has no significant lagoon and thus is considered a reef island, or in some literature a ‘table reef’ (Fosberg, 1969). The island is a semi-circular, elongate island with maximum dimensions 1.35 km north-to-south and 1.8 km east-to-west. The maximum elevation on Satawal is at least 7 meters and by some definitions would not be considered low-lying (Richmond, Mieremet, & Reiss, 1997).



Figure 11 – Satawal Island 2015 (imagery credit: iREi)

2.2 Climate

Yap State lies in the tropical climate zone between the Tropic of Cancer and the equator. Weather is generally warm, humid, and rainy with regional variances occurring due to trade winds. Climatic variables, including seasonal and annual precipitation, mean sea-level, and occasional typhoon events, heavily influence the health and availability of resources on the outer-lying islands, and anticipated climate change would alter these conditions.

2.2.1 Precipitation

Rainfall is the sole source of freshwater for remote, outer-lying atolls, therefore accurate historical data for annual rainfall is important for future planning purposes. Historical precipitation data is available through the National Ocean and Atmospheric Administration (NOAA) for weather stations on several larger islands in Micronesia, including stations at the Yap and Chuuk Weather Service Office Airports. These two stations provide the most complete historical climatic data for Yap State dating as far back as 1951. Average climate indices for the nearest airports are shown in Table 1.

Table 1 – Average annual precipitation and daily temperature for regional airport weather stations

STATION	Annual Precipitation (m)	Average daily temperature (°C) ¹	Maximum daily temperature (°C)	Minimum daily temperature (°C)
YAP ISLAND WEATHER SERVICE OFFICE AIRPORT FM	3.07	27.6	30.2	24.9
CHUUK WEATHER SERVICE OFFICE AIRPORT FM	3.42	28.2	30.9	25.4

¹Data from the National Oceanic and Atmospheric Administration

As shown in Table 1, the amount of annual rainfall varies regionally and generally decreases from south to north and east to west. Variance in rainfall occurs spatially within atolls (Falkland, 1994) (Spennemann, 2006) and the variance can be up to 10% (Falkland, 1994). The climate is also humid with average humidity between 83 – 87% (Alkire, 1959) (Tracey, Abbott, & Arnow, 1961). Yap atolls experience two seasons: a dry season from November to June and a wet season from July to November (Figure 12). Northeasterly trade winds form conditions for the dry season and the wet season occurs when the trade winds subside creating more variable wind patterns at the Intertropical Convergence Zone (ITCZ) (Arnow, 1955) (Anthony, 1997).



Figure 12 – Average daily rainfall for Yap Island (mm)

Droughts occur typically every 6-7 years for coral atoll islands (White, et al., 2007) and occur during the dry season in relation to El Niño Southern Oscillation (ENSO) events (White, Falkland, & Scott, 1999). Severe droughts occur in the months following the start of an intense El Niño event (Landers & Khosrowpanah, 2004) and severity can vary to extremes down to 5% of typical monthly precipitation and 28% of normal seasonal precipitation, as was observed on Yap Island during the dry season in 1983 (Van der Brug, 1986). Historical extreme precipitation years for each airport weather station are shown in Table 2.

Table 2 – Extreme annual precipitation (m) at regional airport weather stations (June to May)

STATION	Precipitation (m), End year - ENSO Event ¹			
	Maximum		Minimum	
YAP ISLAND WEATHER SERVICE OFFICE AIRPORT FM	4.03	(2004)	2.11	(1973 - Strong El Niño)
CHUUK WEATHER SERVICE OFFICE AIRPORT FM	4.59	(1956 - Mild La Niña)	1.82	(1983 - Very Strong El Niño)

¹ Data from the National Oceanic and Atmospheric Administration

As Table 2 demonstrates, annual rainfall can drop to 2/3 the annual average during some El Niño years. The ENSO events are identified using the Oceanic Niño Index (ONI) which is the standard used by NOAA. According to ENSO years categorized by ONI, the strongest El Niño event occurred from August to December of 1997 and impacted the tropical pacific, including Yap outer-lying islands. The drought that followed in the early months of 1998 was subsequently one of the most severe.

2.2.2 Sea-level

ENSO events also alter sea level elevation. El Niño episodes frequently correspond to a mean sea-level drop (Landers & Khosrowpanah, 2004), while conversely La Niña events lead to higher sea-levels due to higher water temperatures and intensified easterly trade winds. For low-lying atolls, the higher tides exhibited during La Niña events may lead to shoreline erosion and episodes of over wash which can harm important resources such as groundwater, stored rainwater, and taro (Hezel, 2009).

2.2.3 Typhoons

Storm events occur frequently in Yap State as small, passing storms or minor weather from large storms at a distance (Tracey, Abbott, & Arnow, 1961). While these events are not regarded as dangerous by the islanders in Yap (Levin, 1976), islanders are concerned with infrequently occurring typhoons. Typhoons historically devastate water resources, vegetation, and human life by extremely strong winds and large waves. For instance, in March 31st, 2015 Typhoon Maysak struck Ulithi and winds that reached 160 miles per hour (258 km per hour) leveled 60% of the structures and devastated the food supply. Damage to natural resources and human life are commonly a result, as well as an alteration to the island geometry. Impacts have reduced in severity in recent years as a result of government aid responses.

The precursor to a typhoon is a tropical cyclone, or rather a circulation of high winds originating over tropical oceans, and typhoon status is reached when the maximum sustained 1-minute winds reach 64 knots (74 mph). Typhoons typically begin as tropical cyclones over eastern Micronesia and travel north to Guam, thereby missing Yap State (Tracey, Abbott, & Arnow, 1961) (Landers & Khosrowpanah, 2004). Historically in the Yap region, typhoons and their impacts have been of varying degrees of severity from small typhoons that over-wash and damage groundwater resources (Levin, 1976) to large typhoons that take human life. Perhaps the strongest typhoon to hit central Yap is the Great Typhoon of 1907, as named by local islanders (Tracey, Abbott, & Arnow, 1961). According to personal accounts from Ifalik islanders, the typhoon leveled most trees, damaged most structures, and took the lives of 35 islanders (Tracey, Abbott, & Arnow, 1961).

Typhoons also alter the island geometry by sweeping sediments in and away from an island, and thus may benefit or harm the islanders. For example, the Great Typhoon of 1907 swept in enough gravel and sediment to fill a narrow channel between two islands on the north side of Ifalik Atoll, which thereby merged the islands into one (Tracey, Abbott, & Arnow, 1961). Refer to Figure 13 and Figure 14 for a comparison prior to and after the typhoon. The same typhoon destroyed part of eastern Eauripik Island (Levin, 1976).

Response to typhoon impacts has evolved over time from a regime backed by neighboring-island rescue and hospitality, to strategy backed by government aid supplies. For instance, when a typhoon struck Eauripik in the late mid-1800s, a party came by boat from Woleai to rescue survivors and bring them to Woleai where they could await recovery of their resources (Levin, 1976). Alternatively, a more recent typhoon that struck Eauripik in 1975 was remediated, instead, by government surplus food. The islanders determined they could ration the

supplies well enough to continue living on the island despite the damage that occurred to the vegetation and the fresh water lens.

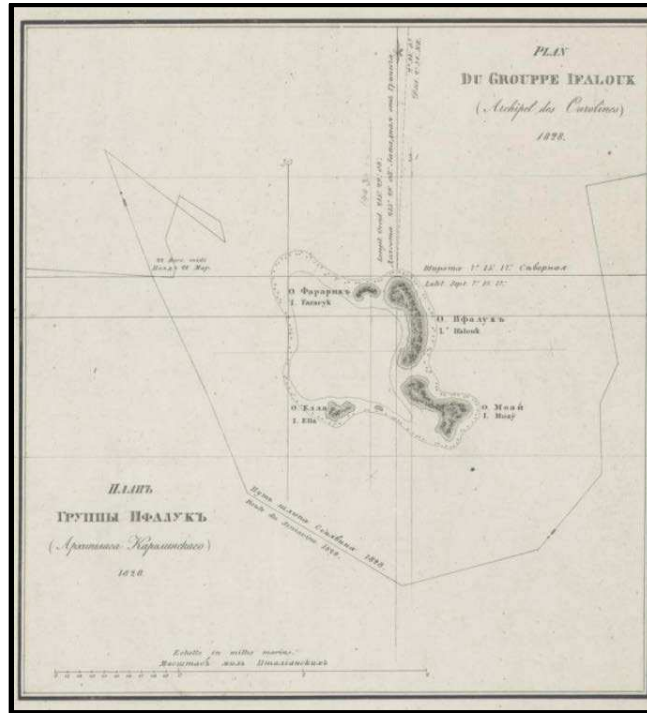


Figure 13 – Hand-drawn map of Ifalik Atoll, 19th Century

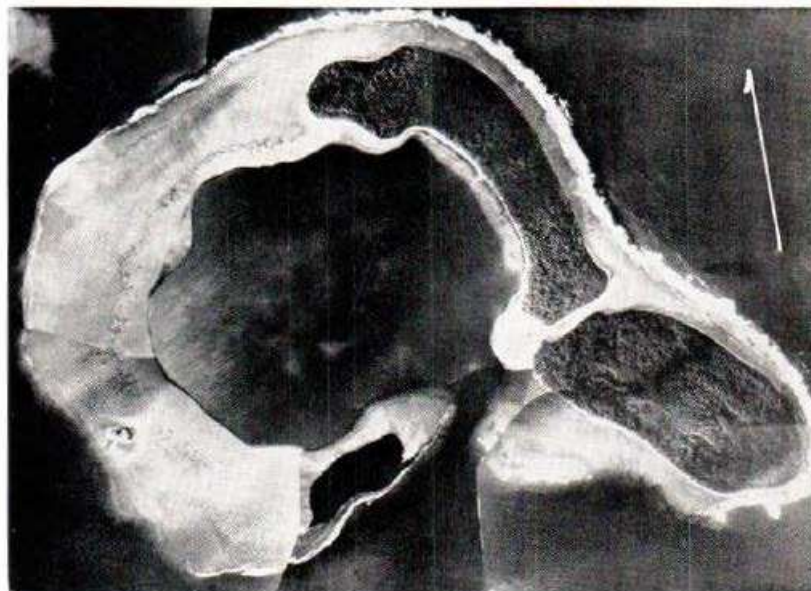


Figure 14 – Geometry of Ifalik Atoll, 1948
(Photograph by U.S. Navy) (Tracey, Abbott, & Arnow, 1961)

2.3 Climate change

Climate change, naturally or anthropogenically accelerated, alters the frequency, duration, and intensity of extreme weather events and low-lying atolls are especially vulnerable to the impacts. Yap State atolls are susceptible to climate change effects due to their remoteness, limited resources, low topography, and easily erodible sediments. The Intergovernmental Panel on Climate Change (IPCC) predicts the following climate change impacts will occur for small island states in the Pacific: more frequent ENSO events, increase in mean sea level, and intensified typhoons (Barros, et al., 2012).

2.3.1 ENSO events

IPCC noted they have a medium confidence that an observed increase in frequency of ENSO events has occurred since 1950 in the equatorial Pacific (Barros, et al., 2012). Future increases in intensity and frequency of ENSO events will increase the occurrence and severity of droughts for the outer-lying atolls which inhibits access to freshwater.

2.3.2 Accelerated sea-level rise

Sea-level rise (SLR) is occurring on a global scale at roughly 1.7 mm/yr based on tide gauge observations, and roughly 2.8-3.6 mm/yr based on satellite altimetry data. This is referred to as the global mean sea level (GMSL) (Kensch, Ford, & McLean, 2015). Pacific island nations have observed an increase in mean sea level and it is very likely to continue in the near future (Barros, et al., 2012). The impacts of SLR include saltwater inundation of the surface, saltwater intrusion into the aquifers, erosion of shoreline, and a landward shift of the saltwater interface (Barros, et al., 2012) (Holding & Allen, 2015). However, atolls have shown dynamic responses and some may be more resilient to SLR than others (Kensch, Ford, & McLean, 2015). In

addition, effects would vary from depending on island location within the atoll and the geologic characteristics.

2.3.3 Intensified typhoons

In addition, the IPCC notes that it is likely that wind speeds of tropical cyclones will intensify in the future, however, frequency will likely remain stable or decrease (Barros, et al., 2012). Intensified typhoons may result in more devastating effects on the natural resources and loss of human life. The landform shape, location, and size would also be more dramatically altered by intensified typhoons.

2.4 Demographics

As of the 2010 census, the population in Yap State was 11,377 residents and most residents reside in Yap Proper while 4,006 residents live in the outer-islands (FSM National Government, 2010). Refer to Table 3 for population of the outer-lying atolls from 1920 to the present.

Table 3 – Historical Population for Yap State and Selected Atolls

Year	Population ¹					
	Yap	Outer-Islands	Ulithi	Eauripik	Ifalik	Satawal
1920	8,338	2,960	450	-	-	292
1925	7,366	2,711	508	103	295	250
1930	6,486	2,465	448	110	305	253
1935	6,006	2,312	408	102	252	264
1958	5,540	2,299	460	141	301	285
1973	7,870	2,731	710	127	314	354
1980	8,100	2,908	710	121	389	386
1987	10,139	3,488	852	101	477	466
1994	11,178	4,259	1,016	118	653	560
2000	11,241	3,850	773	113	561	531
2010	11,377	4,006	847	114	578	501

¹Population data from FSM 2000 and 2010 Census

As shown by Table 3, population fluctuations are most significant in Ulithi which also has the greatest number of inhabitants, and populations remain most stable on Eauripik which has the lowest number of inhabitants. From 2000 to 2010, Ulithi had the highest annual growth rate at 1%. Satawal was the only atoll that decreased in population size, with an annual population growth rate of -0.6%.

2.5 Water consumption

In general, low-lying, Yap island communities use water collected by rain catchments as their most significant source for drinking water (Dillaha & Zolan, 1985) (Detay, et al., 1989). Yap islands, in particular, have shown more careful water practices than other Micronesian islands, perhaps due to more limited rainfall and unavailability of other potable water sources. For instance, one study found that Yap communities cleaned tanks more frequently than other Micronesian islands and utilized a high percentage of the roof area, at approximately 79% on average (Dillaha & Zolan, 1985). Interestingly, fecal and total coliforms are frequently present in RWCS water (Detay, et al., 1989), including one instance on Yap islands in 1985, with measured 58% of 36 samples present with fecal coliform bacteria and 78% of 37 samples present with total coliform bacteria (Dillaha & Zolan, 1985). Although this study found that most RWCS still met the early World Health Organization (WHO) standards for coliform bacteria, most would not meet the current standard of un-detectability in all samples.

Since most other water purposes, including washwater, pose a lower risk of health concerns by water contamination, other sources such as groundwater or seawater are used to conserve the RWCS water. Groundwater is also occasionally used to supplement drinking water supplies during droughts or shortages and it is common for island residents to boil the water first (Anthony, 1997). Coconut water is also frequently used for drinking purposes depending on the

available supply for the particular community. Additionally, residents can ration at great lengths when necessary. For instance, a USGS study in Ulithi during the 1983-1984 drought found that water consumption dropped to 1.89 liters of water per capita per day on Asor and Fassarai islands (Van der Brug, 1986).

3. DATA COLLECTION

This section covers two collections of data that are integral to the rainwater catchment system and groundwater modeling portions of this thesis. The first section summarizes the objectives and results from a field survey conducted by a collaborative research team on Ifalik Island in August 2015. The second section covers the development of and rationale behind selection of the rainfall scenarios used in the following analyses.

3.1 Field survey on Ifalik

3.1.1 Overview

As part of this research, a field team conducted a hydrologic field assessment on Ifalik Atoll in Yap, Micronesia from August 15, 2015 to August 22, 2015. The team consisted of seven scientists working on behalf of Island Research & Education Initiative (iREi) based out of Pohnpei, FSM. The objectives of the fieldwork included:

- Conduct a detailed inventory of the rainwater catchment infrastructure, including dimensions of effective roof area, storage tank capacity, guttered roof area, and qualitative assessment of gutter-downspout condition (Figure 15).
- Survey groundwater by measuring well water levels and salinity.
- Locate through GPS and document by photograph groundwater wells and rainwater catchment systems.
- Examine water quality from both sources by measuring temperature, pH, zinc, lead, and E. coli.
- Interview households to collect information regarding the main sources of water, purposes of water from those sources, demand, quality, scarcity, and health concerns.
- Perform a survey of vegetation, particularly typical density of coconut trees.

- A more detailed account of the hydrologic assessment may be found in the technical report published by Water and Environmental Research Institute (Kottermair, Taborosi, & Jenson, 2016).

A brief survey was also conducted on Eauripik Island on the return trip, however due to time constraints, the survey was limited to a photo inventory of the RWCS storage tanks and brief interviews.



Figure 15 – Photograph of a rainwater catchment storage tank on Ifalik (Photo credit: iREi, 2015)

3.1.2 *Rainwater catchment inventory*

The field team inventoried over 100 rainwater catchment systems on Ifalik (Appendix A), most of which were household catchments and the remaining were schools, churches, dispensaries, and men or women’s meeting houses. To get the effective roof area and storage tank size for unlabeled tanks, a laser distance meter (Tuirel T100) was used to measure the dimensions of the catchment. Catchments were briefly observed on Eauripik and there are at

least 30 household RWCS and 2 community systems. Observations from the RWCS assessment include:

- Several catchments had a guttered roof area smaller than the full area of the roof.
- Concrete cisterns used to store water collected from large, community structures were in general disrepair and residents expressed a preference for the 2,000 liter high-density polyethylene (HDPE) tanks (Figure 15). These were the most common tanks inventoried on both Ifalik and Eauripik.
- Many catchments were integrated into small cooking or storage huts due to easier implementation over existing thatched roof households.
- Larger catchment systems may have multiple storage tanks.
- Eauripik has a noticeably higher bird population which results in continual maintenance for the roof catchments.

3.1.3 Groundwater survey

The field team inventoried over 60 groundwater wells on Ifalik. To get water table levels, a laser distance meter (Tuirel T100) is used in conjunction with a tripod to measure water table elevations. Two-level loggers (HOBO U20 Titanium Water Level Loggers) were installed to measure tidal data, one open to the atmosphere and one installed a few meters from the shoreline on the lagoon side. Wells were briefly observed on Eauripik and there are at least 8 wells.

Observations from the well assessment include:

- A survey benchmark made in limestone during a USGS study in 1953 (Tracey, Abbott, & Arnow, 1961) not found during the field assessment. In addition, wells described in the earlier study were filled in and used to grow taro.
- Thirteen wells were surveyed for water level, depth to bottom, diameter, materials, and uses. Due to complications that arose during the field work, the accuracy was determined to be uncertain and therefore was not used in further analysis of this thesis.

- Observations indicated low tide occurred earlier on the ocean side than on the lagoon side. In addition, the team recommended installing tidal gages on both the lagoon and ocean side to improve results.

3.1.4 *Surveyed locations*

Locations of the rainwater catchment storage tanks and groundwater wells were shot using a Trimble Juno 5 GPS unit which documented latitude and longitude. Elevation data was determined to be unreliable. In addition, over 1,000 photographs were taken using an Olympus TG2 camera of the water structures, vegetation, island residents, etc. (Figure 16).



Figure 16 – Photograph of a young, Ifalikian woman collecting water from a storage tank on Ifalik (Photo credit: iREi, 2015)

3.1.5 *Water quality*

Important water quality parameters were measured, including E.coli, pH, and zinc. pH was measured qualitative using pH paper, E.coli was tested for on Ifalik and Eauripik using a presence/absence test kit, and zinc was tested through off-site laboratory analysis to see leaching

occurred from coatings on the metal panels. For the water quality assessment, several observations and findings were made, and include:

- pH: Values for twenty wells and catchments ranged between 6 and 7 on the pH scale.
- E.coli: All samples from 10 well sites and 6 storage tanks tested on Ifalik were positive, except for 1 of the storage tanks, and all 4 samples from storage tanks on Eauripik were positive.
- Zinc: Samples taken from 3 community RWCS were all well below the recommended limit of 100 milligrams per liter.

3.1.6 Household interviews

Household interviews with the residents of Ifalik and Eauripik lent information regarding sources, demand, quality, scarcity, and health concerns and the following conclusions were made from the surveys:

- Ifalik residents use water from the rainwater catchments for drinking water purposes and to cook higher quality foods, such as rice. Also, coconuts are a supplement to the rainwater and each person consumes an average of 3 per day. Groundwater is used for other purposes, such as laundry and washing dishes.
- Eauripik residents rainwater only for drinking purposes and do not drink coconut water. Groundwater and seawater are used for other purposes.
- Water demand on Ifalik and Eauripik is typically around 3 gallons (11.5 liters) of water per person per day, depending on showers and food preparation.

3.1.7 Vegetation survey

To survey the vegetation, seven 10 x 30 meter plots were identified in disparate parts of the island, on both the windward and leeward side. Species were recorded for the low, immature layer designated as 2 meters or below, the understory which contained trees between 2-10 meters in height, and the overstory that exists above. The following observations were found:

- An average of 6.57 coconut trees were identified for the plots, which is equivalent to a density of approximately 89 trees per acre.
- Breadfruit was present in most plots. Banana, papaya, and pandanus trees were also present in several.
- Wild taro was consistently identified at the inland locations.

3.2 Rainfall conditions

3.2.1 Average conditions

Average rainfall conditions are simulated using normal daily rainfall data from Yap Island Weather Service Office Airport station averaged over the active period from July 1st, 1951 to July 1st, 2015 (Figure 12). Due to little information for rainfall in Eauripik, Ifalik, and Satawal, the weather station for the main island in Yap State is assumed to be valid for the entire state. Intermittent data is available for Ulithi, however it is much less complete and due to proximity to Yap Island, Falalop rainfall should be similar.

3.2.2 Drought conditions

According to ENSO years categorized by the Oceanic Niño Index, the strongest El Niño event occurred from August to December of 1997 and impacted the tropical pacific, including Yap outer-lying islands. The drought that followed in the early months of 1998 was subsequently one of the most severe. Due to the recent nature and severity of this drought, the meteorological period from August 1st, 1997 to July 31st, 1998 is selected to simulate drought conditions for rainwater and groundwater evaluations.

3.2.3 Future climate conditions

General Circulation Models (GCMs) are used to examine the effects of future rainfall conditions on the rainwater and groundwater storage supplies due to climate change. GCMs are

numerical models created to represent physical earth processes under climate change induced by greenhouse gas (GHG) concentrations. According to the IPCC, the GCMs provide a credible, overall simulation of future climate conditions at large spatial and temporal scales, for instance at the sub-continental spatial scales and decadal scales (Perkins, et al., 2007) (Barros, et al., 2012). Since data from GCMs are provided in monthly rainfall amounts, they must be downscaled to daily values to model performance of rainwater catchment systems and simulate groundwater dynamics (Wallace, Bailey, & Arabi, 2015).

At least 62 GCMs participate in the Coupled Model Intercomparison Project 5 (CMIP5) and the models that best represent historical rainfall in the region of western Micronesia will be used to simulate future precipitation. For each GCM, there are four variations based on representative concentration pathways (RCPs): RCP2.6, RCP 4.5, RCP 6.0, and RCP 8.5. RCPs are the four radiative forcing scenarios selected by the IPCC, of which RCP 2.6 is the lower concentration projection and RCP 8.5 is the highest. For purposes of this thesis, future climate models will consider the range of models and will therefore evaluate the best fit model at RCP 2.6 and the best fit model at RCP 8.5. Qualitatively, RCP 2.6 assumes that anthropogenic greenhouse gas (GHG) emissions peak in the 2010-2020 decade and decrease in annual emissions in years following. Conversely, RCP 8.5 assumes that emissions continue to rise for the next several decades.

A previous study by Wallace et al. evaluated the participating GCMs to find the best models for Western and Eastern regions of Micronesia at each RCP variation. The study evaluated the models by downscaling the monthly data and testing the precipitation data against historical records for each region (Wallace, Bailey, & Arabi, 2015). The study utilized a multi-score, statistical method that implemented the Skill Score (S_{score}) and the Brier Score (BS) to

evaluate replication of historical precipitation data (Fu, et al., 2013). The S_{score} is a statistic that measures the area between the probability density function (PDF) curves of the historical and GCM rainfall data (Wallace, Bailey, & Arabi, 2015). This is calculated as the cumulative, minimum value of the distributions of each bin value for a PDF generated by a specified number of bin values. Mathematically, the S_{score} is represented by Equation 2 where n is the number of bins for the PDF, Z_m is the frequency of values in a bin from the model and Z_0 is the frequency of values in a bin from the observed data (Perkins, et al., 2007).

$$S_{score} = \sum_1^n \text{minimum}(Z_m, Z_0) \quad \text{Equation 2}$$

An S_{score} value close to 1 indicates the PDF for historical data and modeled data overlap well and the GCM is an excellent model, whereas a score value near 0 is a poor model. Typically when using this metric, a floor value is selected at roughly 0.7 or 0.8 to indicate the threshold of acceptable models, with values above the threshold value considered acceptable for further evaluation (Perkins, et al., 2007) (Wallace, Bailey, & Arabi, 2015).

The second metric is the Brier Score which is a mean squared error for metric for probability forecasts (Brier, 1950) (Fu, et al., 2013). Equation 3 shows the calculation for the Brier Score, where P_{mi} is the modeled i th probability value of a given bin, and P_{oi} is the observed i th probability value for that given bin (Wallace & Bailey, 2015). For this metric, a value of zero is perfectly projected climate model and a value of 2 is a poor climate model.

$$BS = \frac{1}{n} \sum_1^n (P_{mi} - P_{oi})^2 \quad \text{Equation 3}$$

For the Western region, which includes Yap State, models of correlation to historical precipitation records were created by the National Aeronautics and Space Administration

(NASA) Goddard Institute for Space Studies (GISS), a laboratory in the Earth Sciences Division (ESD) of NASA. Specifically, the study found that for the radiative forcing scenarios of RCP 2.6 and RCP 8.5 in the region of Western Micronesia, the best correlated general climate models were GISS-E2-H and GISS-E2-H-p2 (Wallace, Bailey, & Arabi, 2015). Statistical metrics for the GISS-E2-H model under RCP 2.6 were a BS of 0.0029 and an S_{score} of 0.833 and statistical metrics for the GISS-E2-H-p2 model under RCP 8.5 were a BS of 0.0024 and an S_{score} of 0.839. Corresponding, downscaled daily precipitation data from these models are used to evaluate the effects to performance of rainwater catchment systems and groundwater lens dynamics under future climate conditions.

4. RAINWATER COLLECTION AND STORAGE

4.1 Overview of methods

For communities in Yap State that rely on rainwater catchments for drinking water, the supply must meet the demand, otherwise the deficit must be supplemented by boiled groundwater or an emergency supply of bottled water. A simple mass balance model is an excellent way to evaluate the reliability of a rainwater catchment system. For the remainder of this thesis, the term ‘reliability’ refers to the percentage of days during a simulation that the daily demand is met by the storage tank (Liaw & Chiang, 2014) (Wallace, Bailey, & Arabi, 2015). On a day in which the supply from the storage tank is less than the demand, the stored volume becomes the daily output and that day is counted against the overall reliability. In other words, maximum reliability for a simulation occurs when the demand is met every day and it is equivalent to a value of 1.00 or 100%. A system that provides insufficient water for the entire period is unreliable and the reliability is 0.00 or 0%.

The mass balance is a conceptual model that assumes the RWCS is a closed system with a single input, a single output, storage, and losses. Rainfall depth is the sole input of water, and this is typically taken from the nearest airport weather station. The output is water demand which depends on the number of users and the per capita demand of the users. Design constants included in the model are specific to the RWCS and include roof area (the guttered portion) and storage tank size. Finally, to consider losses from the gutter-downspout system, an efficiency factor must be approximated based on the condition, which considers age, presence of cracks, and sufficiency in length and width to convey the entire volume collected from the roof. This

factor establishes a more realistic estimate of the portion of rainwater volume delivered from the roof to the storage tank.

Weather stations in Yap State collect precipitation data on a daily basis, therefore the conceptual model is used to estimate the supply and reliability on a daily basis. The volume stored at the end of the selected time step is calculated by Equation 4. Note that dimension L represents a length unit (e.g. meter) and dimension T represents a time unit (e.g. day).

$$V_t = \max \{ \min [V_{t-1} + AR_t \varepsilon, S] - O_t, 0 \} \quad \text{Equation 4}$$

Where:

V_t : volume of stored rainwater at the end of the day [L^3]

V_{t-1} : volume of stored rainwater at the end of the previous day [L^3]

A: effective rooftop catchment area (area projected from bird's eye view and enclosed by gutters) [L^2]

R_t : depth of rainfall per time step [L/T]

ε : efficiency of the gutter-downspout system [-]

S: storage tank size [L^3]

O_t : water demand per time step [L^3/T]

The mass balance equation calculates the volume at the end of each day and satisfies two criteria: 1) storage in the tank cannot exceed the volume of the tank, imposed by the minimum function, and 2) storage in the tank cannot be less than zero, as imposed by the maximum function.

This section uses the field data collected by this study on Ifalik Island to determine the existing reliability of the rainwater catchment systems and evaluate how improvements can be made to increase water. To determine the existing reliability of the RWCS and the effects due to changes in design, a daily mass balance model is implemented with varying rainfall conditions. In addition, the mass balance model is implemented to develop design curves based on common values for a RWCS (e.g. roof area, storage tank size). Design curves are a tool developed to

evaluate the relationships between reliability and size of the catchment for design and retrofitting of RWCS.

4.2 Rainwater catchment systems of Ifalik

The mass balance model provides estimates of stored rainwater volumes, and it is used to evaluate the performance of the typical RWCS found on Ifalik, to examine the influence of parameters through a sensitivity analysis, and to evaluate the community water supply by evaluating the performance of each household RWCS. The model is used to estimate daily stored volumes for a RWCS that exhibits average characteristics of a rainwater catchment system on Ifalik. This hypothetical 'base' RWCS is then analyzed for sensitivity of the parameters by modeling scenarios that exhibit a single, small alteration to a parameter of the RWCS. Analyses for sensitivity are evaluated for the average rainfall conditions and severe drought conditions. Then, reliability of the Ifalik catchment system network is assessed on a community level using severe drought and future rainfall conditions. The drought imposed uses rainfall data from a severe drought that occurred during 1997-1999, and future climate conditions are modeled for 2010-2040 using downscaled, daily rainfall data for GCM GISS-E2-H for the RCP2.6 forcing scenario and GISS-E2-H-p2 for the RCP8.5 forcing scenario.

4.2.1 Evaluation of Ifalik RWCS parameters

There are over one hundred operational rainwater catchment systems on Ifalik Island, as identified through field work conducted in mid-August 2015. Data collected for RWCS evaluation are included in Appendix A of this thesis. The measurable and qualitative characteristics for each RWCS were recorded, including guttered roof area, potential guttered roof area, storage tank volume, gutter-downspout condition, and the number of residents (water users) within each compound. This information becomes included in the mass balance model

(Equation 4) as RWCS-specific constants and parameters, namely: effective roof area A (actual or potential), storage tank capacity S , system efficiency ε , and daily output (or demand) O . Since measurements in the field were done with measuring tapes, the guttered roof area, potential roof area, and storage tank capacity is considered accurate enough and used directly in the mass balance model. Table 4 provides summary statistics for the Ifalik rainwater catchment systems.

Table 4 – Statistics for rainwater catchment systems on Ifalik Island

Statistic	Effective roof area, A (m ²)			Storage tank volume, S (L)
	Actual	Potential - Case 1 ^a	Potential - Case 2 ^b	
Average				
Mean	16.5	25.6	20.1	5,870
Median	10.0	12.2	7.8	1,880
Mode	6.0	6.0	2.3	2,000
Range				
Maximum	253.7	546.7	546.7	337,720
Minimum	1.56	1.56	0.88	11

^a. Case 1 assumes gutters on existing catchments are expanded to full potential area

^b. Case 2 assumes gutters on existing catchments are expanded to full potential area *and* full-area catchments are added to roofs of all remaining structures

The field work conducted in Ifalik determined that several RWCS had a guttered roof area, or effective roof area, smaller than the total roof area (Kottermair, Taborosi, & Jenson, 2016). Figure 17 shows the measured effective roof area for all rainwater catchment systems on Ifalik, as well as the potential effective roof area.

System efficiency, ε , is estimated from the qualitative assessment of the gutter-downspout system made by the field team and therefore has the greatest level of uncertainty. A scale was developed to obtain a numeric value for the efficiency based on the qualitative assessment, which ranged from ‘Very Poor’ condition to ‘Very Good’ condition. Since a newly constructed RWCS typically has an efficiency of 0.8 (or 80%) (USAID - Washington, DC, US, 1982), this was used for the ‘Very Good’ condition while lower assessments were given smaller

values, as shown in Table 5. At least 90 of the catchments surveyed received a rating of ‘Good’ condition.

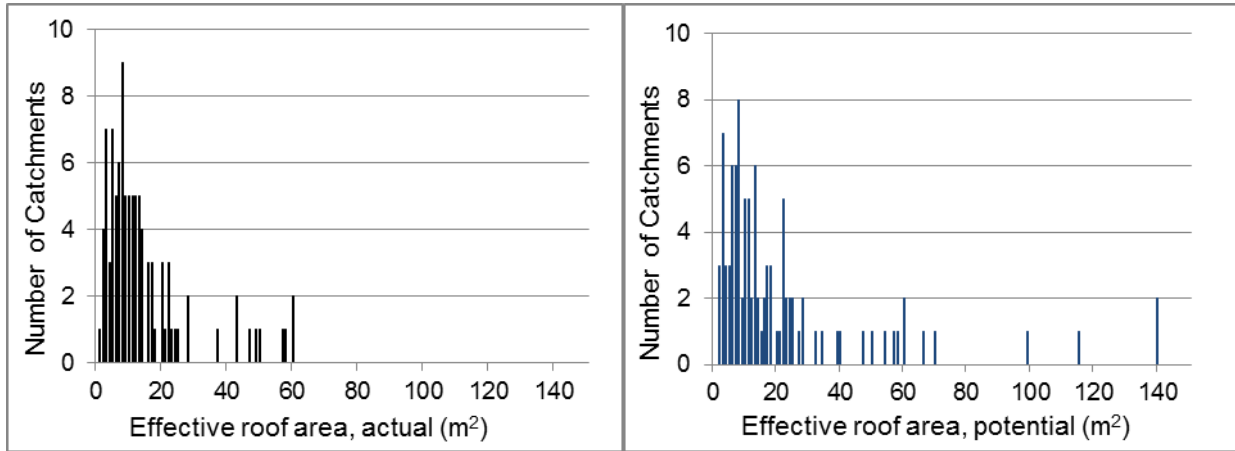


Figure 17 – Effective roof area of rainwater catchment systems on Ifalik Island, actual and potential

Table 5 – Rainwater catchment system efficiency scale

Condition of gutter-downspout system	Designated efficiency, ϵ (-)
Very good	0.8
Good or average	0.7
Fair	0.55
Poor	0.4
Very poor	0.2

The demand or output, O , was determined by estimating the number of users and the daily per capita demand. To determine the number of users for each RWCS, the residents in each compound were allocated as users to a single RWCS based on the storage tank sizes in the compound. For example, the model would assume that a compound with ten people and two RWCS, one with a 2,000 liter tank and the other with a 500 liter tank, has eight residents using the former RWCS and two residents using the latter. In general, typical number of users for each catchment ranged from 3 to 12 users, with a mean average of 7 users per catchment. It should be noted that although estimating the number of users is important for modeling the reliability of the

rainwater catchment systems, the residents of Ifalik readily share water with one another on a daily basis, which extends the reliability of the entire island supply.

The daily per capita demand was estimated using results from Question 13 of the household interviews, which asked: “*If it stopped raining from now on, how long would your full supply last?*” The answers ranged from 2 weeks to 1 month to deplete a full water tank with the majority of answers indicating 2 weeks. Using this information with the number of residents in the interviewees’ compound and corresponding tank sizes, the average per capita demand rate is estimated to be approximately 12 L/day, with minimum and maximum of 8 L/day and 16 L/day. Based on the average number of water users per catchment and average water demand per person, the typical daily demand from a RWCS is 84 L day⁻¹. By comparison, the U.S. national average demand is 81 gallons per capita per day, or 307 liters per capita per day (Maupin, et al., 2014).

One final condition that is important to consider for this mass balance model is the initial condition. The stored volume, V_{t-1} , for the first time step represents this initial condition and it has a strong influence on the results. For evaluations in this analysis, simulations were started several months prior to the time period of interest at a time when there was high rainfall to limit the impact of this condition.

To begin simulating the reliability of the typical rainwater catchment system on Ifalik, a base scenario is created using the average values for the model inputs. This scenario is for a rainwater catchment system that has a demand from seven users at 12 liters per person per day, has a 16.5 m² roof area, a 2,000 liter tank capacity, a gutter-downspout system efficiency of 70%, and an initial volume at 50% the tank capacity. Then, modifications were made to the base scenario in twelve additional scenarios to observe the impact to reliability. Each scenario

includes either an increase or decrease to a RWCS variable and when possible, the modification corresponds to a meaningful number for that variable. For instance, the efficiency is adjusted in Scenario 6 to 40% to simulate a decline from ‘good’ to ‘poor’ gutter-downspout conditions. The first set of six scenarios uses decreased input values, and the second set uses increased values (Table 6).

Table 6 – Scenario parameters for performance evaluation of typical RWCS on Ifalik Island

Scenario	Variable					
	Number of water users	Demand per water user (L/day)	Effective roof area (m ²)	Storage tank size (L)	Gutter-downspout efficiency (%)	Initial volume (% tank)
1 (Base)	7	12	16.5	2,000	70%	50%
2	3	12	16.5	2,000	70%	50%
3	7	8	16.5	2,000	70%	50%
4	7	12	10	2,000	70%	50%
5	7	12	16.5	1,000	70%	50%
6	7	12	16.5	2,000	40%	50%
7	7	12	16.5	2,000	70%	5%
8	12	12	16.5	2,000	70%	50%
9	7	16	16.5	2,000	70%	50%
10	7	12	25.6	2,000	70%	50%
11	7	12	16.5	3,000	70%	50%
12	7	12	16.5	2,000	80%	50%
13	7	12	16.5	2,000	70%	100%

For this section of the rainwater catchment system analysis, a second metric is included in addition to reliability termed *volumetric reliability* (Liaw & Chiang, 2014). This metric is added to show the actual water deficiency between the RWCS supply and the demand required by the users. The computation for volumetric reliability is shown in Equation 5.

$$r_v = \frac{V_{collected}}{V_{demanded}} \quad \text{Equation 5}$$

Where:

r_v : volumetric reliability [-]

$V_{collected}$: volume of stored rainwater during the simulation [L³]

$V_{demanded}$: volume of rainwater demanded during the simulation [L³]

In other words, the metric includes the portion of water consumed on days in which stored water was insufficient and counted against the reliability. Volumetric reliability is more significant for averaged precipitation data, as shown in the following section.

4.2.1.1 Average rainfall conditions

Analyses of the mass balance model are performed to test the influence of parameters under average rainfall conditions. Results are shown in Table 7 and Figure 18 and Figure 19 for the first and second set of scenarios.

Table 7 – Results for typical RWCS and parameter scenarios, average rainfall conditions

Scenario	Parameter Variation	Reliability (%)	Volumetric reliability (%)
1 (Base)	-	77%	93%
2	Decrease to 3 water users	100%	100%
3	Decrease to 8 L/day demand per water user	100%	100%
4	Decrease to 10 m ² effective roof area size	39%	73%
5	Decrease to 1,000 L storage tank size	71%	92%
6	Decrease to 40% gutter-downspout efficiency	17%	69%
7	Decrease to 5% tank size for initial storage volume	64%	90%
8	Increase to 12 water users	21%	69%
9	Increase to 16 L/day demand per water user	63%	84%
10	Increase to 25.6 m ² effective roof area size	100%	100%
11	Increase to 3,000 L storage tank size	82%	95%
12	Increase to 80% gutter-downspout efficiency	87%	97%
13	Increase to 100% tank size for initial storage volume	85%	96%

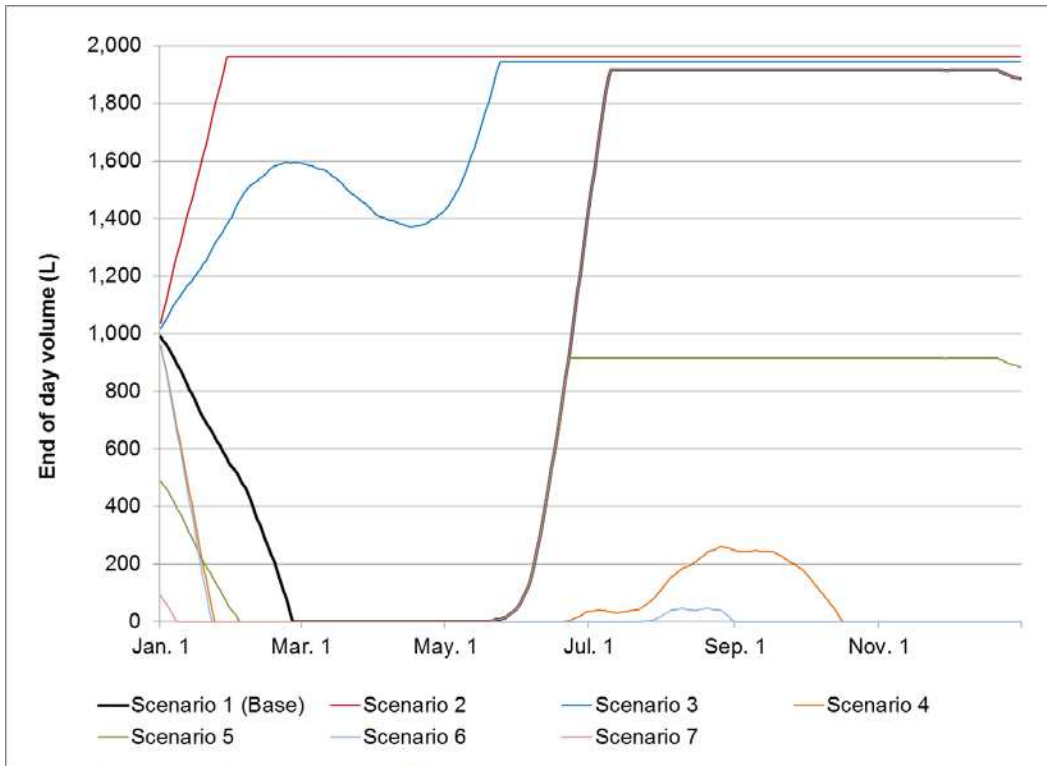


Figure 18 – Modeled storage volume for Scenarios 2 through 7, average rainfall conditions

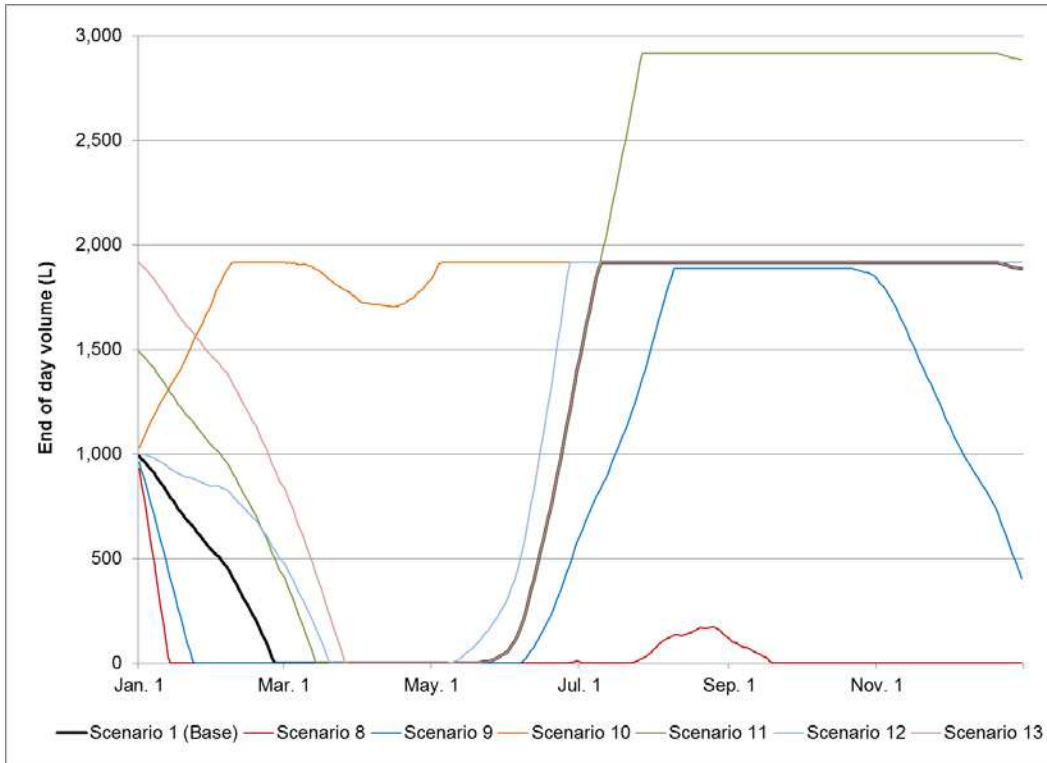


Figure 19 – Modeled storage volume for Scenarios 8 through 13, average rainfall conditions

As shown in the figures, the base scenario that is based on typical RWCS characteristics has a relatively low reliability of 77% for the average rainfall conditions. This is for several reasons: 1) days with a stored water supply between zero liters and the daily demand are neglected, 2) the school rainwater catchment system is neglected from statistics summary of household RWCS due to the large size, 3) community water practices, especially neighbor-neighbor water sharing, and 4) over-simplification of the rainwater catchment system network.

With regard to the former reason, days in the base simulation with a stored supply between zero and 84 liters are neglected as shown by the volumetric reliability of 93%. There are 83 days in this simulation which have a stored water supply between 50 and 84 liters, all of which are not included in the original reliability term and lead to a low reliability score of 77%. Therefore, the volumetric reliability metric is better suited for use with averaged precipitation data in which variance from day-to-day is small. In reality, the rainwater catchment systems are more reliable under average rainfall conditions due to assistance from large community rainwater catchments, in this case the school, community water practices, and site-specific catchment considerations.

Evident from the reliability estimates is that relatively small alterations to the rainwater catchment design have a large impact when designing for average rainfall conditions. For instance, an increase in the gutter-downspout efficiency from 70% to 80% results in a 10% increase in overall reliability to 87%. Certain parameters are more influential than others for this analysis, and the results indicate that the most influential variables are daily demand, roof area, and gutter-downspout system efficiency.

4.2.1.2 Severe drought conditions

Analyses of the mass balance model are also performed to test the influence of parameters under severe drought rainfall conditions. Results are shown in Table 8 and Figures 20 and 21 for the first and second set of simulations.

Table 8 – Results for typical RWCS and parameter scenarios, severe drought rainfall conditions

Scenario	Parameter Variation	Reliability (%)	Volumetric reliability (%)
1 (Base)	-	64%	67%
2	Decrease to 3 water users	90%	91%
3	Decrease to 8 L/day demand per water user	77%	79%
4	Decrease to 10 m ² effective roof area size	44%	51%
5	Decrease to 1,000 L storage tank size	59%	64%
6	Decrease to 40% gutter-downspout efficiency	43%	49%
7	Decrease to 5% tank size for initial storage volume	64%	67%
8	Increase to 12 water users	40%	49%
9	Increase to 16 L/day demand per water user	53%	58%
10	Increase to 25.6 m ² effective roof area size	74%	77%
11	Increase to 3,000 L storage tank size	68%	71%
12	Increase to 80% gutter-downspout efficiency	66%	70%
13	Increase to 100% tank size for initial storage volume	64%	67%

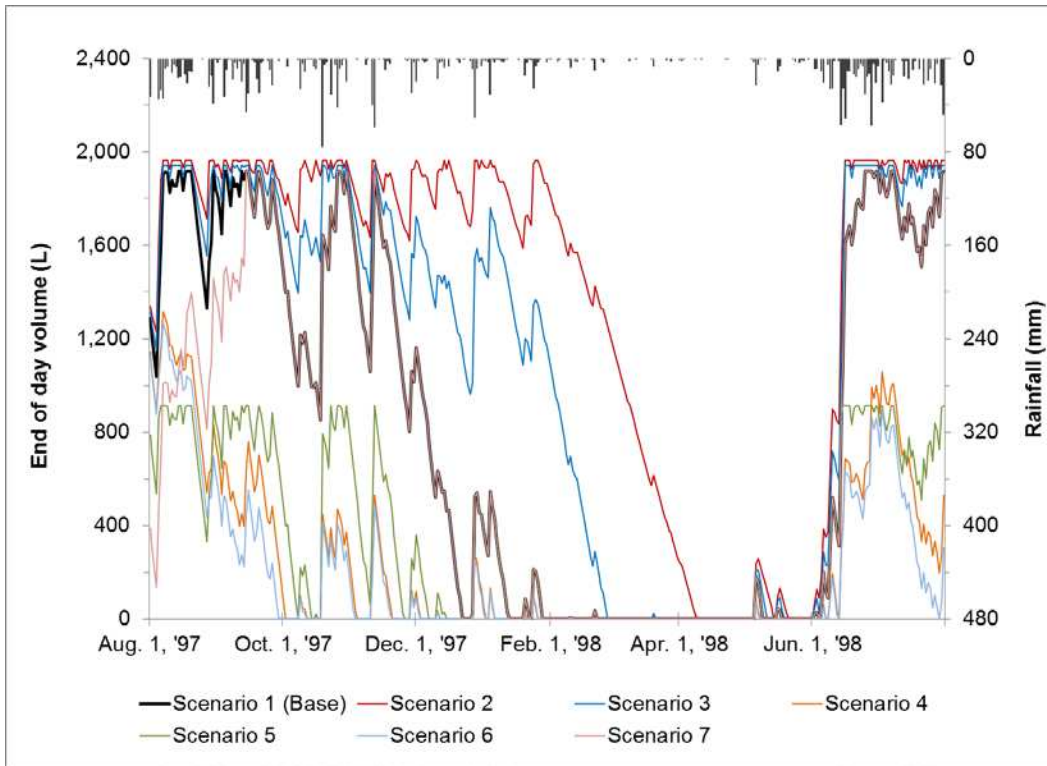


Figure 20 – Modeled storage volume for Scenarios 2 through 7, severe drought conditions

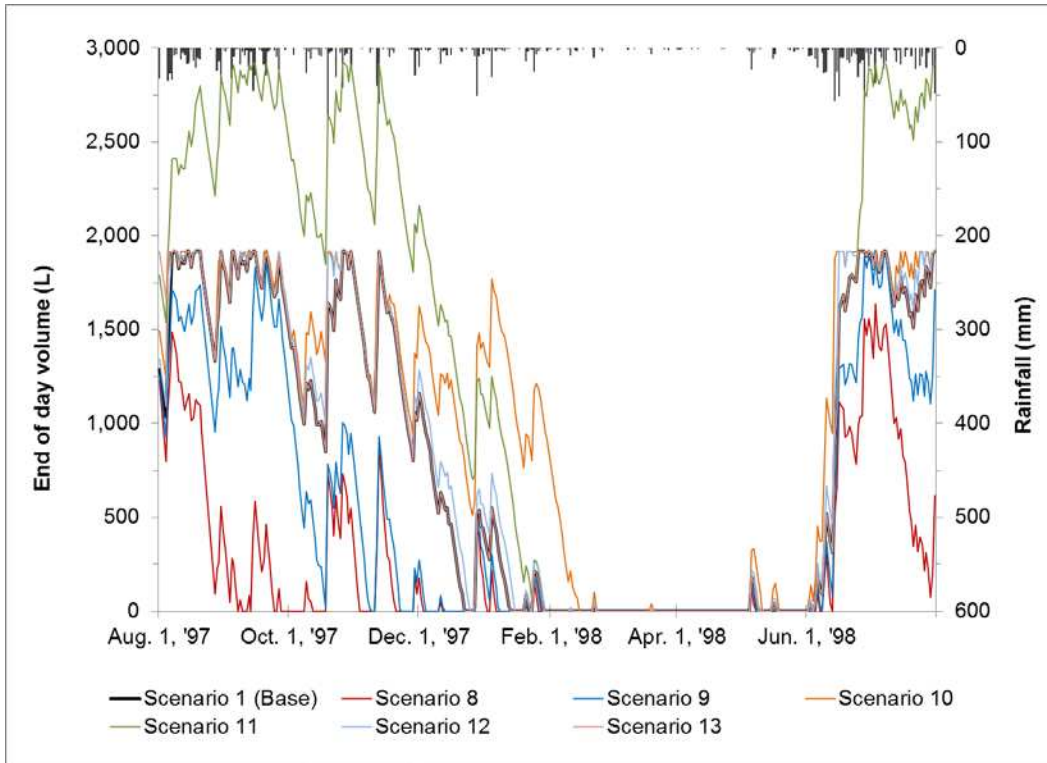


Figure 21 – Modeled storage volume for Scenarios 8 through 13, severe drought conditions

For all simulated scenarios, a steep decrease in stored water begins in November 1997 which is followed by a period of severe drought that begins between December 1st, 1997 and February 1st, 1998 for most scenarios. The drought remains severe for most scenarios until June and all experience at least 38 days of insufficient water supply during this period. By comparison to the results from the average rainfall conditions, the base scenario has a lower overall reliability under severe drought conditions by approximately 15%. Additionally, there is a smaller difference between the metrics of reliability and volumetric reliability for the severe drought conditions. This is because there are 131 days in this simulation which have a stored water supply below the daily demand of 84 liters, and 102 of these days have a water supply below 10 liters. Due to similar results for actual annual precipitation data, it appears that both reliability based on percentage of time met and percentage of supply met are appropriate for real, continuous precipitation data.

Results also show that the same alterations to the rainwater catchment design have a smaller impact to the overall reliability. For instance, an increase in the gutter-downspout efficiency to 80% results in a 2% increase in overall reliability compared to the 10% increase found using the average rainfall conditions. Also by comparison, the results from the average rainfall conditions show more or less whether the RWCS design under each scenario is reliable or unreliable overall. Thus, for instances of new construction in which bare minimum design parameters must be met due to limited funds, materials or time, planning with regard to the average rainfall conditions would be advantageous.

Although none of the drought scenarios provided sufficient water during the drought, some modifications improved reliability better than others, most notably the daily demand (number of users, demand per person), effective roof catchment area, and gutter-downspout

efficiency. This confirms the same findings from the average rainfall conditions. Demand is the greatest influence due to the magnitude of the changes for Scenario 2 and Scenario 8 which showed a decrease in demand by 71.5% and an increase in demand by 71.5%. Results for Scenario 2 and Scenario 8 were such that there were 93 more days of sufficient water supply and 87 fewer days of sufficiently water supply, respectively under severe drought conditions.

Interestingly, the influence of effective rainwater catchment area, as shown by Scenario 4 and 10, appears to impact the overall reliability much more than storage tank size, as shown by Scenario 5 and 11. Scenario 4 reduced the catchment size by approximately 40% and the result was an additional 74 days without sufficient water supply under severe drought conditions. Scenario 5, which reduced the storage tank size by 50% resulted in only an additional 22 days without sufficient water supply. Thus, if expansion of an existing RWCS is desired, the best measure to make is an increase in the effective catchment area.

One additional parameter that has a significant impact is gutter-downspout system efficiency, shown by Scenario 6 and Scenario 12. The reduction to 'poor' conditions which assume 60% of the roof run-off is lost from the gutter-downspout systems, heavily influences the reliability and adds 78 days of insufficient water supply to the base scenario under severe drought conditions. However, a 10% increase in efficiency shown by Scenario 12 only slightly improves the reliability by 7 days additional days with sufficient water. This suggests that it is best to fix highly damaged RWCS to a 'good' condition rather than make minor improvements to a RWCS already determined to be in 'good' condition.

Finally, for this simulation two variables appear to have a minor effect on the reliability of the base RWCS scenario: initial storage volume and storage tank size. The initial storage volume had a minimal effect because the simulation began several months before a decline in

precipitation occurred, and because it was started during a period of wet weather. More surprisingly, storage tank size had a minimal impact on the reliability, evident by a maximum change of 19 days as a result of a 50% change in the tank size. For a RWCS of this nature, an investment in additional storage is likely a minimally effective modification.

4.2.2 Evaluation of Ifalik RWCS community water supply

The daily water storage was also estimated using the mass balance model for each of the one hundred rainwater catchment systems. For this, each catchment is simulated individually with respect to the dimensions measured in the field survey, the qualitatively assessed gutter-downspout efficiency, and the number of people at the compound. Then, the performance of each specific RWCS is evaluated using the mass balance model for the severe drought conditions and future rainfall conditions.

4.2.2.1 Severe drought conditions – parameter assessment

The reliability of each RWCS is determined through the mass balance model and shown in Figure 22. As shown, a small fraction of the RWCSs on the island had sufficient water during the drought.

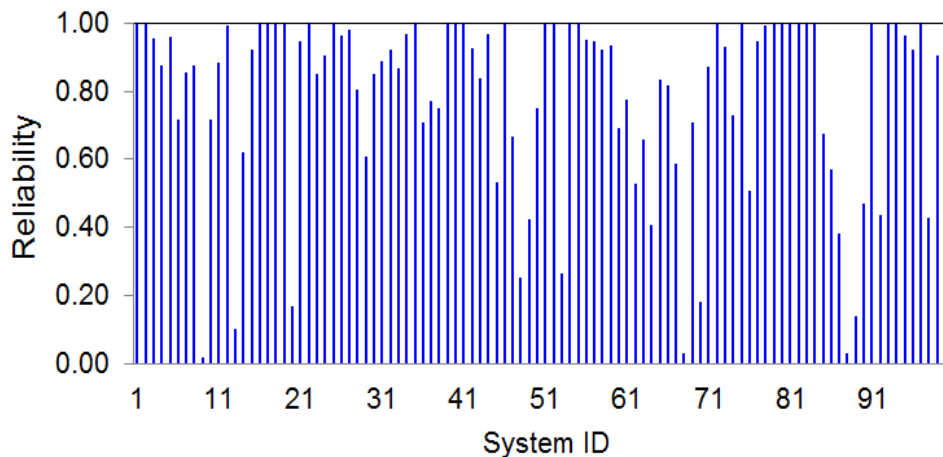


Figure 22 – Reliability of each RWCS on Ifalik for severe drought conditions

To determine which system parameters should be modified to increase future water storage, parameters were plotted against reliability for each RWCS (Figure 23). The primary parameters of interest are analyzed, including tank size, roof area, gutter-downspout efficiency, and number of residents.

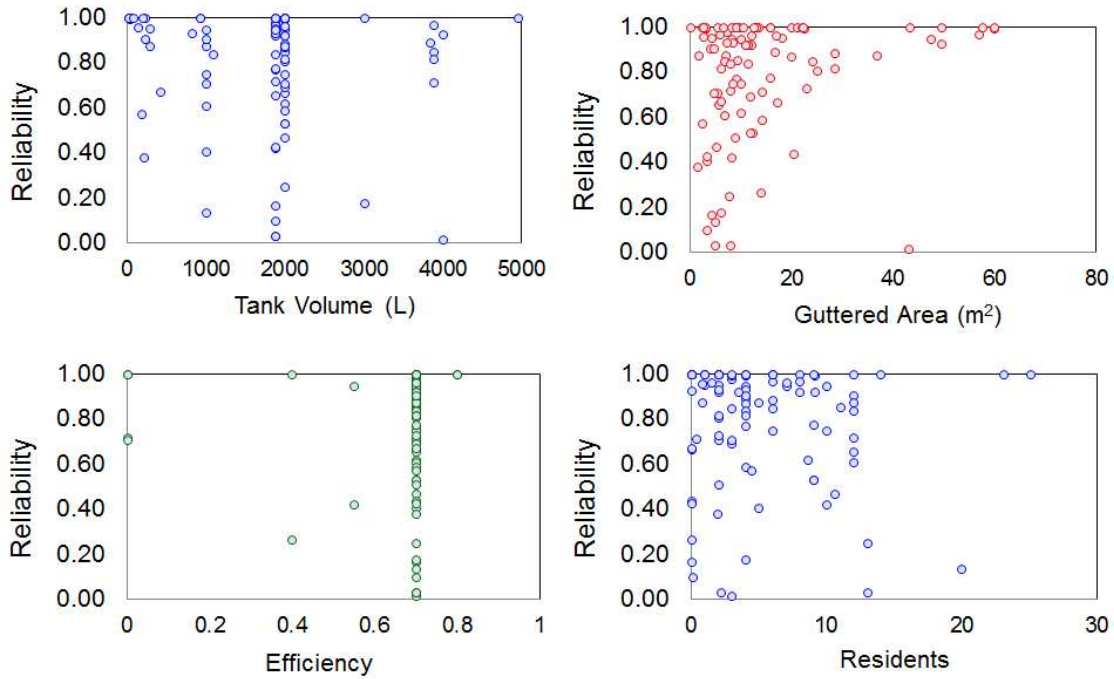


Figure 23 – Plots of reliability for parameter values: tank size, roof area, efficiency, and number of residents

As seen in the figure, there is no identifiable trend between reliability and tank volume or gutter-downspout efficiency, and there is a minor correlation between number of residents and reliability. Efficiency shows no identifiable trend due to the large percentage of catchments that have an estimated efficiency of 70%. Finally, a strong, direct relationship exists between effective roof area and reliability; therefore increasing the effective roof area is the most effective measure to increase reliability. This confirms the positive correlation found in the previous section.

4.2.2.2 Severe drought conditions – community water assessment

Although fewer simplifications are required for this method due to inclusion of actual effective roof area, storage tank size, efficiency, and water users, a few variables will still affect the volume of water captured and stored for a RWCS, including the fraction of tank filled at the beginning of the simulation and the daily per capita demand. To test the influence of these parameters, four scenarios are run that deviated from the base scenario of 50% initial volume and 12 liters per capita per day. The scenarios model an initial tank volume ranging from 30% to 70%, and a daily per capita demand ranging between 8 liters per capita per day and 16 liters per capita per day. For simulation, the total stored water for the community is estimated by adding the volumes at each RWCS. Results are shown in Figure 24 and the base scenario is shown in black. As seen in the figure, there is a significant range of estimated stored volumes and this represents the level of uncertainty due to uncertainty in the parameters. Also shown by the figure is that the stored volumes do not reach zero, which agrees with the household surveys that indicated the community water has not reached zero in the past.

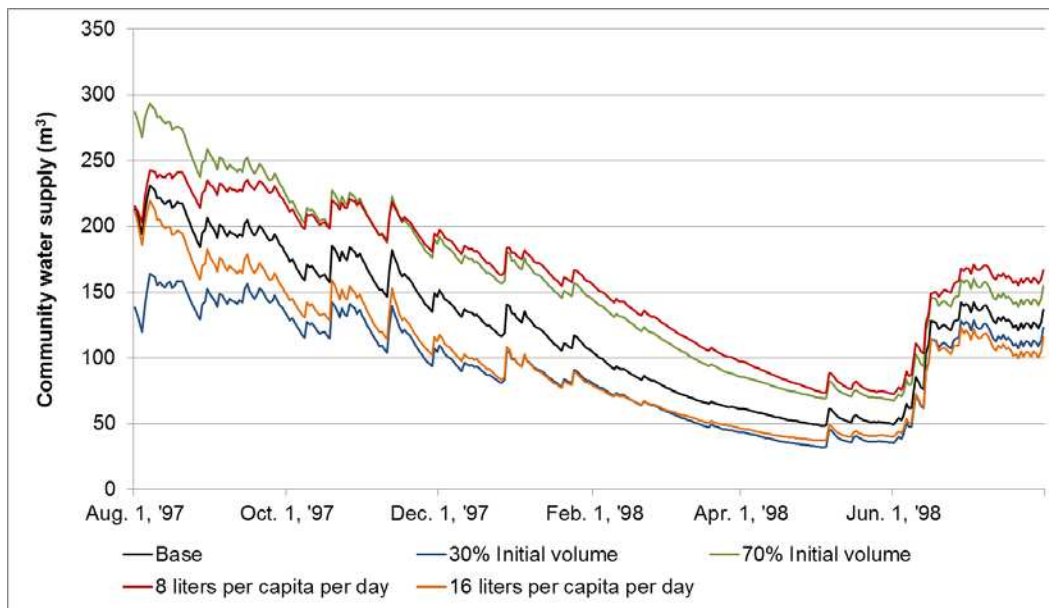


Figure 24 – Ifalik community water supply under severe drought conditions, actual roof area

To further evaluate the effect of roof area on RWCS reliability, additional simulations are performed using the potential roof area using the same scenarios from the actual roof area analysis for severe drought conditions. Results from the potential effective roof area analysis are shown in Figure 25 and a statistical summary comparison between the results is shown in Table 9.

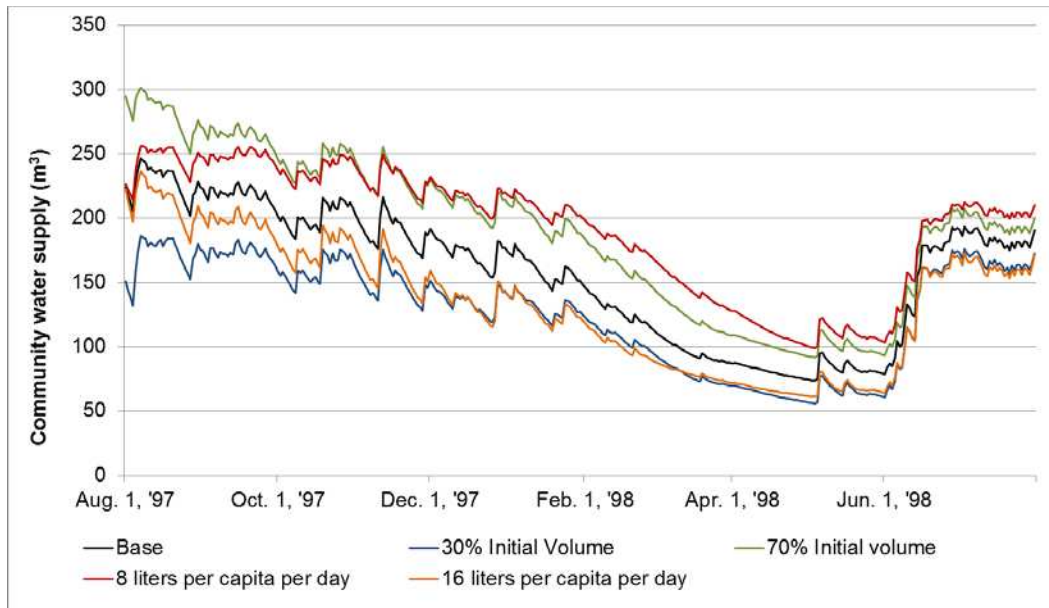


Figure 25 – Ifalik community water supply under severe drought conditions, potential roof area

Table 9 – Summary statistics comparing actual and potential effective roof area use during 1997-1998 drought

Effective roof area	Daily community water supply, base scenario (m ³)		
	Average	Maximum	Minimum
Actual	123	231	48
Potential	158	246	74

Findings show that increasing the community rainwater catchments to the full potential roof area increases the community water supply during severe drought conditions. For instance, the supply modeled for the base scenario decreases to a minimum of 48 cubic meters when using catchments with existing gutter reaches, and this increases to 74 cubic meters when potential area is used. In addition, the storage volume prior to February 1st, 1998 is declining at a much

smaller rate in the potential roof area simulations compared to actual roof simulations. The results suggest that using the full potential area of the roof is beneficial in extending water supply during severe droughts.

4.2.2.3 Future rainfall condition assessment

The water balance model also was applied to future climate conditions using rainfall output from General Circulation Models. As previously discussed, the GCMs that best correlate to historical rainfall data for Yap State are GISS-E2-H for RCP 2.6 and GISS-E2-H-p2 for RCP 8.5 (Wallace, Bailey, & Arabi, 2015) and since RCP 2.6 models the lowest atmospheric concentrations of greenhouse gases and RCP 8.5 models the highest, the models together provide a good range of climate scenarios. Varying scenarios that consider fluctuations in daily per capita demand are included since it is the strongest, influencing parameter that is not intrinsic to the rainwater catchment system design and conditions, as shown in Figure 25. The two GCM models consider the average daily demand of 12 liters per capita per day, and the bounding ranges of 8 liters per capita per day and 16 liters per capita per day. The simulation is run for the time period 2010-2040 for each of the scenarios, since the stability of atoll formations and their resources is limited and long-term scenarios are minimally informative. Results from the simulations are shown in Figure 26 and Figure 27 for the actual and potential effective roof area, and a summary of statistics is shown in Table 10.

Table 10 – Summary statistics comparing actual and potential effective roof area use during future climate conditions

Effective roof area	Daily stored water supply (m ³)		
	Average	Maximum	Minimum
RCP 2.6, Actual	76	186	52
RCP 2.6, Potential	140	187	80
RCP 8.5, Actual	78	203	52
RCP 8.5, Potential	143	222	96

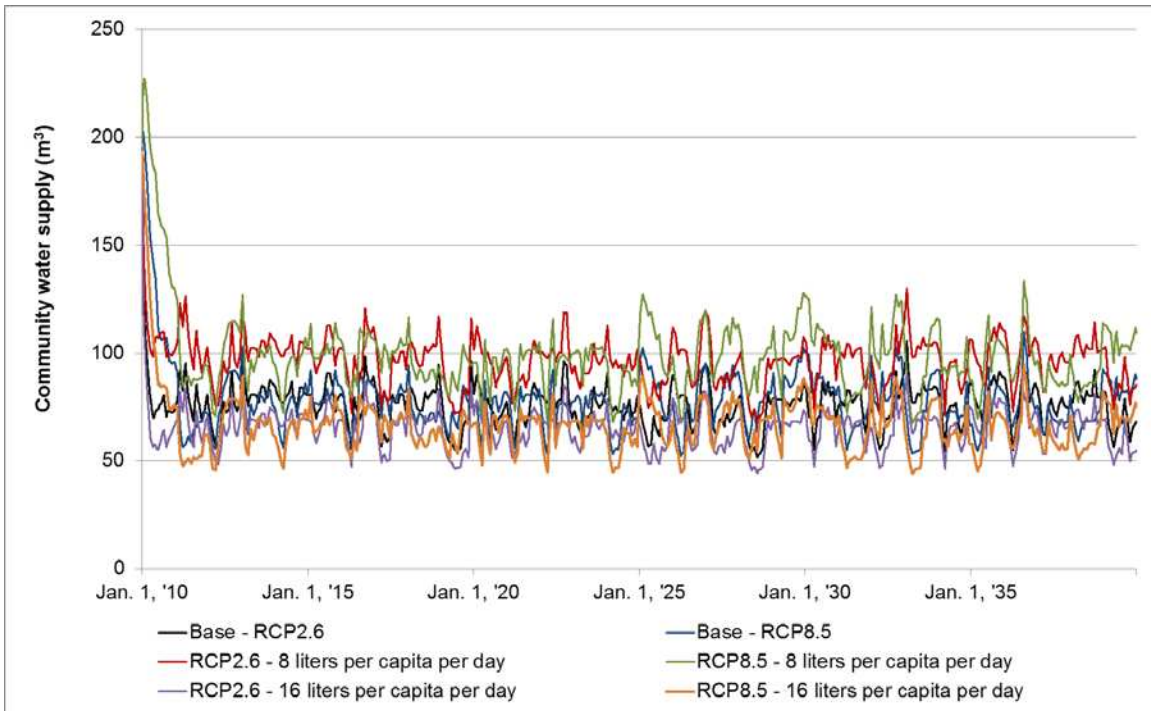


Figure 26 – Ifalik community water supply under future climate conditions, actual roof area

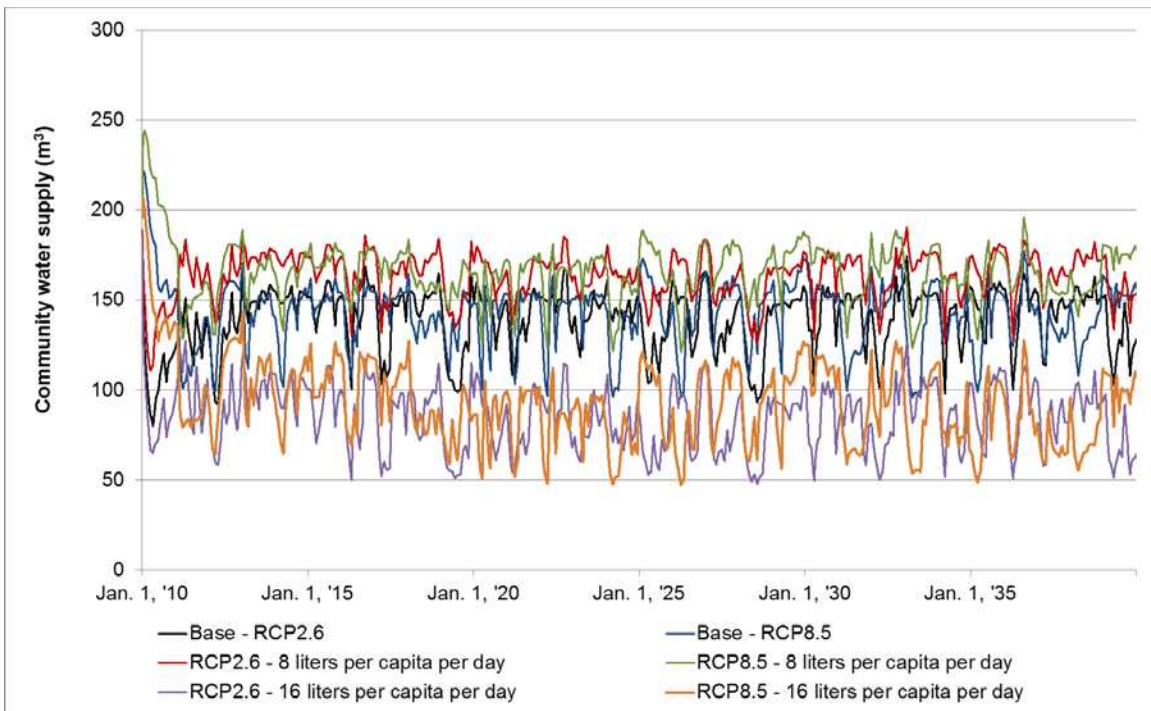


Figure 27 – Ifalik community water supply under future climate conditions, potential roof area

As seen in the figures, the total community water never depletes fully during the 30-year period, and using potential areas greatly increases the stored water volume over time. Comparing the results between future rainfall conditions and the severe drought conditions, it appears that the minimum obtained by using severe drought conditions is lower and thus, drought conditions are recommended for a conservative rainwater catchment designs.

4.3 Design curves for rainwater catchment system design

4.3.1 Overview of design curves

The water balance model of Equation 4 also can be used to develop combinations of roof area and tank size that meet a certain level of reliability, with reliability defined as the portion of time that the system meets the water demand based on rainfall patterns. The result is a plot referred to here as a design curve, and Figure 28 shows an example set.

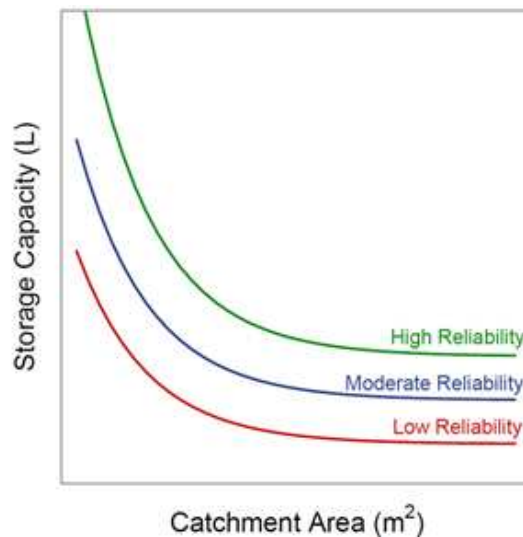


Figure 28 – Example design curve for rainwater catchment systems

The curves can be used to find the set of catchment area and storage tank size that will meet a certain level of reliability. For example, the capacity of an available storage tank is measured, and the curve can be used to determine which roof area is required to meet that degree

of reliability. In this thesis, design curves are created using the severe drought rainfall data and the GCM rainfall data for the years 2010-2040. The design curves are created using the following method:

1. Select a rate of reliability (e.g. 95%).
2. Select a roof catchment area.
3. Run the water balance model for the selected period of rainfall records and find the storage tank size that will provide the desired rate of reliability.
4. Repeat Steps 2 and 3 until a sufficient number of area-capacity pairs are assessed and a curve can be drawn through the data points.

4.3.2 Design curves for severe drought conditions

The design curves using the 1997-1998 rainfall data are shown in Figure 29. A different set of design curves is presented for differing number of residents using water from the RWCS. These design curves can be used to determine required roof catchment area for a given tank volume, or vice versa, to achieve a certain level of reliability. Reliability rates of 80%, 90%, 95%, and 99% are presented. Notice that larger roof areas and tank volumes are required to achieve a higher rate of reliability, and also that larger areas and volumes are required for households with a higher number of residents.

4.3.3 Design curves for future climate conditions

Design curves also were created using downscaled rainfall data from the RCP 2.6 GISS-E2-H GCM (Figure 30) and the RCP 8.5 GISS-E2-H-p2 (Figure 31). These curves are much different than the curves created using the severe drought conditions, due to the fact that the GCMs have difficulty simulating major drought periods.

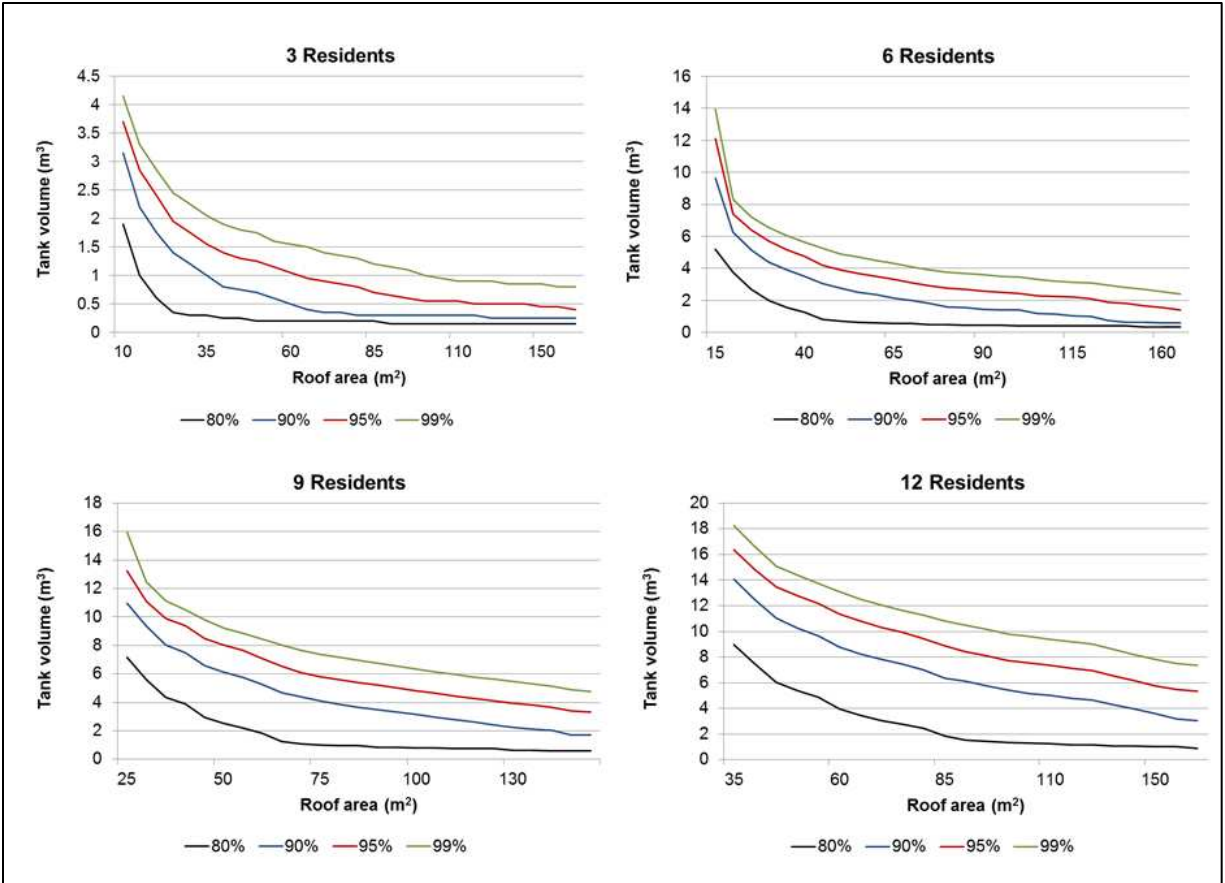


Figure 29 – Design curves for the 1997-1998 severe drought, varying residents per RWCS

The IPCC advocates the use of GCMs primarily for long-term and large-scale applications, since short-term or local events are softened by their formulation. Results from the GCM design curves and severe drought curves confirm the earlier finding that severe drought conditions provide a more conservative design. For example, the design curves for the 95% reliability rate for a 9 resident user catchment is quite different from the severe drought conditions to the GCM conditions. For an existing catchment area of 50 m², a 4 m³ (4,000 L) storage tank and a 3.8 m³ tank are required under the RCP 2.6 GISS-E2-H and RCP 8.5 GISS-E2-H-p2 future rainfall conditions. Design curves using the severe drought conditions, however, indicate that for this same design goal, two times that volume is required by a 8 m³ tank. Thus, isolated and severe drought events are better use for conservative planning measures.

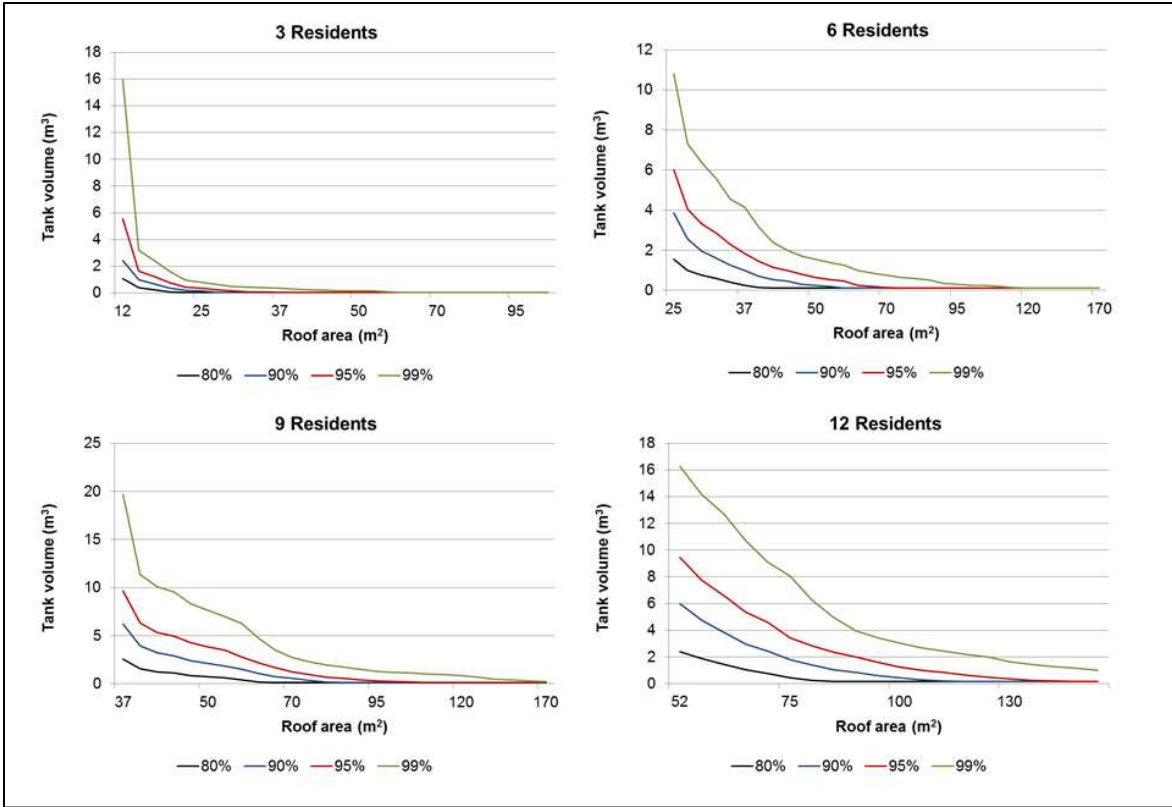


Figure 30 – Design curves for the 2010-2040 period using GCM GISS-E2-H for RCP 2.6

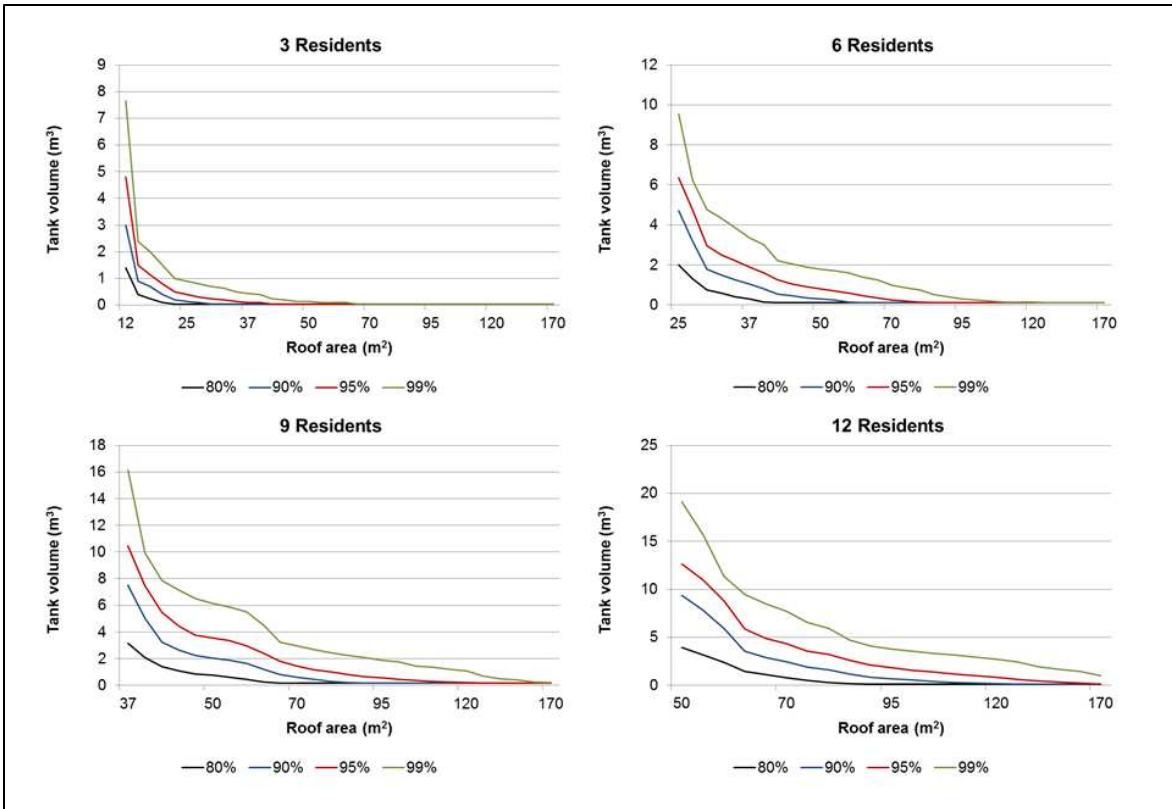


Figure 31 – Design curves for the 2010-2040 period using GCM GISS-E2-H-p2 for RCP 8.5

4.4 Proposed RWCS network for Eauripik, Falalop, and Satawal

Using the information found on Ifalik, a network of rainwater catchment systems is proposed for the three remaining islands of study. The main objective of this analysis is to determine how many rainwater catchments are required on each island for a certain reliability and what corresponding effective roof areas are required. This evaluation assumes that there is no existing infrastructure, since no information is available for these islands.

To create the proposed network, the overall community RWCS is pared down to a single RWCS which is selected for the network based on the reliability. Two reliability curves are used for selection based on two rainfall conditions, one simulating average annual precipitation and the other severe drought. For reliability in this analysis, effective roof area is the dependent variable since it is a highly influential variable and also provides beneficial tool for water users. Three scenarios are modeled for both sets of conditions to simulate water storage for the range of typical water users per catchment on Ifalik: 3 users, 7 users, and 12 users per catchment. All other parameters are held constant are the average values found on Ifalik Island. For storage volume, the capacity will be 2,000 liters, since the 2,000 liter HDPE storage tanks are popular among the island residents and the materials are available to them. Additional assumptions are made on the basis of the Ifalik survey, including: a typical water demand of 12 liters per capita per day, average gutter-downspout conditions with 70% efficiency, and 50% initially filled. The resulting reliability curves are shown in Figure 32 and Figure 33.

As shown in Figure 32, water reliability dramatically increases for the household water supply at an effective roof area size of 9 m². Most household roof areas are larger, and further, the mean average catchment area on Ifalik was 16 m² which corresponds to a roughly 80%

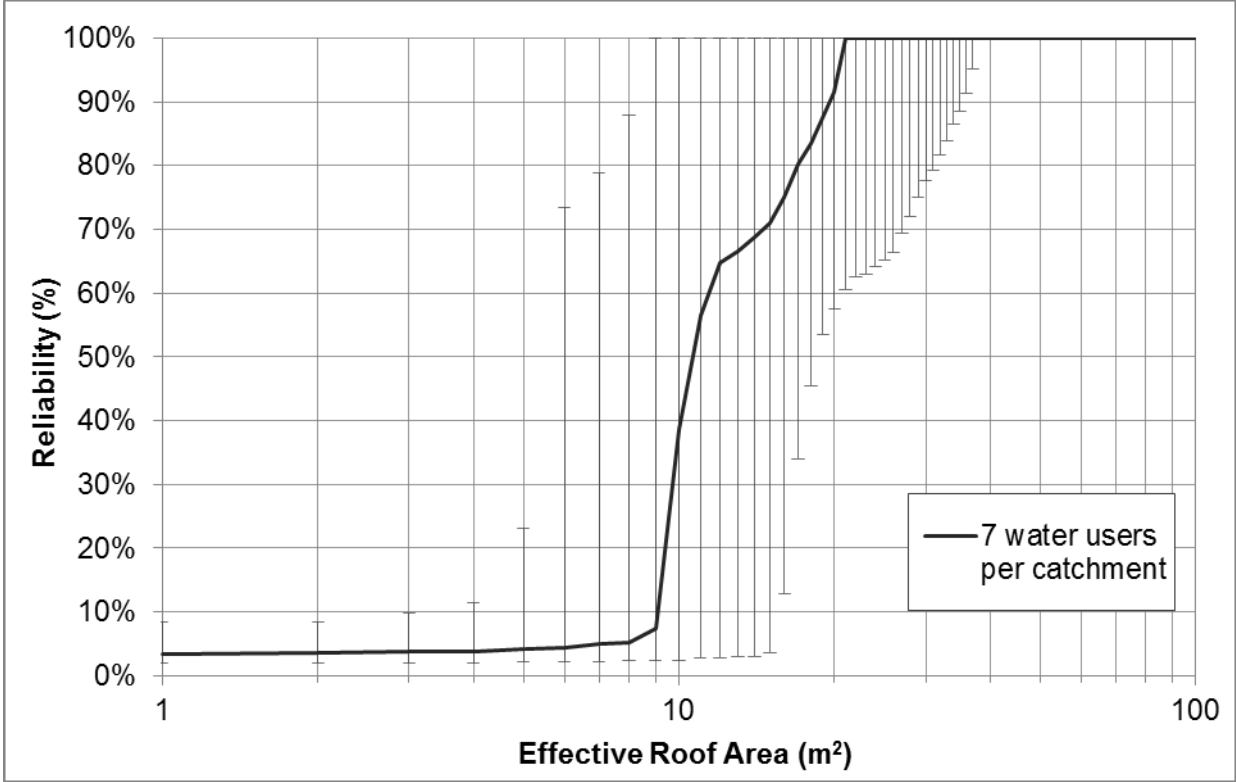


Figure 32 – Reliability curve for average rainfall conditions, 3 – 12 water users per catchment

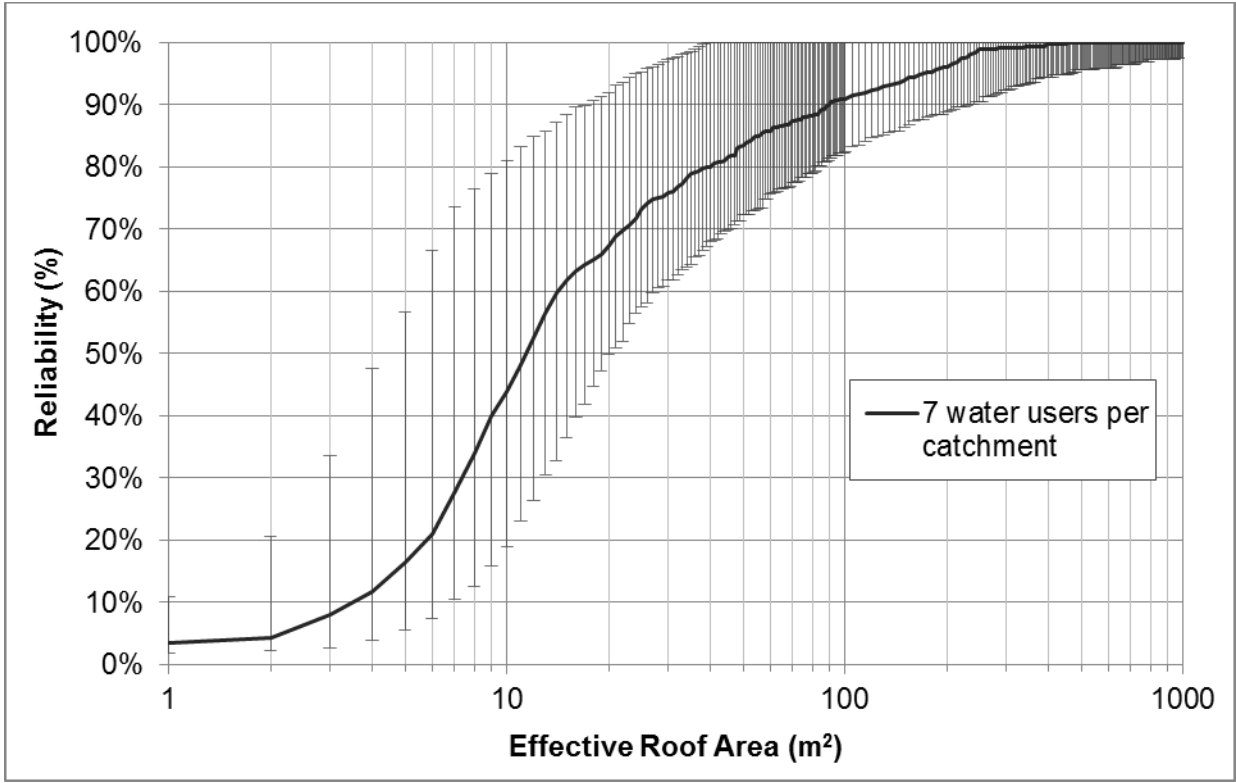


Figure 33 – Reliability curve for severe drought conditions, 3 – 12 water users per catchment

reliability in water supply for average rainfall conditions. This is especially good considering the supplemental community water supplies and opening sharing between neighbors. Water supply reliability during a severe drought requires a much larger effective roof area, as shown in Figure 33. By comparison, to reach 80% reliability for a 7 water user household, the existing 16 m² rainwater catchment determined by average rainfall conditions needs to be expanded to 40 m², which requires significant amounts of space, materials, and money.

Finally, using the catchment sizes that correspond to 80%, 90%, 95%, and 99% reliability, the size and number for catchments for each island is determined. Using the number of users for each scenario, the number of catchments is found based on the population of each island. According to the 2010 FSM census, the population of Eauripik, Ifalik, and Satawal islands are 114, 578, and 501, respectively. The population of Falalop is given as part of the overall Ulithi population, however other sources indicate the population is close to 475. The effective roof area for each reliability goal and rainfall conditions, taken from Figure 32 and Figure 33, is plotted against the island-specific required catchment number to give potential catchment networks for each island. The 99% reliability curves for the drought simulations are not pictured as most catchment areas for this goal did not converge to 99% by 1,000 m².

As shown in the design curves, the severe drought condition requires several times more effective catchment area compared to the average rainfall conditions, approximately 15 times as many square meters. Also, the average rainfall plots demonstrate how minor increases to the roof catchment area result in a significantly higher reliability. With this tool, water managers can access how their community rainwater network is performing compared to a reliability goal. For instance, achieving a 95% reliability for the severe drought conditions would be costly and required substantial quantities of roofing material. However, achieving an 80% for this extreme

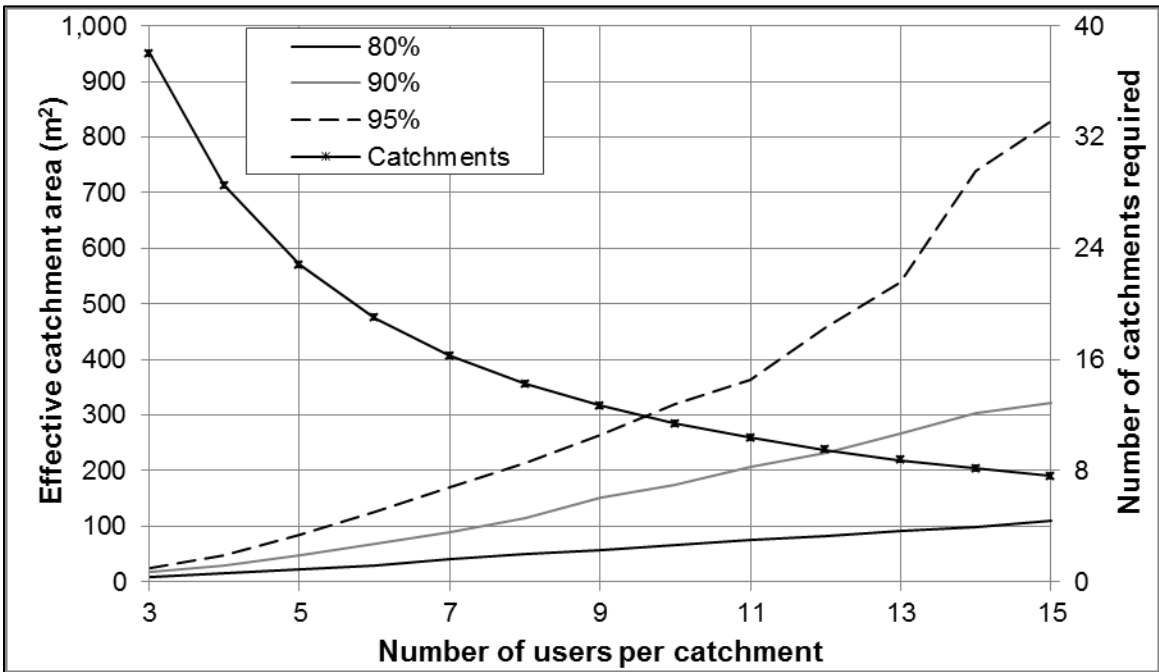
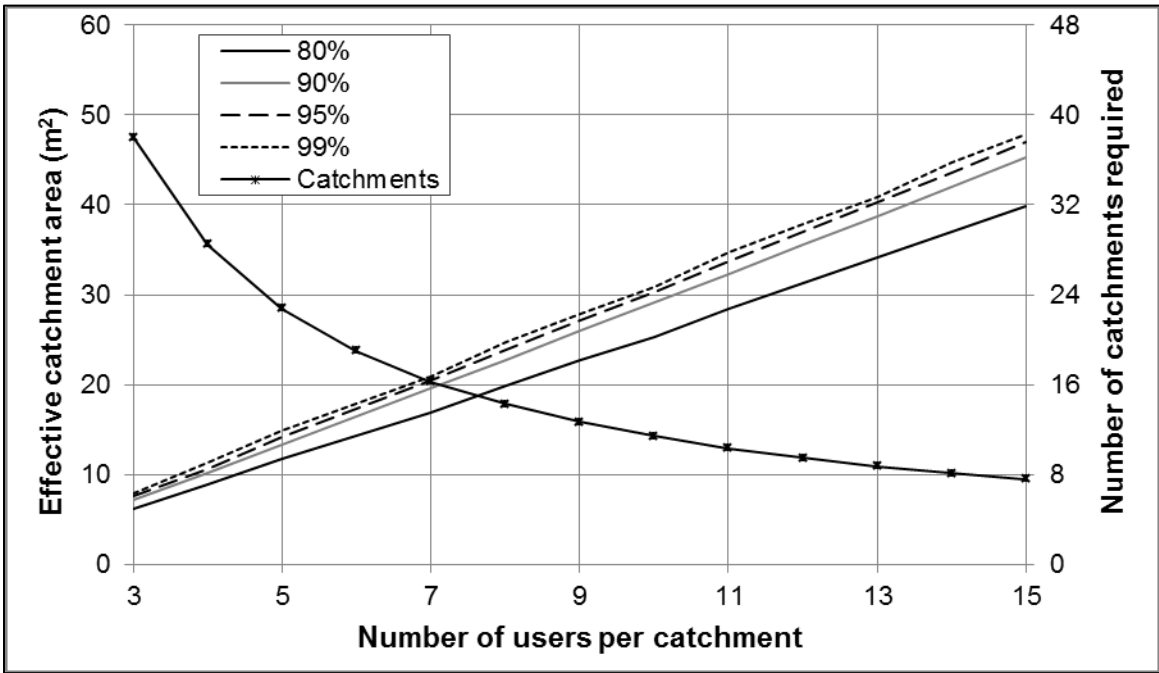


Figure 34 – Design curves for a network of rainwater catchment systems on Eauripik under average rainfall conditions (top) and severe drought conditions (bottom)

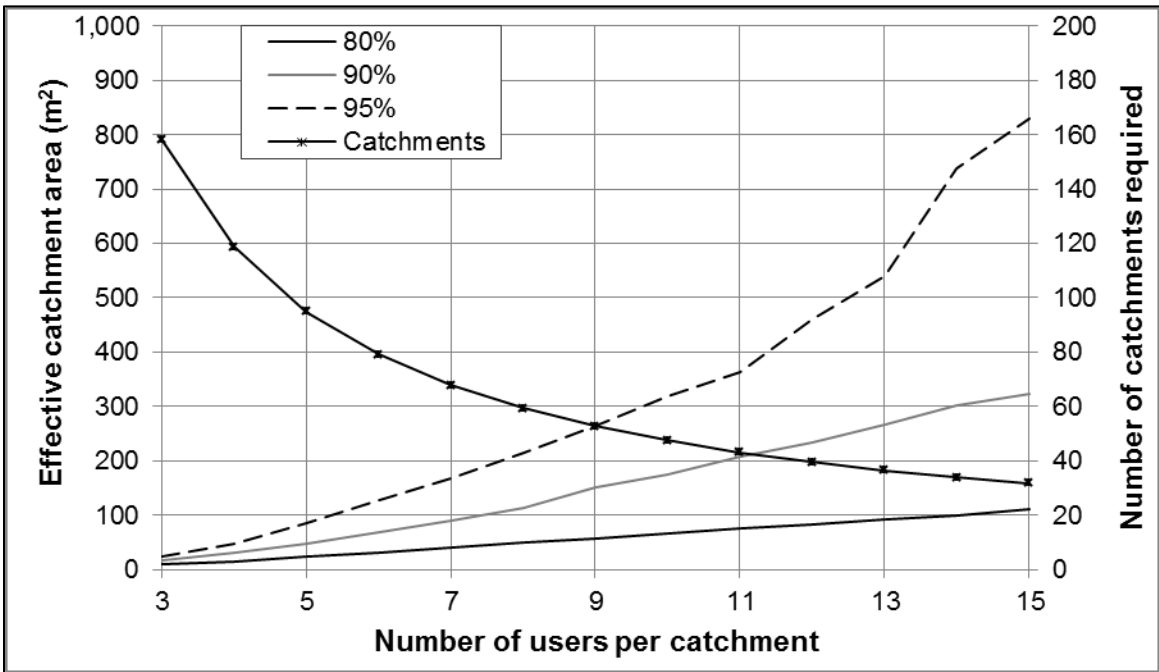
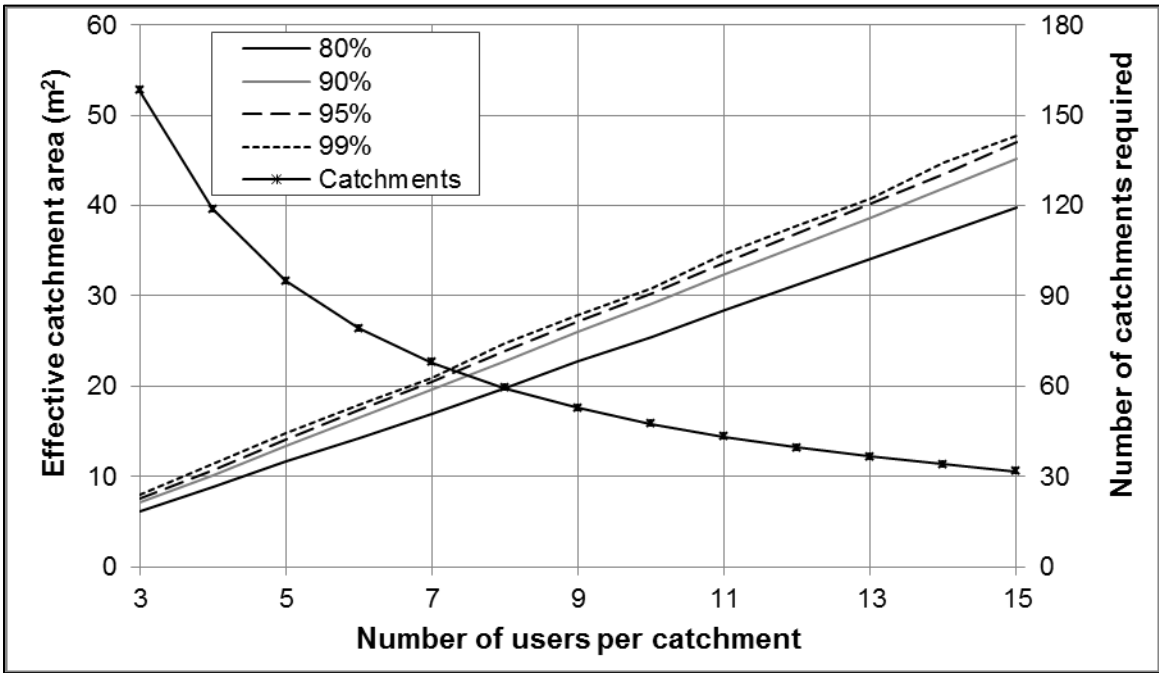


Figure 35 – Design curves for a network of rainwater catchment systems on Falalop under average rainfall conditions (top) and severe drought conditions (bottom)

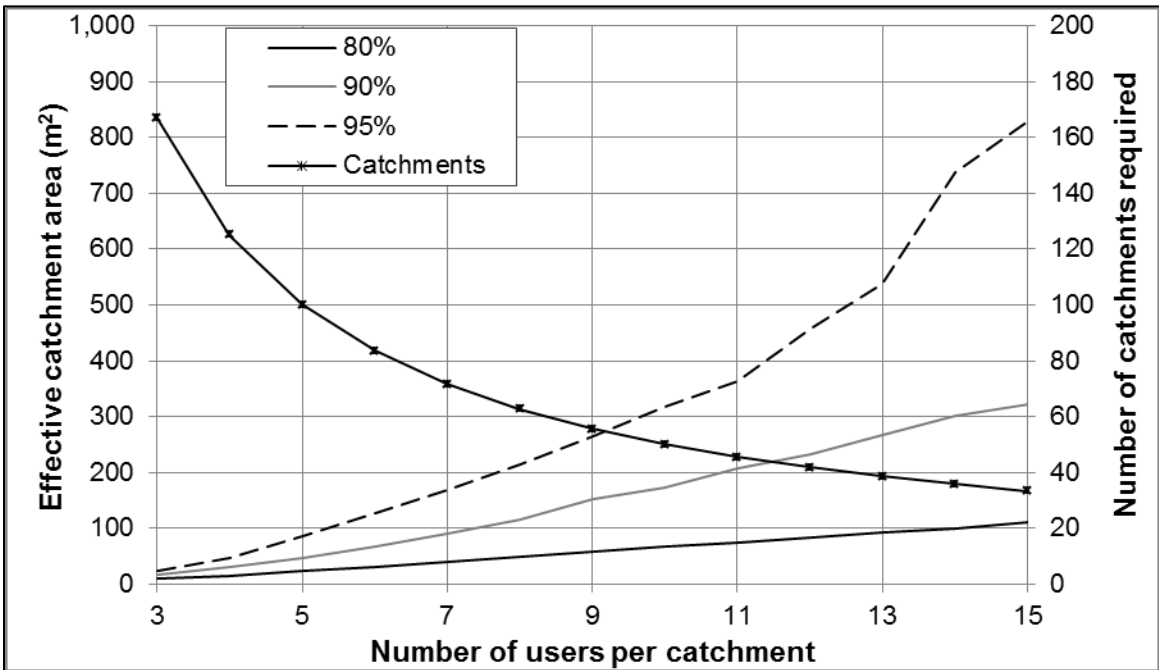
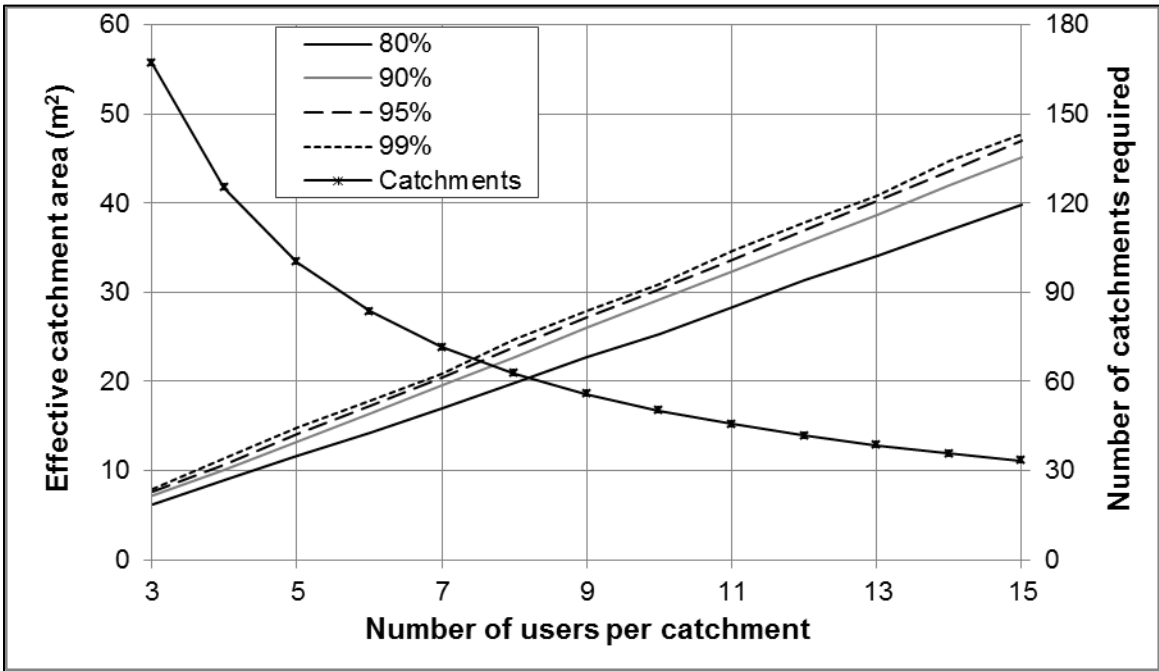


Figure 36 – Design curves for a network of rainwater catchment systems on Satawal under average rainfall conditions (top) and severe drought conditions (bottom)

rainfall condition is far more reasonable and practical for real implementation. This tool aids in making those planning decisions and will help water managers justify their plans to their island neighbors, funders, and contractors.

Design curves, shown in Figures 34, 35, and 36, are generated for each of the three remaining islands, Eauripik Island, Falalop Island, and Satawal Island. The curves rely on two important pieces of information for water managers: reliability goal and number of users per catchment. Based on selected reliability goal and the approximate number of water users per catchment, a water manager on these islands can determine the number of catchments required and the effective roof area of the catchment. As shown in Figures 34, 35, and 36, the drought scenario provides a more conservative rainwater catchment system network that requires a larger catchment area. It should be noted that this is an oversimplification, however, results are valuable provided the water manager is able to approximate the number of water users per catchment and the average catchment size of the existing network.

5. THREE-DIMENSIONAL GROUNDWATER LENS DYNAMICS

5.1 Introduction

This section of the thesis utilizes three-dimensional (3-D) modeling to analyze transient groundwater lens dynamics for the four atolls of study in Yap State. The freshwater lens is the body of fresh groundwater that floats atop the underlying seawater within the Holocene aquifer. Rainfall conditions modeled are steady rainfall conditions at downscaled, average annual rainfall rates, and future rainfall rates obtained from GCM data. Results will be shown in terms of the thickness of the freshwater lens under the center of each island.

5.2 Previous numerical modeling work

For small, coral atoll islands, previous studies have primarily focused on using numerical modeling to estimate groundwater lens thickness as well as finding the maximum sustainable yield for pumping. Perhaps one of the first examples of numerical modeling for groundwater lens dynamics in coral atoll islands was in 1974 by Ronald K. Lam who used the finite difference method to estimate permeability from tidal data (Lam, 1974). Other studies used the Ghyben-Herzberg relationship for finite difference, numerical modeling to find the thickness of the freshwater lens (Chidley & Lloyd, 1977). This relationship assumes an abrupt transition occurs between the freshwater and saltwater, however, it is known that a broad transition zone exists instead. In 1984, a two-dimensional, finite element U.S. Geological Survey code called SUTRA, was developed to simulate saturated-unsaturated, density dependent groundwater flow. This program is still one of the preferred codes that models density dependent groundwater flow, and several studies have considered 2-D SUTRA models for groundwater dynamics in coral atoll

islands (Underwood, Peterson, & Voss, 1992) (Peterson & Gingerich, 1995) (Bailey, Jenson, & Olsen, 2009) (Bailey, Jenson, & Taborosi, 2013) (Bailey, Khalil, & Chatikavanij, 2014).

Three-dimensional modeling for coral atolls started in 2003 with a study that used TOUGH2 hydrology models to determine the thickness of the freshwater lens and the effects of different model parameters (Lee, 2003). This study also found that two flow components exist in the groundwater system: vertical movements driven by tidal fluctuations that occur over small length and time scales, and flow governed by long-term recharge patterns. Since then, several modeling studies have been conducted to analyze the effects of sea-level rise and overwash on groundwater lenses using SUTRA (Terry & Chui, 2012) (Chui & Terry, Modeling Fresh Water Lens Damage and Recovery on Atolls After Storm-Wave Washover, 2012) (Chui & Terry, 2013) (Bailey & Jenson, 2014) (Mahmoodzadeh, et al., 2014). The studies by Chui & Terry focus on a “typical coral atoll islet in the tropical pacific” (Chui & Terry, 2012), whereas the study by Mahmoodzadeh et al. (2014) studies inundation of the groundwater lens on an arid island in the Persian Gulf, Iran. The SUTRA study conducted by Bailey & Jenson (2014) models groundwater lens dynamics on a hypothetical island in Yap, similar to test various island parameter effects on overwash. SEAWAT has been used less frequently to model freshwater lenses. One study used SEAWAT to model impacts of sea-level rise, rainfall conditions, and evapotranspiration on the freshwater lens of Grande Glorieuse Island in the Western Indian Ocean (Comte, et al., 2014). Another study used SEAWAT to model the effects of various climatic changes on the groundwater lens of Andros Island in the Bahamas (Holding & Allen, 2015). Previous studies have not used SEAWAT to model the effects of future rainfall conditions on the freshwater lenses of several islands in Yap State, Micronesia.

5.3 Freshwater lens dynamics

5.3.1 Model development

This thesis uses SEAWAT to model three-dimensional, variable-density, saturated groundwater flow for the islands studies. The U.S. Geological Survey developed the code for SEAWAT by coupling codes for MODFLOW and MT3DMS. The species considered for variable density flow was aqueous chloride, which is specified at concentrations for seawater and freshwater. Four islands are modeled in the outer-lying areas of Yap State, Micronesia: Eauripik, Falalop, Ifalik, and Satawal.

For the four islands of interest, a preliminary model was created to simulate steady, average rainfall conditions under average annual rainfall. To discretize the model, ArcGIS map software was implemented to create a shapefile outline of each island. Then, each shapefile was exported into ModelMuse, the USGS MODFLOW program, to aid in creating the grid space. The grid space for the larger islands was composed of 10-meter cells and 5-meter cells were used for smaller islands. Refer to Figure 37 for a visual representation of the Ifalik grid space and Table 11 for the grid cell size selected for each island. Each model used thirty layers of cells and layers were thinned near the surface to improve precision in the most active region. Cell thickness becomes coarser with depth, with the first layer a thickness of 0.25 meters and the bottom layer a thickness of 8 meters. The freshwater lenses for islands of this size are limited to the top 1 – 8 meters, therefore, a finer grid space in this section provides more accurate model results.

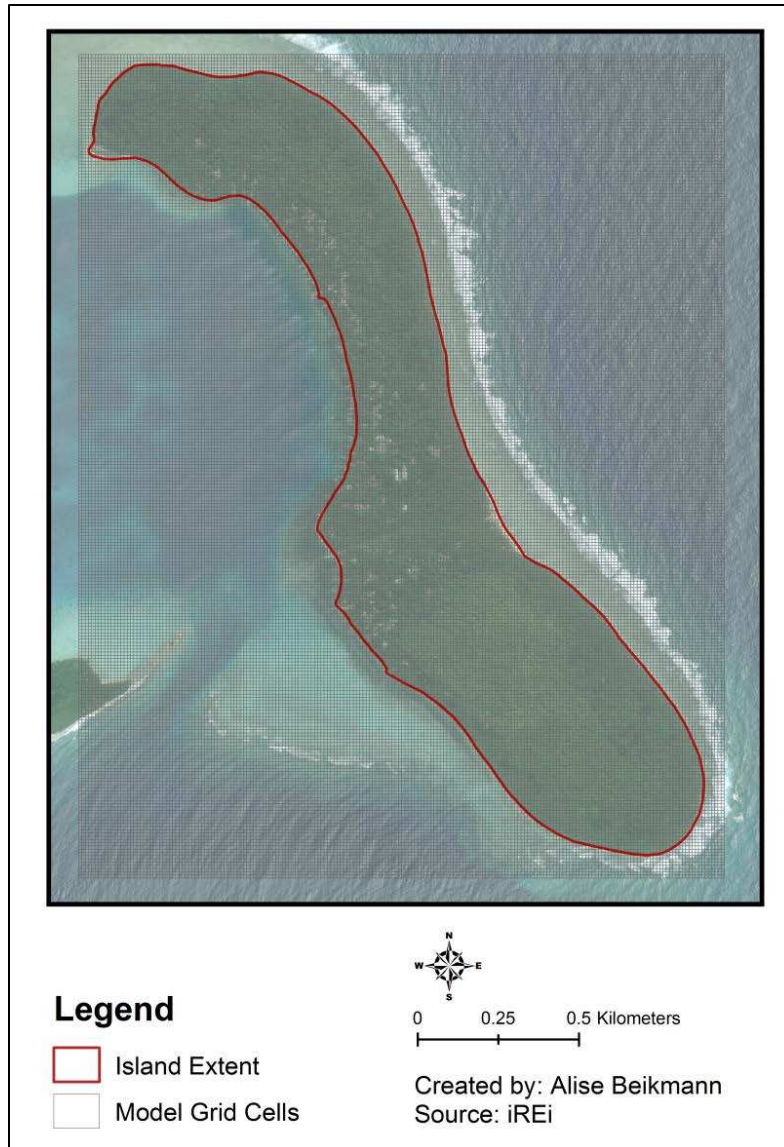


Figure 37 – Discretization for Ifalik SEAWAT Model (10 meter cell size)

Table 11 – Grid cell discretization

Island	Island Area (km ²)	Cell size (m)	Rows	Columns
Eauripik	0.10	5 x 5	62	142
Falalop	0.92	10 x 10	130	120
Ifalik	1.33	10 x 10	255	200
Satawal	1.29	10 x 10	150	190

Eauripik is a small island and the original 10 m x 10 m grid space was not discrete enough for SEAWAT to solve it. In this case, changing the cell size to 5 m x 5 m is sufficient.

The largest model is Ifalik with a grid space of 255 x 200 cells for a total of 51,000 cells. Simulations for Ifalik had run times often twice as long as the runs for the other islands.

For the steady, average rainfall simulations, 4-hour time steps were used since all islands were able to converge by the end of a 30-day period during a trial run. Daily time steps are not discrete enough to converge for every time step, and 1-hour time steps conflicted with Eauripik and Satawal, the former of which did not accumulate a lens and that latter which continued to oscillate without converging. Refer to Appendix B for plots of maximum thickness using these time step increments under steady, average rainfall conditions. Stress periods were daily and outputs were printed every 30 days to get monthly lens sizes.

The average annual rainfall conditions for Yap Island were simulated, which annually amounts to 3.07 meters of precipitation. All precipitation scenarios were recalculated to have average monthly rainfall distribute equally between the number of days. SEAWAT does not simulate daily rainfall data well for this application. Recharge to the groundwater lens for all scenarios is assumed to be 50% based on simplifications made in previous literature. Hydrogeologic properties, including hydraulic conductivity, porosity, specific storage, and specific yield were selected based on commonly observed values for coral atoll islands. The initial horizontal hydraulic conductivity is selected based on the results from Bailey et al. 2008 which found that windward islands may be approximated to 400 m day⁻¹ in the Holocene aquifer (Bailey, Jenson, & Olsen, 2009). Additionally, the results also found that the vertical hydraulic conductivity may be approximated to 20% of the horizontal hydraulic conductivity and the underlying Pleistocene aquifer may be estimated at 5,000 m day⁻¹ for the horizontal hydraulic conductivity and 1,000 m day⁻¹ for the vertical hydraulic conductivity. Porosity is 0.2 in the Holocene aquifer and 0.3 in the Pleistocene aquifer, consistent with values found in literature for

small, coral atolls. Based on the average range of 15 – 25 meters for the thickness of the Holocene sediments, a depth of 20 meters is selected to modeling the discontinuity of the geology. Parameters for the Holocene and Pleistocene aquifer were selected based on previous work done on similar islands, and these are included in Table 12.

Table 12 – Initial SEAWAT Parameters

Holocene Aquifer	
Hydraulic conductivity (m/day)	400
Vertical hydraulic conductivity (m/day)	80
Porosity	0.2
Specific storage (m ⁻¹)	7.50E-04
Specific yield	0.2
Longitudinal dispersivity (m)	5
Transverse dispersivity(m)	1.00E-02
Diffusion (m ² /day)	1.00E-04
Pleistocene Aquifer	
Hydraulic conductivity (m/day)	5,000
Vertical hydraulic conductivity (m/day)	1,000
Porosity	0.3
Specific storage (m ⁻¹)	7.50E-04
Specific yield	0.3
Longitudinal dispersivity (m)	5
Transverse dispersivity(m)	1.00E-02
Diffusion (m ² /day)	1.00E-04

Calibration of the models was performed using salinity data collected on Falalop by Stephen Anthony (United States Geological Survey, Pacific Island Water Science Center, Honolulu, Hawaii) in 1987-1988 (unpublished data). This data was used for calibration for two reasons: 1. salinity data for Eauripik or Satawal is undocumented and data collected in 1953 on Ifalik is unusable due to a new island geometry, and 2. field data collected as part of this study is limited and unreliable due to issues that arose in the field. Therefore, calibration proceeds uses the detailed salinity profile data collected by Stephen Anthony of USGS (1988, unpublished) to calibrate the Falalop model and extrapolate findings to the remaining models.

Stephen Anthony collected salinity profile data from five drilled wells on Falalop at disparate locations on the island. The data was measured on two separate dates, on a day in October 1987 and another in January 1988. Since locations were marked on a rough map by hand, well locations were approximated and added to ArcGIS along with the MODFLOW grid cells (Figure 38).

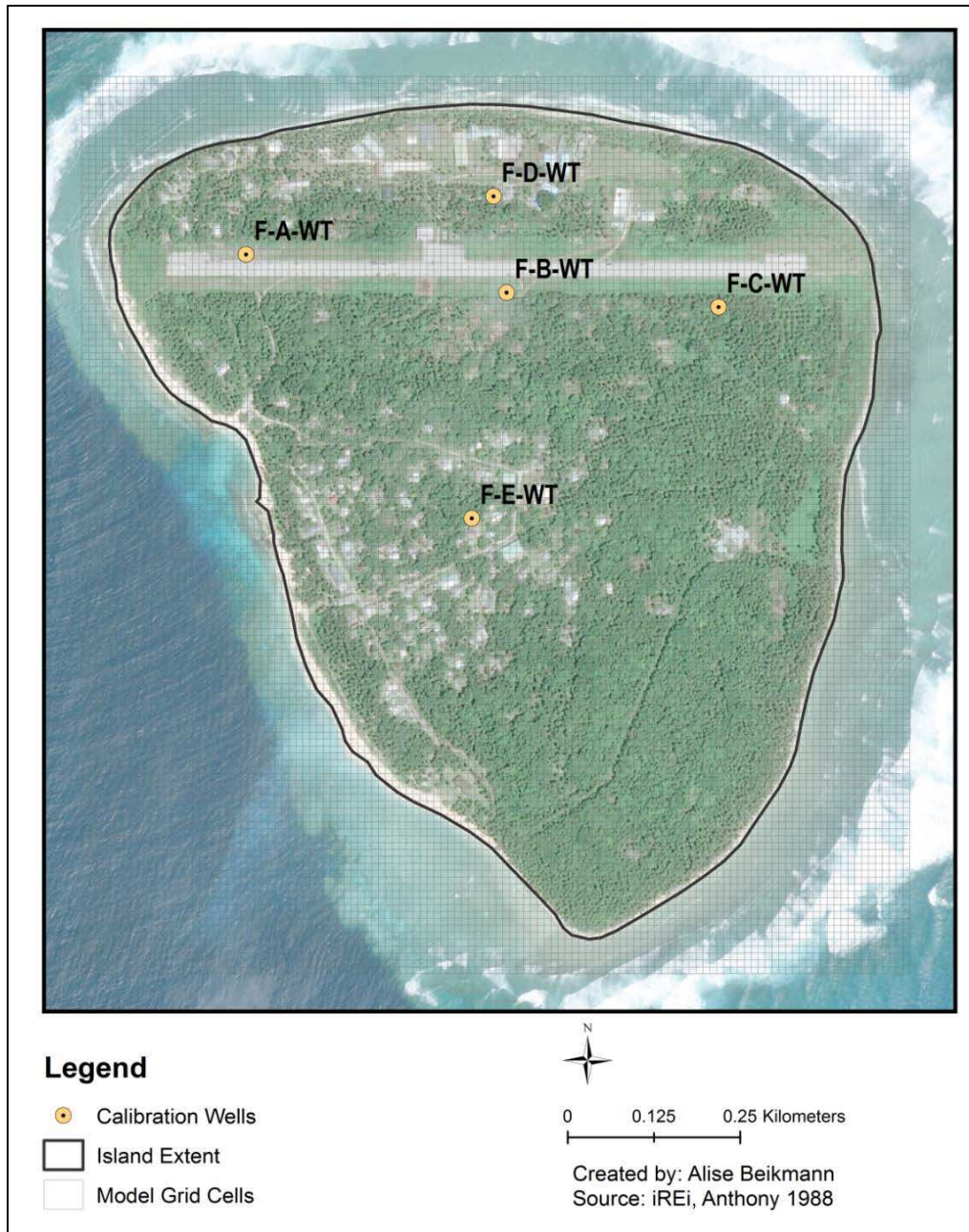


Figure 38 – Map of calibration wells on Falalop

This designated the reference cells in SEAWAT at which each observation wells are located, and the groundwater lens thickness at each of the five cells is tracked throughout the calibration process. To calibrate the model, hydraulic conductivity was modified until the error between the modeled and observed freshwater lens thickness was minimized. Error is estimated using two metrics, residual error and root mean squared error (RMSE). The residual errors for each observation point are calculated using Equation 6 below, where d_e is the lens thickness of the model and d_a is the observed lens thickness for the same observation point. The RMSE estimates error by summing the squared residuals for each observation point (total of m points) and taking the square root, as shown in Equation 7.

$$e_i = d_m - d_a \quad \text{Equation 6}$$

$$RMSE = \sqrt{\frac{1}{m} \sum_{i=1}^m e_i^2} \quad \text{Equation 7}$$

Since five wells were measured during this study, the hydraulic conductivity with the lowest average error and lowest RMSE is chosen for further modeling. At conclusion of the calibration, the hydraulic conductivity is reduced to 175 m day^{-1} to develop a thicker lens. Results from the calibration are shown in Table 13 and the summary of errors are shown in Table 14.

Table 13 – Calibration of SEAWAT model to observed salinity profile data on Falalop, 1987-1988

October 1987 Calibration Point

Well Name	Description	Date	Measured freshwater lens depth (m)	Modeled			Error		
				HK = 125 m/day	HK = 150 m/day	HK = 175 m/day	HK = 125 m/day	HK = 150 m/day	HK = 175 m/day
F-A-WT	West	10/14/87	1.80	2.43	1.97	1.57	0.63	0.16	-0.23
F-B-WT	Central	10/13/87	6.71	5.70	5.08	4.54	-1.01	-1.63	-2.17
F-C-WT	East	10/14/87	1.34	4.29	3.69	3.17	2.96	2.35	1.83
F-D-WT	North	10/23/87	4.56	3.45	2.90	2.42	-1.12	-1.67	-2.14
F-E-WT	South	10/12/87	1.75	5.94	5.53	4.87	4.18	3.78	3.12
Average Error (m/day)							1.13	0.60	0.08
RMSE (m/day)							5.38	5.03	4.74

January 1988 Calibration Point

Well Name	Description	Date	Measured freshwater lens depth (m)	Modeled			Error		
				HK = 125 m/day	HK = 150 m/day	HK = 175 m/day	HK = 125 m/day	HK = 150 m/day	HK = 175 m/day
F-A-WT	West	1/28/88	-	1.62	1.07	0.56	-	-	-
F-B-WT	Central	1/28/88	6.81	5.03	4.41	3.77	-1.78	-2.40	-3.04
F-C-WT	East	1/28/88	-	3.49	2.85	2.30	-	-	-
F-D-WT	North	1/28/88	1.51	2.56	1.95	1.40	1.05	0.44	-0.11
F-E-WT	South	1/28/88	1.45	5.38	4.77	4.15	3.93	3.33	2.70
Average Error (m/day)							1.07	0.46	-0.15
RMSE (m/day)							4.44	4.13	4.07

Table 14 – Summary of calibration statistics for varying horizontal hydraulic conductivity

	125 m day ⁻¹	150 m day ⁻¹	175 m day ⁻¹
Overall Average Error (m/day)	1.10	0.53	-0.03
Overall RMSE (m/day)	4.91	4.58	4.40
Rank (1-Best, 3-Worst)	3	2	1

As shown by the summary table in Table 14, a hydraulic conductivity of 175 m day⁻¹ minimizes the residual error and the RMSE which reduces bias in the model and the collective error. Refer to Table 15 for the final model parameters of the Holocene Aquifer and Figure 39 for a cross-section of the calibrated SEAWAT model for Falalop Island.

Table 15 – Calibrated SEAWAT Parameters

Holocene Aquifer	
Hydraulic conductivity (m/day)	175
Vertical hydraulic conductivity (m/day)	35
Porosity	0.2
Specific storage (m ⁻¹)	7.50E-04
Specific yield	0.2
Longitudinal dispersivity (m)	5
Transverse dispersivity(m)	1.00E-02
Diffusion (m ² /day)	1.00E-04
Pleistocene Aquifer	
Hydraulic conductivity (m/day)	5,000
Vertical hydraulic conductivity (m/day)	1,000
Porosity	0.3
Specific storage (m ⁻¹)	7.50E-04
Specific yield	0.3
Longitudinal dispersivity (m)	5
Transverse dispersivity(m)	1.00E-02
Diffusion (m ² /day)	1.00E-04

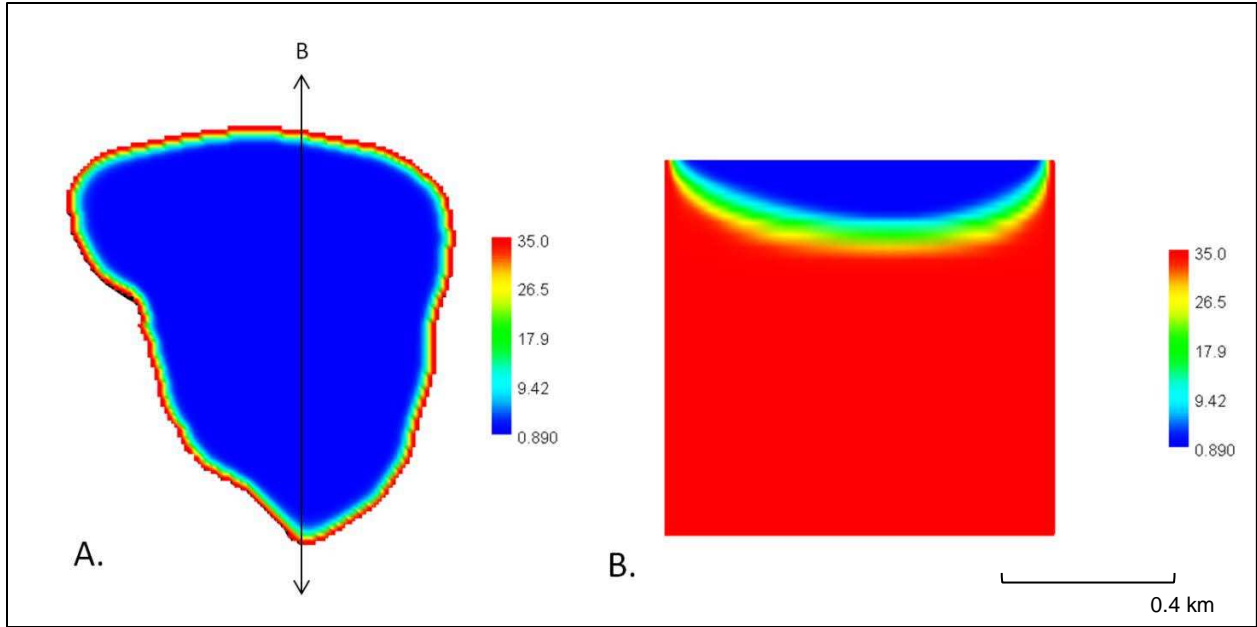


Figure 39 – Falalop calibrated, steady average rainfall model; A. Plan view, B. Profile view. Red indicates a chloride concentration for seawater of 35 g/kg and blue indicates a chloride concentration of 0.89 g/kg for freshwater.

With the calibrated hydraulic conductivity, the freshwater lens is regenerated under steady, average rainfall conditions for the islands. Plan and profile views of these islands are shown in Figure 40, Figure 41, and Figure 42. The maximum freshwater lens thickness and total lens volume for each island is shown in Table 16.

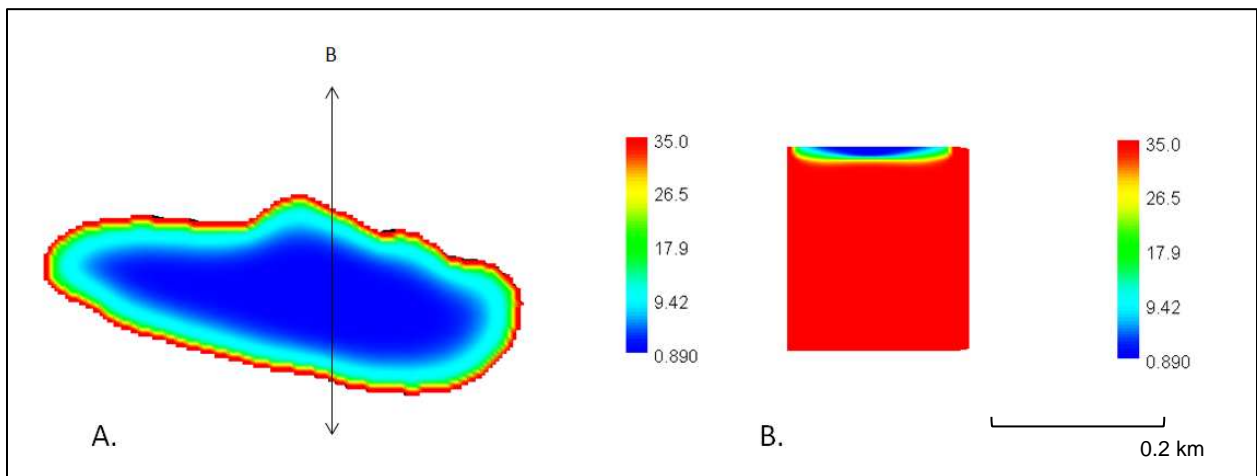


Figure 40 – Eauripik calibrated, steady average rainfall model; A. Plan view, B. Profile view. Red indicates a chloride concentration for seawater of 35 g/kg and blue indicates a chloride concentration of 0.89 g/kg for freshwater.

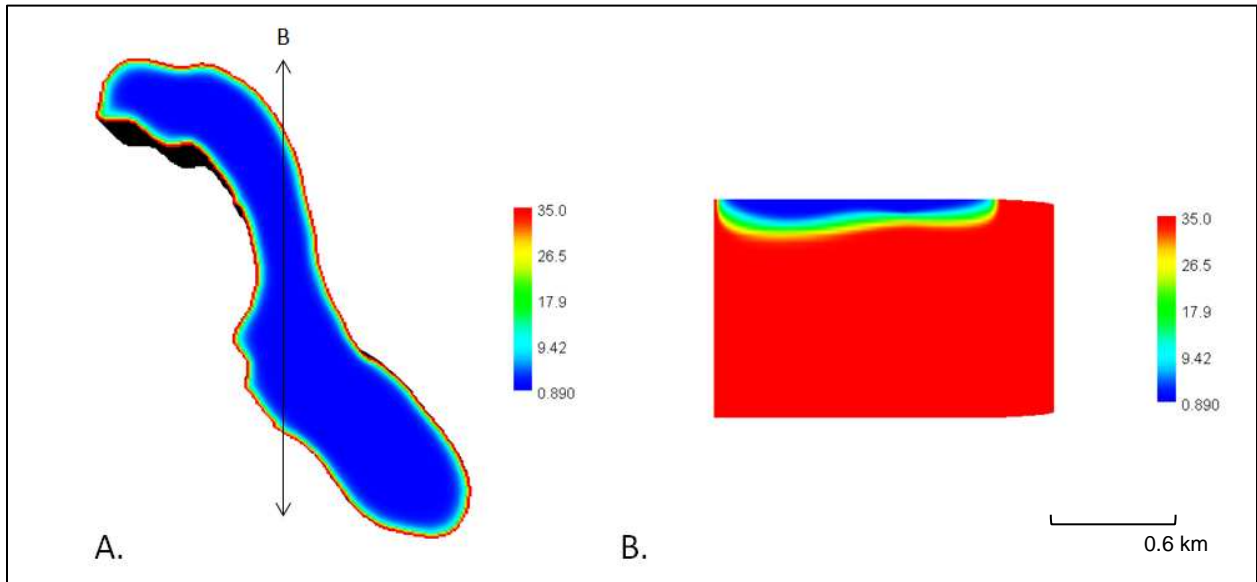


Figure 41 – Ifalik calibrated, steady average rainfall model; Plan view, B. Profile view. Red indicates a chloride concentration for seawater of 35 g/kg and blue indicates a chloride concentration of 0.89 g/kg for freshwater.

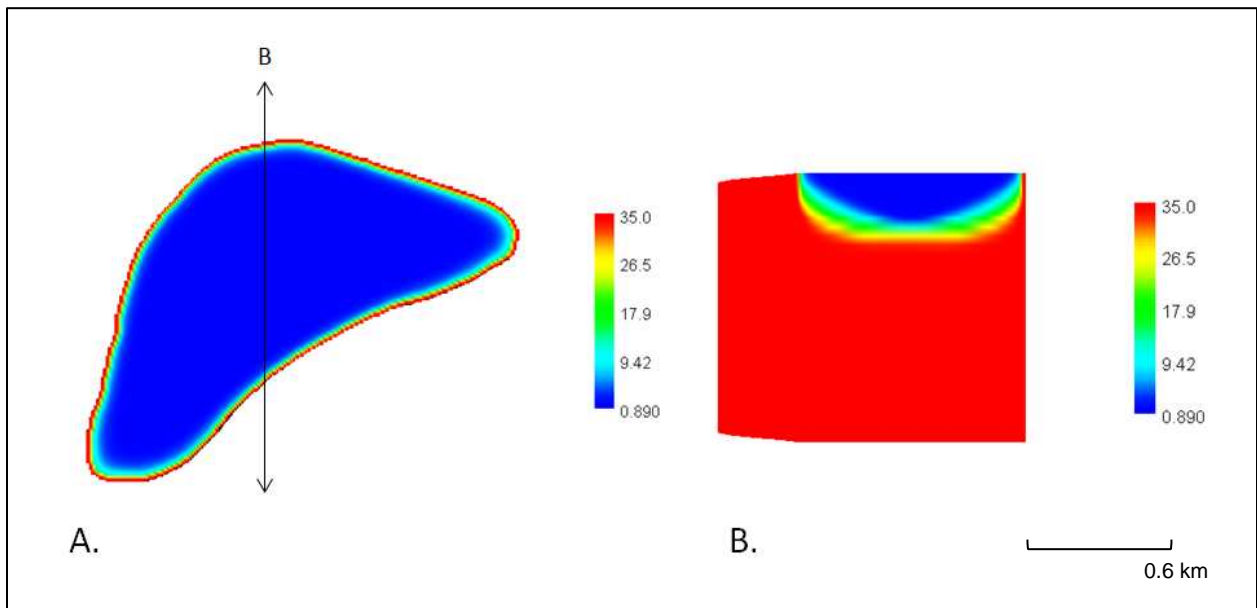


Figure 42 – Satawal calibrated, steady average rainfall model; A. Plan view, B. Profile view. Red indicates a chloride concentration for seawater of 35 g/kg and blue indicates a chloride concentration of 0.89 g/kg for freshwater.

Table 16 – Freshwater lens characteristics under steady, average rainfall conditions

Island	Maximum Lens Thickness (m)	Lens Volume (m ³)
Eauripik	0.86	8,700
Falalop	7.64	2,881,000
Ifalik	5.60	2,473,000
Satawal	7.65	4,100,000

As shown in Table 16, the freshwater lens on Eauripik is less than 1 meter at maximum thickness for average rainfall conditions due to the small island width. Actual lens thickness is most likely smaller since the island is frequently over-washed. The lens thicknesses for the other islands make sense relative to each other. Ifalik, which is a long, infinite strip island and the largest island is shallower due to the elongated shape. Satawal, a semi-circular island with a size similar to Ifalik, has the thickest lens and a lens volume 40% larger than the next largest, Falalop. Falalop is smaller in area, however it is a triangular shape which increases the groundwater storage.

5.3.2 Future rainfall conditions

General Circulation Models are used to examine the effects of global climate change, and subsequently precipitation, on the size of the fresh groundwater lens. Two representative GCM climate models were selected based on the lower and upper representative concentration pathways, GISS-E2-H for RCP 2.6 and GISS-E2-H-p2 for RCP 8.5. Qualitatively, RCP 2.6 models low level climate change in which anthropogenic GHG emissions peak in the 2010-2020 decade and decrease in annual emissions in years following. Conversely, RCP 8.5 models strong climate change and assumes that emissions continue to increase annually for the next several decades. These models capture the range of groundwater lens sizes expected with respect to climate change from 2010 to 2040.

5.3.2.1 RCP 2.6 Scenario

Results from the 30-year RCP 2.6 climate change scenario are shown graphically as the maximum freshwater lens depth (Figure 43, Figure 44), and as the total freshwater lens volume (Figure 45, Figure 46). Two figures are shown for each plot type because the groundwater lens thickness and volume for Eauripik is typically orders of magnitude smaller than the remaining islands. A statistical summary of the results is displayed in Table 17.

Table 17 – Statistics for RCP 2.6 GCM GISS-E2-H groundwater model (2010-2040)

Island	Maximum Thickness (m)				Volume (m ³)			
	Average	Maximum	Minimum	Range	Average	Maximum	Minimum	Range
Eauripik	0.05	0.46	0.00	0.46	240	4,599	0	4,599
Falalop	5.55	6.66	4.54	2.12	2,221,676	2,881,682	1,452,704	1,428,978
Ifalik	3.35	4.22	2.46	1.76	1,442,197	2,151,803	737,526	1,414,277
Satawal	5.94	6.95	4.77	2.17	3,272,475	4,195,318	2,189,538	2,005,780

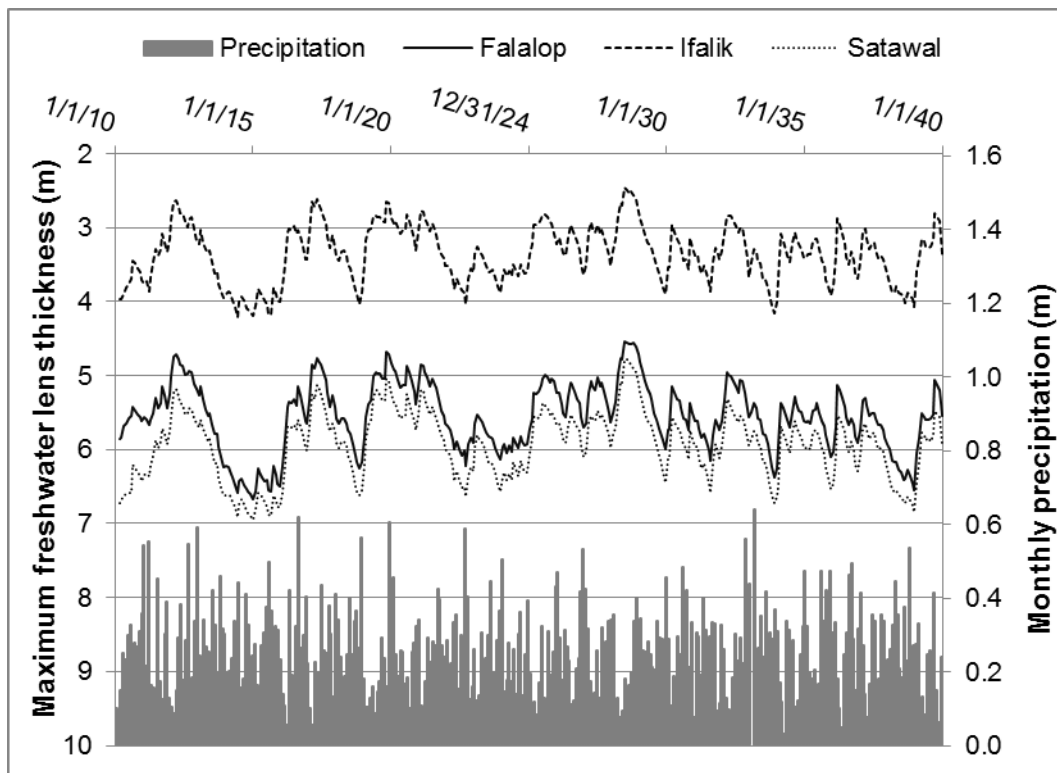


Figure 43 – Groundwater lens thickness (m) for RCP 2.6 Scenario (Falalop, Ifalik, and Satawal)

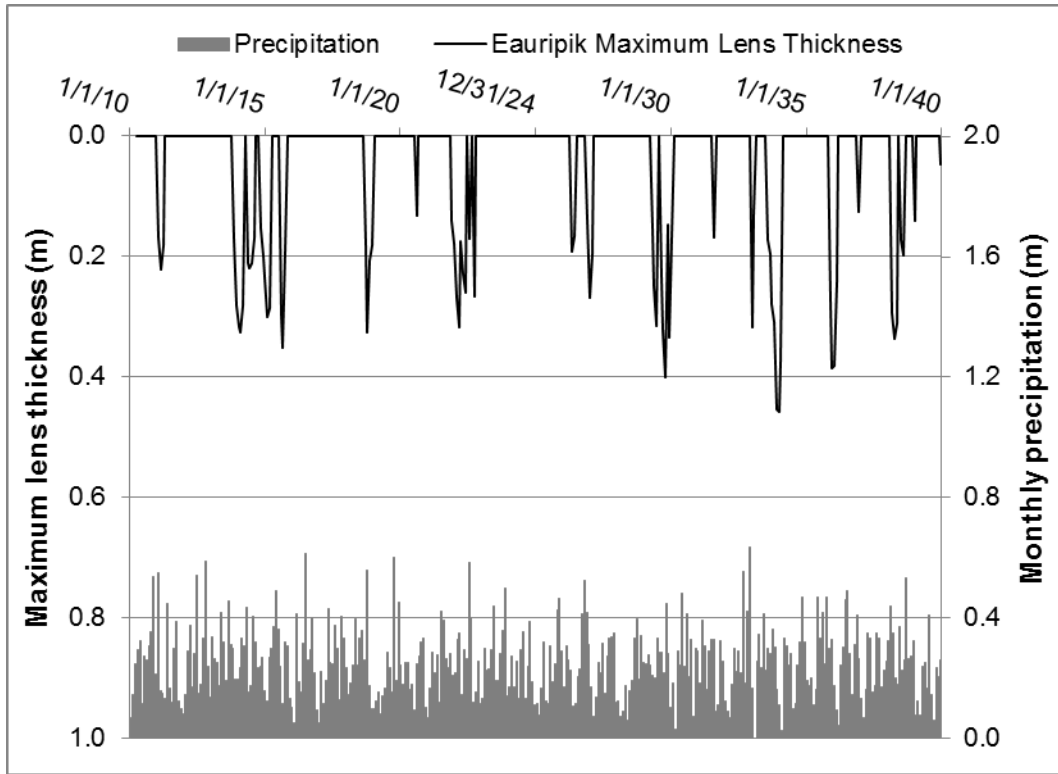


Figure 44 – Groundwater lens thickness (m) for RCP 2.6 Scenario (Eauripik)

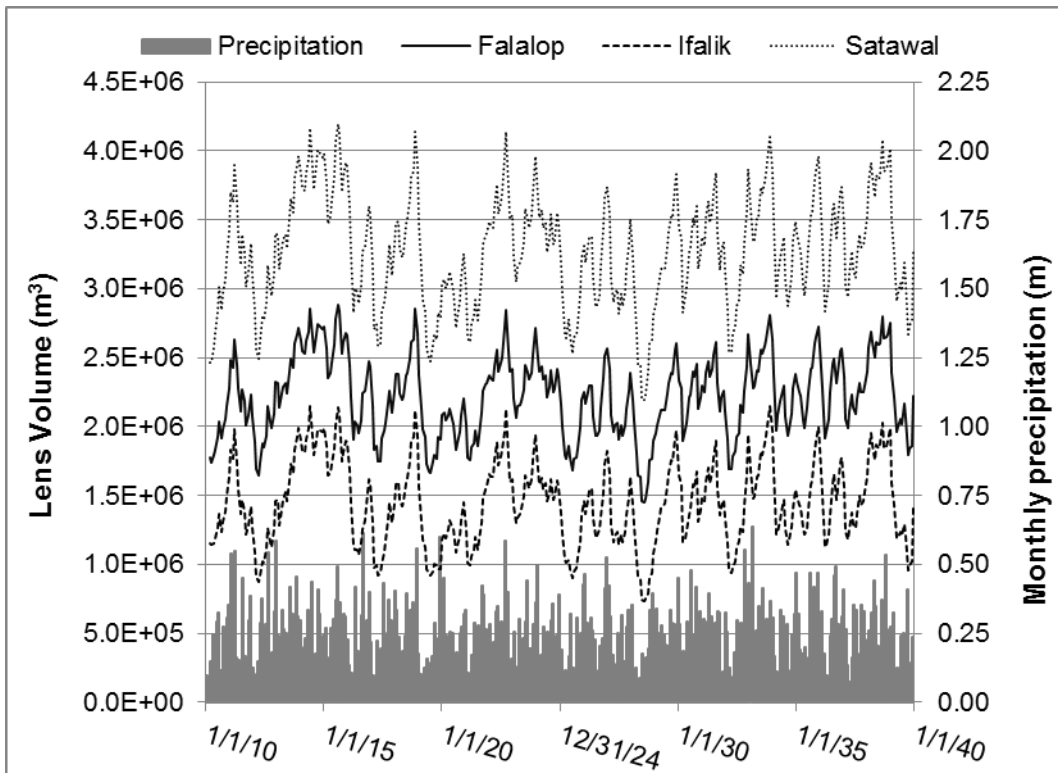


Figure 45 – Groundwater lens volume (m³) for RCP 2.6 Scenario (Falalop, Ifalik, and Satawal)

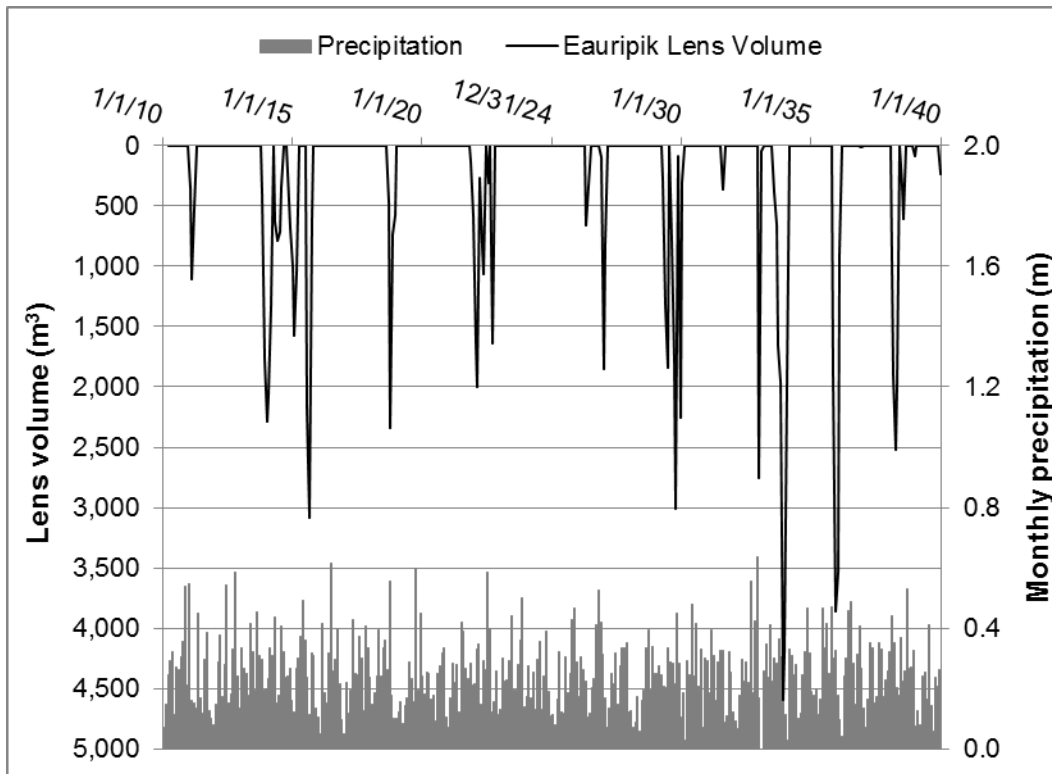


Figure 46 – Groundwater lens volume (m^3) for RCP 2.6 Scenario (Eauripik)

As shown by the figures, the freshwater lens thickness and volume varies in time for the islands in response to recharge. The response, or trend, of the freshwater lens thickness and volume is similar for the three larger islands. A significant increase in maximum lens thickness occurs early in the simulation period between year 2012 and 2015 that leads to a 1.5 – 2 meter variance in groundwater thickness over a 3-year period. In contrast, the maximum freshwater lens thickness for Eauripik never exceeds 0.45 meters and does not exceed 0 meters for over 50% of the 30 year simulation.

5.3.2.2 RCP 8.5 Scenario

Results from the 30-year RCP 8.5 climate change scenario, based on the GISS-E2-H-p2 global circulation model, are shown graphically in Figure 47 and Figure 48, as the maximum

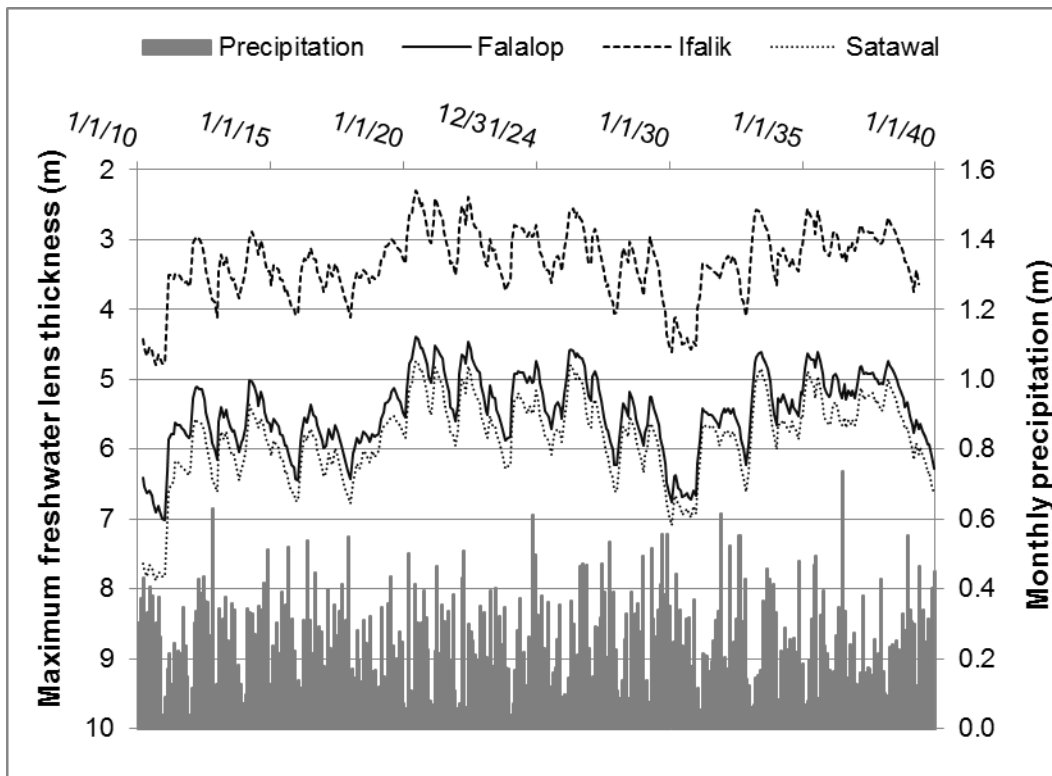


Figure 47 – Groundwater lens thickness (m) for RCP 8.5 Scenario (Falalop, Ifalik, and Satawal)

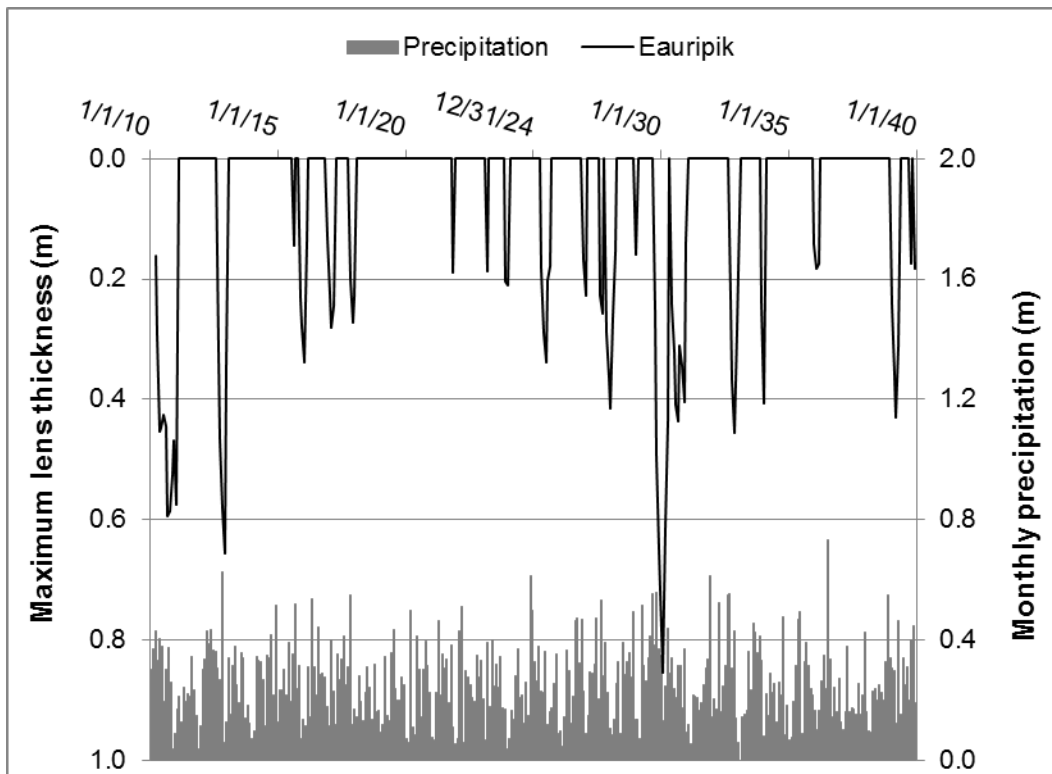


Figure 48 – Groundwater lens thickness (m) for RCP 8.5 Scenario (Eauripik)

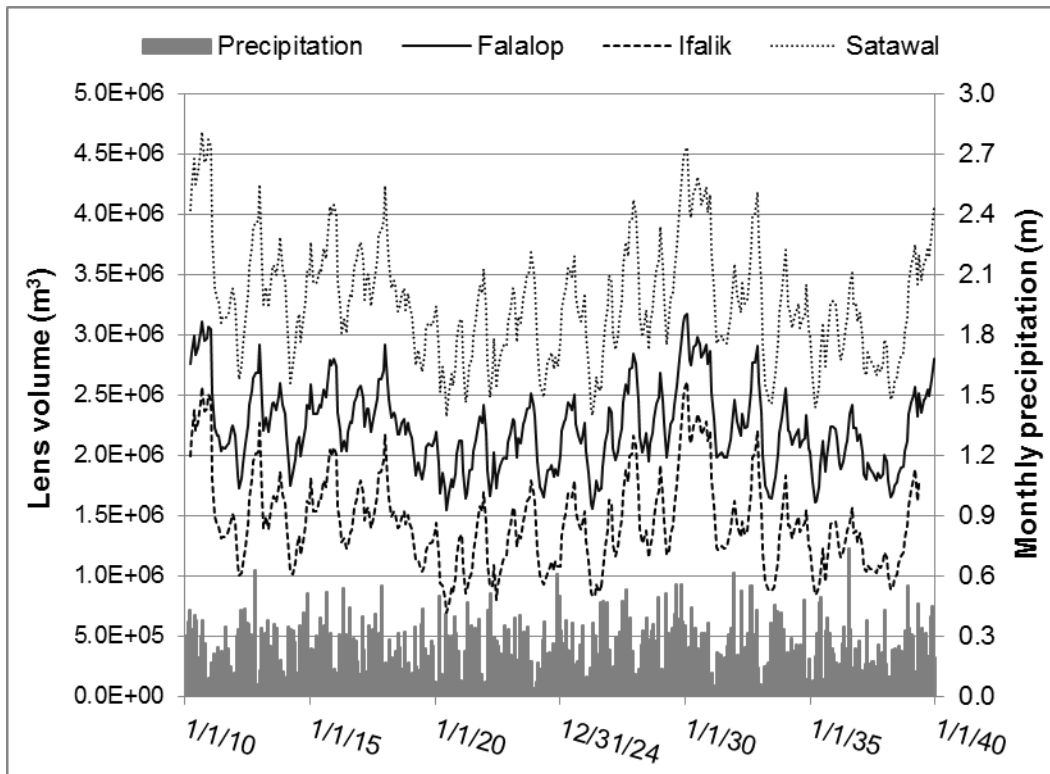


Figure 49 – Groundwater lens volume (m³) for RCP 8.5 Scenario (Falalop, Ifalik, and Satawal)

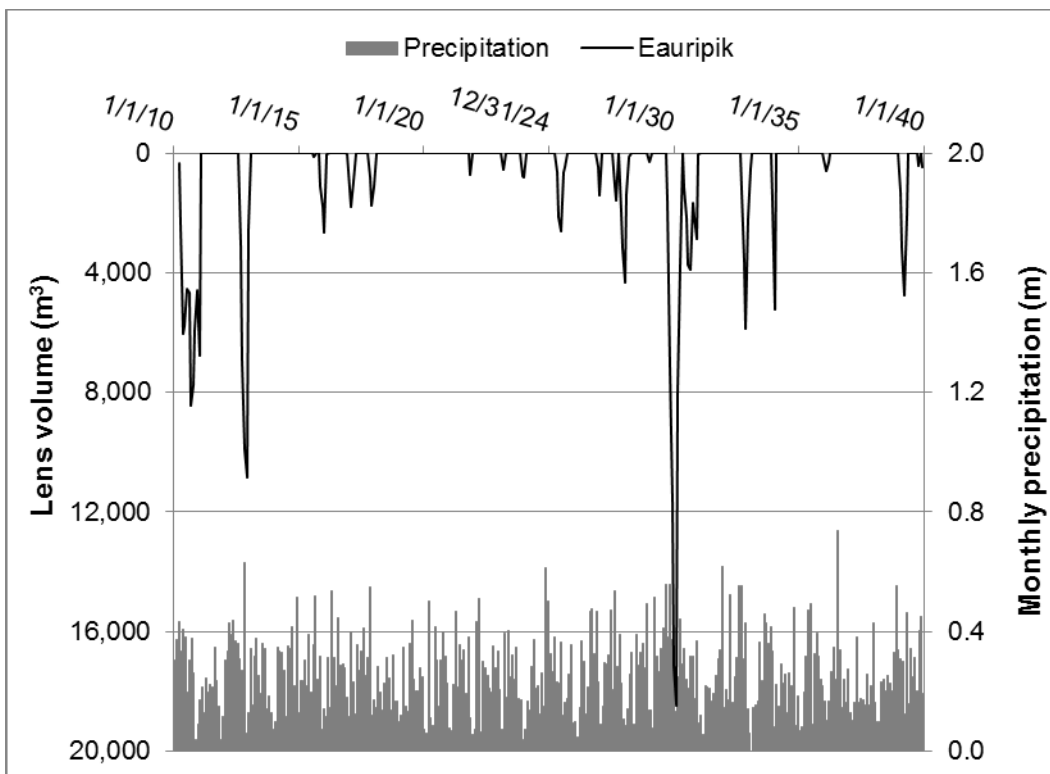


Figure 50 – Groundwater lens volume (m³) for RCP 8.5 Scenario (Eauripik)

freshwater lens depth, and in Figure 49 and Figure 50 as the lens volume. A statistical summary of the results is displayed in Table 18.

Table 18 – Statistics for RCP 8.5 GCM GISS-E2-H-p2 groundwater model (2010-2040)

Island	Maximum Thickness (m)				Volume (m ³)			
	Average	Maximum	Minimum	Range	Average	Maximum	Minimum	Range
Eauripik	0.07	0.85	0.00	0.85	683	18,503	0	18,503
Falalop	5.46	7.01	4.40	2.62	2,225,293	3,173,582	1,550,548	1,623,034
Ifalik	3.33	4.80	2.29	2.51	1,443,308	2,607,779	692,558	1,915,221
Satawal	5.84	7.88	4.73	3.15	3,274,714	4,682,408	2,320,881	2,361,527

The response for this climate scenario appears distinctly different than the RCP 2.6 conditions. The groundwater lens appears much more dynamic in this scenario, with wider oscillations of lens thickness and volume. There are also decadal episodes of general increases and decreases in lens size. Compared to the previous climate scenario, the range of lens sizes is larger by over a half meter, yet the overall average conditions are dryer than the RCP 2.6 scenario. It is apparent based on these findings that climate change strength may have strong a significant impact on the Pacific climate and subsequently the groundwater lens profile. This GCM, RCP 8.5 GISS-E2-H-p2, represents highly unpredictable climate patterns and if actually followed in the Pacific environment, it could be disastrous. This is especially true if any of the IPCC projected climate changes occur in FSM, namely an increase in typhoon frequencies and consistent sea-level rise. However, at this time there is no indication whether the Pacific will experience a scenario like RCP 2.6 GISS-E2-H or one like RCP 8.5 GISS-E2-H-p2.

6. CONCLUSIONS AND RECOMMENDATIONS

Water security on Pacific atoll islands is a growing concern and the state of water security depends on several factors, specifically the availability of rainwater, the reliability of the network of rainwater catchment systems, and the availability of fresh groundwater as a secondary source to use during periods of low rainfall.

6.1 Rainfall conditions

Rainfall conditions must be carefully selected in water resources analyses, and selection is dependent on the purpose and time-scale. To quantify the reliability of rainwater catchment systems, it is recommended that users model with short-term, historical rainfall conditions that simulate an average year or a severe drought with daily time increments. Severe drought rainfall conditions provide a more conservative rainwater catchment system design. General Circulation Models may also be used for RWCS analysis, however, the conditions provide a less conservative design. GCM rainfall conditions are ideal for a long-term, climate analysis and are recommended for long-term groundwater analyses. For instance, the freshwater lenses observed a dynamic response during the 30-year simulation of the RCP8.5 GCM. Historical rainfall data and severe drought rainfall data are also acceptable for modeling in SEAWAT, provided the purpose is still achievable with the use of scaled-down, monthly rainfall data.

6.2 Rainwater collection

Optimizing the capacity of the rainwater collection network is the best course of action for improving water security on remote, Pacific Islands. Evaluation of rainwater catchments should be conducted at the community level to reduce over-simplification by average statistics.

The three most important parameters to consider in RWCS analysis is daily demand, catchment area, and gutter-downspout efficiency. Design curves included in this thesis supplement the planning process. Finally, the network of rainwater catchment systems on Ifalik Island are sufficient to meet the needs of the community during average conditions, future climate change conditions, and severe drought conditions.

6.3 Groundwater collection

Atoll islands large enough to develop a useful groundwater lens may wish to manage this source for future droughts. Findings from this study suggest the freshwater lens volume may fluctuate more significantly from year-to-year as a result of higher levels of climate change. Climate change impacts to the freshwater lens were quite different for between the high- and low-level climate change scenarios, which indicates that the degree of climate change will be important to water resource managers in this region. The groundwater analysis also found that a hydraulic conductivity of 175 m day^{-1} is appropriate for the upper-lying, Holocene aquifer in the Yap outer-islands, and the groundwater lens for Eauripik Island is insufficient for use as a source of drinking water.

6.4 Other applications and future research

The methods for rainwater catchment systems analysis presented in this thesis are adaptable to any region, especially applications for community-based evaluations. Mass balance models are customizable and will fit specific needs, like specific precipitation scenarios, conditions of existing systems, configurations of community catchment systems, etc. Design curves are an excellent resource for constructing new catchment systems and are readily usable as presented. Groundwater modeling methods are applicable to any atoll island community in the Pacific or Indian oceans.

7. REFERENCES

- Alkire, W. H. (1959). Residence, Economy, and Habitat in the Caroline Islands: A Study in Ecologic Adaptation. *University of Hawaii, Thesis*.
- Anthony, S. S. (1997). Hydrogeology of selected islands of the Federated States of Micronesia. In L. Vacher, & T. M. Quinn, *Geology and Hydrogeology of Carbonate Islands* (Vol. 54, pp. 693-707). Amsterdam: Elsevier.
- Arnow, T. (1955). The hydrology of Ifalik Atoll, Western Caroline Islands. *Atoll Research Bulliten No. 44*.
- Ayers, J. F., & Vacher, H. L. (1986). Hydrogeology of an Atoll Island: A Conceptual Model from Detailed Study of a Micronesian Example. *Ground Water*, 24(2), 185-198.
- Bailey, R. T., & Jenson, J. W. (2014). Effects of Marine Overwash for Atoll Aquifers: Environmental and Human Factors. *Groundwater*, 52(5), 694-704.
- Bailey, R. T., Jenson, J. W., & Olsen, A. E. (2009). Numerical Modeling of Atoll Island Hydrogeology. *Groundwater*, 184-196.
- Bailey, R. T., Jenson, J. W., & Olsen, A. E. (2010). Estimating the Ground Water Resources of Atoll Islands. *Water*, 1-27.
- Bailey, R. T., Jenson, J. W., & Taborosi, D. (2013). Estimating the freshwater-lens thickness of Atoll Islands in the Federated States of Micronesia. *Hydrogeology Journal*, 441-457.
- Bailey, R. T., Khalil, A., & Chatikavanij, V. (2014). Estimating transient freshwater lens dynamics for atoll islands of the Maldives. *Journal of Hydrology*, 247-256.
- Barros, V., Field, C. B., Dahe, Q., & Stocker, T. F. (2012). *Managing the Risks of Extreme Events and Disasters to Advance Climate Change Adaptation*. New York City, New York: Intergovernmental Panel on Climate Change.
- Bates, M., & Abbott, D. (1958). *Ifaluk - Portrait of a Coral Island*. London: Museum Press Limited.
- Batu, V. (1998). *Aquifer Hydraulics: A Comprehensive Guide to Hydrogeologic Data Analysis*. New York: John Wiley & Sons.

- Brier, G. W. (1950). Verification of forecasts expressed in terms of probability. *Mon Wea Rev*(78), 1-3.
- Bryan, E. H. (1953). Check list of atolls. *Atoll Research Bulletin*(19), pp. 1-38.
- Chidley, T. R., & Lloyd, J. W. (1977). A Mathematical Model Study of Fresh-Water Lenses. *Ground Water*, 215-222.
- Chui, T. F., & Terry, J. P. (2012). Modeling Fresh Water Lens Damage and Recovery on Atolls After Storm-Wave Washover. *Groundwater*, 50(3), 412-420.
- Chui, T. F., & Terry, J. P. (2013). Influence of sea-level rise on freshwater lenses of different atoll island sizes and lens resilience to storm-induced salinization. *Journal of Hydrology*, 502, 18-26.
- Comte, J.-C., Join, J.-L., Banton, O., & Nicolini, E. (2014). Modelling the response of fresh groundwater to climate and vegetation changes in coral islands. *Hydrogeology Journal*, 1905-1920.
- Dana, J. D. (1872). Corals and Coral Islands. *The American Naturalist*, 674-680.
- Davis, W. M. (1928). The Formation of Coral Reefs. *The Scientific Monthly*, 289-300.
- Detay, M., Alessandrello, E., Come, P., & Groom, I. (1989). Groundwater Contamination and Pollution in Micronesia. *Journal of Hydrology*, 149-170.
- Dillaha, T. A., & Zolan, W. J. (1985). Rainwater Catchment Water Quality in Micronesia. *Water Resources*, 741-746.
- Falkland, A. C. (1994). Climate, Hydrology and Water Resources of the Cocos (Keeling) Islands. *Atoll Research Bulletin No. 400*. Washington, D.C.: National Museum of Natural History.
- Fosberg, F. R. (1969). Plants of Satawal Island, Caroline Islands. *Atoll Research Bulletin No. 132*.
- FSM National Government. (2010). *2010 FSM Census of Population and Housing*. National Government of the Federated States of Micronesia, Department of Economic Affairs, Division of Statistics.
- Fu, G., Liu, Z., Charles, S. P., Xu, Z., & Yao, Z. (2013). A score-based method for assessing the performance of GCMs: A case study of southeastern Australia. *Journal of Geophysical Research: Atmospheres*, 4154-4167.

- Hamlin, S. N., & Anthony, S. S. (1987). *Ground-water resources of the Laura area, Majuro Atoll, Marshall Islands*. Honolulu, Hawaii: U.S. Geological Survey.
- Hezel, F. X. (2009). March Toward Self-Government. *Micronesian Counselor*(76). Pohnpei, FM: Micronesian Seminar.
- Holding, S., & Allen, D. M. (2015). From days to decades: numerical modeling of freshwater lens response to climate change stressors on small low-lying islands. *Hydrology and Earth System Sciences*, 933-949.
- Hunt, C. D., & Peterson, F. L. (1980). *Groundwater Resources of Kwajalein Island, Marchall Islands*. Manoa: Water Resources Research Center, Univesity of Hawaii.
- Kensch, P. S., Ford, M. R., & McLean, R. F. (2015). Coral islands defy sea-level rise over the past century: Records from a central Pacific atoll. *Geology*, 515-518.
- Kottermair, M., Taborosi, D., & Jenson, J. (2016). *Enough water for everyone? A field study of freshwater resources on Ifalik and Eauripik atolls, Yap State, FSM*. Mangilao, Guam: Water and Environmental Research Institute of the Western Pacific, University of Guam.
- Lam, R. K. (1974). Atoll Permeability Calculated from Tidal Diffusion. *Journal of Geophysical Research*, 3073-3081.
- Landers, M. A., & Khosrowpanah, S. (2004). Rainfall Climatology for Pohnpei Islands, Federated States of Micronesia. *Water and Environmental Research Institute*.
- Lee, A. G. (2003). *3-D Numerical Modeling of Freshwater Lens on Atoll Islands*. Berkeley, CA: Lawrence Verkeley National Laboratory.
- Levin, M. J. (1976). Eauripik Population Structure. *University of Michigan, PhD dissertation*.
- Liaw, C. H., & Chiang, Y. C. (2014). Dimensionless Analysis for Designing Domestic Rainwater Harvesting Systems at the Regional Level in Northern Taiwan. *Journal of Water*, 3913-3933.
- Lloyd, J. W., Miles, J. C., Chessman, G. R., & Bugg, S. F. (1980, August). A Ground Water Resources Study of a Pacific Ocean Atoll - Tarawa, Gilbert Islands. *Water Resources Bulletin, American Water Resources Association*, pp. 646-653.
- Mahmoodzadeh, D., Ketabchi, H., Ataie-Ashtiani, B., & Simmons, C. T. (2014). Conceptualization of a fresh groundwater lens influenced by climate change: A modeling study of an arid-region island in the Persian Gulf, Iran. *Journal of Hydrology*, 519, 399-413.

- Maupin, M. A., Kenny, J. F., Hutson, S. S., Lovelace, J. K., Barber, N. L., & Linsey, K. S. (2014). *Estimated Use of Water in the United States in 2010 (No. 1405)*. Reston, Virginia: U.S. Geological Survey.
- Merlin, M. (2015). *People and Plants of Micronesia*. Retrieved from University of Hawaii at Manoa, Botony Department: http://manoa.hawaii.edu/botany/plants_of_micronesia/
- Perkins, S. E., Pitman, A. J., Holbrook, N. J., & McAneney, J. (2007). Evaluation of the AR4 Climate Models' Simulated Daily Maximum Temperature, Minimum Temperature, and Precipitation over Australia Using Probability Density Functions. *Journal of Climate*, 4356-4376.
- Pernetta, J. C. (1992). Impacts of climate change and sea-level rise on small island states: national and international responses. *Global Environmental Change*, 19-31.
- Peterson, F. L., & Gingerich, S. B. (1995). Modeling atoll groundwater systems. *Groundwater Models for Resources Analysis and Management*, 275-292.
- Presley, T. K. (2005). *Effects of the 1998 Drought on the Freshwater Lens in the Laura Area, Majuro Atoll, Republic of the Marshall Islands*. Reston, Virginia: U.S. Geological Surey.
- Richmond, B. M., Mieremet, B., & Reiss, T. E. (1997). Yap Islands natural coastal systems and vulnerability to potential accelerated sea-level rise. *Journal of Coastal Research*, 153-172.
- Roy, P., & Connell, J. (1991). Climatic Change and the Future of Atoll States. *Journal of Coastal Research*, 1057-1075.
- Scourse, A., & Wilkins, C. (2009). Impacts of modernisation on traditional food resource management and food security on Eauripik atoll, Federated States of Micronesia. *Food Security*, 169-176.
- Spennemann, D. H. (2006). Freshwater Lens, Settlement Patterns, Resource Use and Connectivity in the Marshall Islands. *Transforming Cultures eJournal*, 44-63.
- Swartz, J. H. (1962). *Some physical constants for the Marshall Island area*. Washington, D.C.: U.S. Geological Survey.
- Terry, J. P., & Chui, T. F. (2012). Evaluating the fate of freshwater lenses on atoll islands after eustatic sea-level rise and cyclone-driven inundation: A modelling approach. *Global and Planetary Change*(88-89), 76-84.

- Tracey, J. I., Abbott, D. P., & Arnow, T. (1961). *Natural History of Ifaluk Atoll: Physical Environment*. Honolulu: Bernice P. Bishop Museum.
- U.S. Geological Survey. (1996). *U. S. Geological Survey programs in Hawaii and the Pacific*. Honolulu: U.S. Geological Survey.
- Underwood, M. R., Peterson, F. L., & Voss, C. J. (1992). Groundwater lens dynamics of atoll islands. *Water Resources Research*, pp. 2889-2902.
- USAID - Washington, DC, US. (1982). *Designing Roof Catchments (Water for the World Technical Note No. RWS. 1.D.4)*. Washington, DC: USAID.
- USAID - Washington, DC, US. (1982). *Evaluating Rainfall Catchments (Water for the World Technical Note No. RWS. 1.P.5.)*. Washington, DC: USAID.
- Vacher, H. L. (1997). Introduction: Varieties of Carbonate Islands and a Historical Perspective. In H. L. Vacher, & T. M. Quinn, *Geology and Hydrogeology of Carbonate Islands* (pp. 1-33). Amsterdam: Elsevier Science B.V.
- Van der Brug, O. (1986). 1983 Drought in the Western Pacific. *USGS Open-File Report 85-418*.
- Wallace, C. D. (2015). Atoll island freshwater resources: modeling, analysis, and optimization. *Master's Thesis*. Fort Collins, CO: Colorado State University.
- Wallace, C. D., & Bailey, R. T. (2015). Sustainable Rainwater Catchment Systems for Micronesian Atoll Communities. *Journal of the American Water Resources Association*, 185-199.
- Wallace, C. D., Bailey, R. T., & Arabi, M. (2015). Rainwater catchment system design using simulated future climate data. *Hydrology*, 1789-1809.
- White, I. (1996). *Fresh groundwater lens recharge, Bonriki, Kiribati*. Paris: UNESCO.
- White, I., & Falkland, T. (2010). Management of freshwater lenses on small Pacific islands. *Hydrogeology Journal*, 227-246.
- White, I., Falkland, T., & Scott, D. (1999). Droughts in small coral islands: Case study, South Tarawa, Kiribati. *Technical Documents in Hydrology*.
- White, I., Falkland, T., Metutera, T., Metai, E., Overmars, M., Perez, P., & Dray, A. (2007). Climatic and Human Influence on Groundwater in Low Atolls. *Vadose Zone*, 581-590.

APPENDIX A – RAINWATER CATCHMENT SYSTEM DATA FROM IFALIK ISLAND

Compound ID	Roof					Gutter		Storage Tank					
	Structure	Potential (m ²)	Actual (m ²)	Efficiency	Condition	Coverage	Condition	Type	Cap (l)	% Full			
School	Classroom	546.74	253.69	46%	G	100%	VG	Concrete	337722	0%			
	Office	404.47	NA	0%	G	0%							
	Storage	82.84	NA	0%	G	0%							
	Storage	23.85	NA	0%	G	0%							
R2	Smoke HSE	3.08	NA	0%	P	0%		Type A	2000	90%			
	Food STR	4.94	NA	0%	G	0%							
	Catchment	9.52	9.52	100%	G	100%	G						
	Cooking HSE	11.84	NA	0%	F	0%							
	Catchment	9.57	9.57	100%	G	100%	G				Type B	1883.7	100%
R3	Food STR	4.32	4.32	100%	F	100%	G	Barrel	282.7	50%			
	Cooking HSE	8.00	NA	0%	P	0%		Barrel	282.7	100%			
	Food STR	2.25	1.80	80%	F	100%	G						
	Firewood (a)	2.70	2.70	100%	G	100%	G				Barrel	137.4	NA
	Firewood (b)	14.08	14.08	100%	G	100%	G				Type A	2000	100%
	Cooking HSE	6.65	NA	0%	G	0%					Type B	1883.7	Empty
	House	12.00	NA	0%	P	0%							
R-ECE	Headstart	141.86	NA	0%	G	25%	VP	ECE	4950	100%			
R5	Catchment	9.30	9.30	100%	G	100%	G	Type A	2000	100%			
	Cooking HSE	12.21	6.11	50%	G	100%	G	Makeshift (MS)	1000	20%			
	Catchment	7.02	7.02	100%	G	100%	G						
	Plate dryer	3.60	NA	0%	F	0%							
R6	Catchment	53.60	42.88	80%	G	30%		Type A	2000	75%			
						100%		Type A	2000	85%			
	Cooking HSE	22.54	7.89	35%	VG	70%	G	Type B	1883.7	85%			
	Men's HSE	30.40	NA	0%	G	0%		MS	57.7	25%			
	Cooking area	6.40	NA	0%	F	0%							
	Food STR	3.04	NA	0%	G	0%					MS	95.4	30%
											MS1	61.3	NA
	Cooking area	6.33	NA	50%	F						MS2	29.1	NA
							MS3				36.6	NA	

R7	Old Classroom	114.51	28.37	25%	G	100%	G	Type A	2000	75%
	Cooking HSE	10.64	NA	0%	F	0%				
	Cooking HSE	7.83	NA	0%	G	0%				
	Cooking HSE	18.06	NA	0%	VP	0%				
	Food STR	3.04	3.04	100%	G	100%	G	MS	28.3	100%
	Storage HSE	12.24	NA	0%	F	0%				
	Catchment	3.20	3.20	100%	G	100%	G	Type B	1883.7	100%
		9.99	9.99	100%	G	100%	G	Type A	2000	100%
R1	Food STR	5.70	NA	0%	G	100%	G			
	Catchment	24.01	12.01	50%	G	100%	G	Type B	1883.7	30%
	Cooking HSE	16.72	NA	0%	P	0%				
	Cooking HSE	10.20	NA	0%	P	0%				
	Church	59.85	59.85	100%	G	100%	G	Type A	2000	100%
R4 (Women's HSE)	Storage HSE	5.76	NA	0%	G	0%				
	Drying area	7.84	NA	0%	F	0%				
	Cook HSE	10.56	NA	0%	G	0%				
	Storage HSE	4.56	NA	0%	G	0%				
	Catchment	49.50	49.50	100%	G	100%	G	Type B	2000	80%
	Shower	6.00	NA	0%	P	0%				
	Storage HSE	16.10	NA	0%	G	0%				
	Dish Dryer	2.40	NA	0%	F	0%				
	Dish Dryer	3.00	3.00	100%	G	100%	G	MS	24.7	
	Cooking HSE	8.64	NA	0%	F	0%				
	Church	59.85	59.85	100%	G	100%	G	Type A	2000	100%
R10	Catchment	4.25	4.25	100%	G	100%	F	Type B	1883.7	0%
	Church	47.43	47.43	100%	G	100%	G	Type A	2000	100%
	Toolshed	2.72	NA	0%	G	0%				
	Chicken HSE	6.27	NA	0%	P	0%				
	Cooking HSE	7.40	NA	0%	P	0%				
NW Church	NW Church	93.87				0%				

R11	House	66.12	43.32	66%	G	100%	G	Type A	2000	80%
	Shower	5.32	NA	0%	F	100%	G	Type C	1000	
	Dish Dryer	2.72	NA	0%	G	0%				
	Storage	3.80	NA	0%	G	0%				
	Sink	1.20	NA	0%	G	0%				
R12	Storage	2.52	NA	0%	P	0%				
	Storage	6.24	NA	0%	F	0%				
	Cupboard	2.88	NA	0%	F	0%				
	Storage HSE	32.40	24.00	74%	G	100%	G	Type A	2000	100%
	Pot STR	3.91	3.91	100%	G	100%	G	Type B	1883.7	100%
R13	Shower	5.32	NA	0%	G	100%	G	MS	45.4	50%
	Weaving HSE	NA	8.88	NA	G	100%	G	Type D	232.5	100%
R14	Storage HSE	13.32	11.99	90%	F	0%		Concrete	44376	NA
	Storage HSE2	11.02	NA	0%	F	100%	G	Type B	1883.7	NA
	Cupboard	2.85	NA	0%	G	0%				
	Pot STR	8.40	7.14	85%	F	100%	G	Type A	2000	50%
	Cooking area	5.32	NA	0%	P	0%		Type B	1883.7	50%
R9	Cupboard	3.60	NA	0%	G	0%				
	Cooking HSE	6.72	NA	0%	G	0%				
	Storage	25.09	25.09	100%	G	100%	G	Type A	2000	100%
R8	MS							MS	177.3	100%
	Cupboard	1.56	NA	0%	G	0%				
	Drying area	3.23	3.23	100%	F	0%	P			
	Storage	7.13	6.77	95%	G	100%	G	Type C	1000	25%
R15	Cupboard	2.25	NA	0%	F	0%				
	Storage HSE	21.50	6.75	31%	G	100%	G	Type A	2000	90%
	Cupboard	1.68	NA	0%	G	0%				

R16	Drying area	3.06	NA	0%	G	0%				
	Cooking HSE	6.76	NA	0%	G	0%				
	Cupboard	4.18	NA	0%	G	0%				
	Storage HSE	21.56	16.72	78%	G	100%	G	Type B	1883.7	100%
						100%	G	Barrel	1960.6	NA
	Storage HSE	5.25	NA	0%	G	0%				
	Cooking HSE	6.44	NA	0%	G	0%				
	Drying area	11.47	11.47	100%	G	100%	G	Type A	2000	NA
Cupboard	3.20	NA	0%	G	0%					
R17	Drying area	19.98	19.98	100%	F	100%	G	Type A	2000	25%
	Cupboard	1.96	NA	0%	F	0%				
	Cooking HSE	7.54	NA	0%	P	0%				
F18	Cemetery	10.85	5.95	55%	G	100%	G	Type B	1883.7	60%
	Storage	16.50	8.25	50%	G	100%	G	Type A	2000	70%
F17	Cupboard	5.40	5.40	100%	VG	100%	G	Type C	1000	15%
	Drying area	9.50	9.03	95%	G	100%	G	Type B	1883.7	95%
						100%	G	MS	56.5488	0%
	Cooking HSE	11.02	NA	0%	G	0%				
	Drying area	3.12	NA	0%	G	0%				
	Cupboard	1.92	NA	0%	G	0%				
	Cupboard	2.09	NA	0%	F	0%				
	Cupboard	2.25	NA	0%	G	0%				
	Catchment	8.41	8.41	100%	G	100%	G	Type A	2000	0%
	Cooking HSE	14.40	NA	0%	G	0%				
	Cooking HSE	4.65	NA	0%	F	0%				
Cupboard	2.70	NA	0%	G	0%					
Cupboard	2.10	NA	0%	G	0%					
F-ECE	Catchment	39.05	19.88	51%	G	83%	P	Type A	2000	100%
	School	140.00	9.00	6%	G	100%	G	ECE	4950	100%
F16	Cooking HSE	7.35	2.43	33%	G	100%	G			
	Food STR	1.56	NA	0%	G	0%				
	Drying area	3.84	NA	0%	F	0%				
	Cooking HSE	13.60	NA	0%	G	0%				

Store	Store	57.04	49.36	87%	G	100%	G	2000	100%	
								2000	100%	
	Storage/ Cooking	17.68	11.44	65%	G	100%	G	Type B	1883.7	100%
	Drying area	3.23	NA	0%	G	0%				
	Cupboard	3.06	NA	0%	VG	0%				
	Cooking HSE	7.28	NA	0%	G	0%				
F16	Cupboard	2.52	2.39	95%	G	100%	G	MS	25.8	100%
	Drying area	2.24	NA	0%	P	0%				
	Cooking HSE	11.07	NA	0%	F	0%				
F14	Cupboard	1.43	NA	0%	G	0%				
	Drying area	0.88	NA	0%	G	0%				
	Cooking HSE	1.40	NA	0%	G	0%				
	FEMA HSE	69.58	56.80	82%	G	100%	G	Type B	1883.7	100%
								Type A	2000	100%
	Cupboard	3.61	NA	0%	G	0%				
	Cooking HSE	19.20	NA	0%	F	0%				
	Cooking HSE	3.74	NA	0%	P	0%				
F12	Catchment	37.20	NA	0%	G	0%		Concrete	33300	0%
F11	Storage	12.25	12.25	100%	G	100%	VG	Type A	2000	50%
	Cooking HSE	27.72	10.50	38%	F	100%	G	MS	49	NA
	Drying area	17.15	17.15	100%	G	100%	G	Type A	2000	100%
								MS	211	100%
	Cupboard	2.04	NA	0%	G	0%				
	Cooking HSE	13.30	NA	0%	G	0%				
	Cupboard	1.82	NA	0%	F	0%				
	Cooking HSE	14.00	NA	0%	G	0%				
	Storage	4.76	NA	0%	G	0%				
	Cupboard	2.52	NA	0%	G	0%				
F10	Catchment	7.59	7.59	100%	G	100%	F	Type A	2000	25%
	Cupboard	1.69	NA	0%	F	0%				
	House	8.25	8.25	100%	G	100%	G	Type B	1884	20%
	Drying area	10.08	10.08	100%	G	100%	G	Type C	1000	30%
	Cooking HSE	14.44	NA	0%	G	0%				

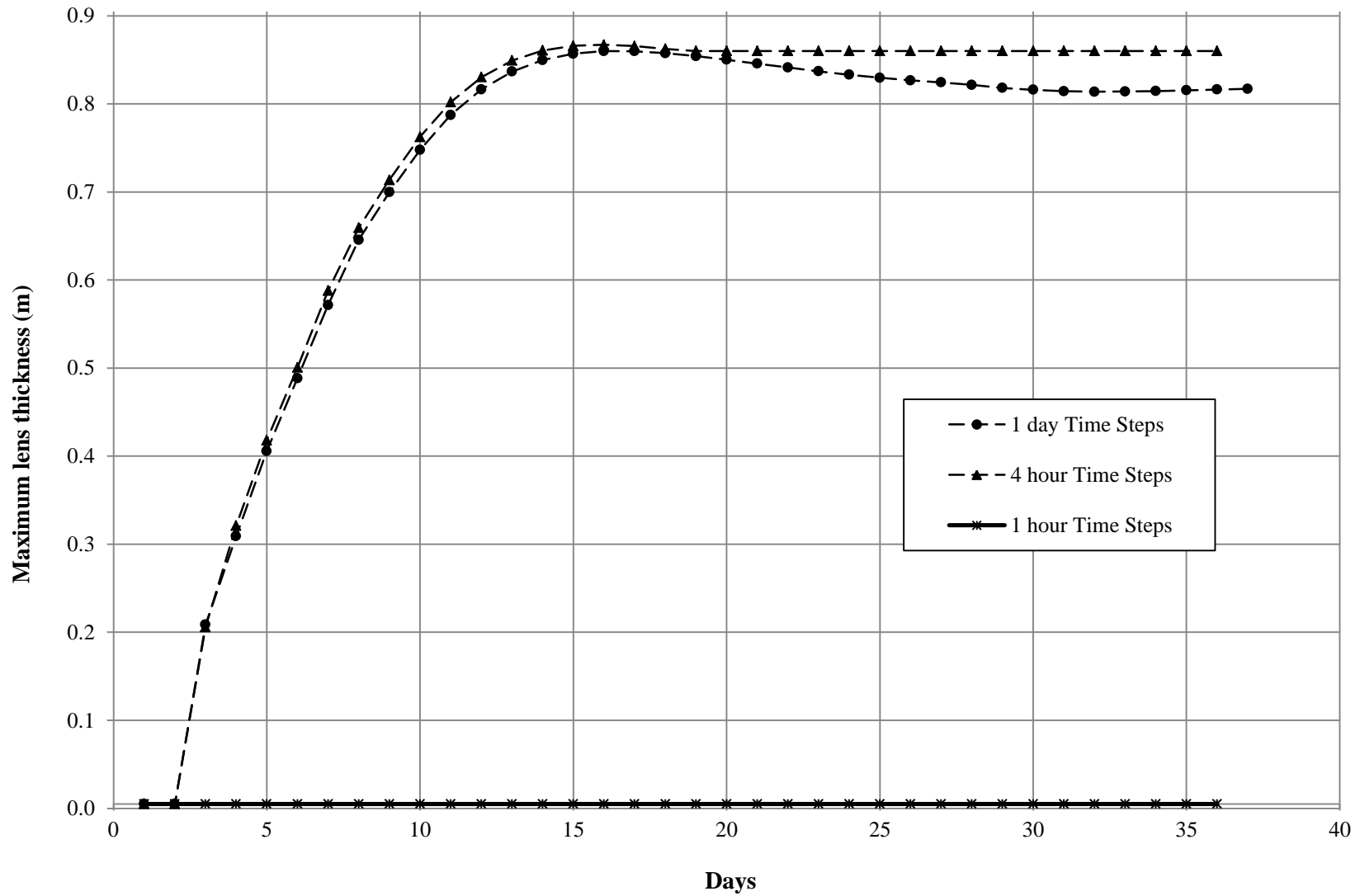
F9	Drying area	6.00	5.40	90%	G	100%	G	Type D	233	100%
	Cupboard	3.60	NA	0%	F	0%				
	Drying area	3.90	NA	0%	F	0%				
	Cupboard	2.21	NA	0%	G	0%				
	Cupboard	2.55	2.55	100%	G	0%	P	MS	26	0%
	House	9.52	NA	0%	G	0%				
	Catchment	27.93	13.97	50%	P	0%		Concrete	47150	0%
	House	25.48	12.74	50%	G	100%	G	Type A	2000	60%
F8	Catchment	13.33	13.33	100%	G	100%	G	Type A	2000	100%
	Cupboard	2.34	NA	0%	G	0%		NA		
F7	Cupboard	2.10	NA	0%	G	0%				
	Cooking HSE	18.00	18.00	100%	G	100%	G	Type B	1884	0%
								Type C	1000	100%
	Storage HSE	8.12	8.12	100%	G	100%	G	MS1	11	100%
								MS2	11	100%
								MS3	11	100%
	Drying area	10.92	10.92	100%	G	100%	G	Type A	2000	100%
	Cupboard	3.42	NA	0%	G	0%				
F4	Catchment	8.37	8.37	100%	F	100%	G	Type B	1884	100%
	Cooking HSE	4.00	NA	0%	F	0%				
	Dishes	2.25	NA	0%	G	0%				
	Drying area	11.84	11.84	100%	G	100%	G	Type A	2000	100%
F3	Storage	15.81	15.81	100%	G	100%	G	Type B	1884	100%
	Cooking HSE	6.24	NA	0%	F	0%		NA		
	Cupboard	2.70	NA	0%	G	0%		NA		
F1	Drying area	14.80	11.84	80%	F	100%	G	Type A	2000	100%
F19	Cupboard	5.58	5.58	100%	G	100%	G	Type B	1884	100%
	Cooking HSE	9.88	NA	0%	G	0%		NA		
Y6	Cupboard	8.00	3.20	40%	F	100%	G	Type C	1000	100%
	Drying area	6.29	NA	0%	G	0%		NA		
	Cooking HSE	2.40	NA	0%	G	0%		NA		
Y5	Cupboard	7.92	7.92	100%	F	100%	G	Type B	1087	100%
	Storage	6.00	6.00	100%	G	100%	G	MS	120.9	
Y4	Type A	2000	75%							
	Drying area	17.60	14.08	80%	F	70%	G	Type A	2000	30%
	Water tank	0.00	NA	0%		0%		Metal	50463	0%

Y7	Storage HSE	10.54	7.91	75%	F	0%		Type B	1884	90%	
	Cupboard	5.89	4.71	80%	G	100%	G	Type A	2000	100%	
Y3	Storage	6.00	6.00	100%	G	100%	G	Type A	2000	100%	
								Type C	1000	100%	
Y8	House	40.32	36.72	91%	G	75%	G	Type A	2000	100%	
								Type C	1000	100%	
								Type B	1884	50%	
Y1	Drying area	13.02	13.02	100%	G	100%	G	Type A	2000	100%	
	Storage	7.20	7.20	100%	G	100%	G	Type B	816	100%	
	Community tank	23.00	23.00	100%	G	100%	G	Type A	2000	100%	
								Type A	2000	100%	
								Type C	1000	0%	
	House	24.08	15.88	66%	G	100%	G	Concrete	62426	0%	
Type A								2000	50%		
								MS	157	30%	
I14	Storage	8.75	8.75	100%	G	100%	G	Type A	2000	0%	
	Cupboard	12.60	10.08	80%	F	100%	G	Concrete	6664	NA	
I13	House		22.40	22.40	100%	G	100%	G	Type B	1884	30%
			57.60	57.60	100%	G	100%	G	Type A	2000	50%
			21.12	21.12	100%	G	100%	G	Type A	2000	0%
			13.50	13.50	100%	G	100%	G	Type A	2000	40%
			13.00	13.00	100%	G	100%	G	Type A	2000	100%
			13.00	13.00	100%	G	100%	G	Type B	1884	20%
			22.08	22.08	100%	G	100%	G	Stainless steel	921	0%
			22.20	22.20	100%	G	100%	G	MS	196	70%
I12	Storage	6.72	6.05	90%	F	100%	G	Type B	421	30%	
	Cupboard	2.40	2.40	100%	G	100%	G	MS	183	10%	
	Cupboard	1.56	1.56	100%	G	100%	G	MS	206	100%	
	Storage	6.90	4.83	70%	F	100%	G	Type B	1884	20%	
I10	Catchment	5.75	5.18	90%	F	100%	G	Type A	2000	100%	
		0.00	NA	0%				Type B	1884	15%	
I12	House	5.00	5.00	100%	G	100%	G	Type C	1000	25%	
I11	Storage	12.58	12.58	100%	G	100%	G	Type B	1884	20%	
								MS	552	70%	

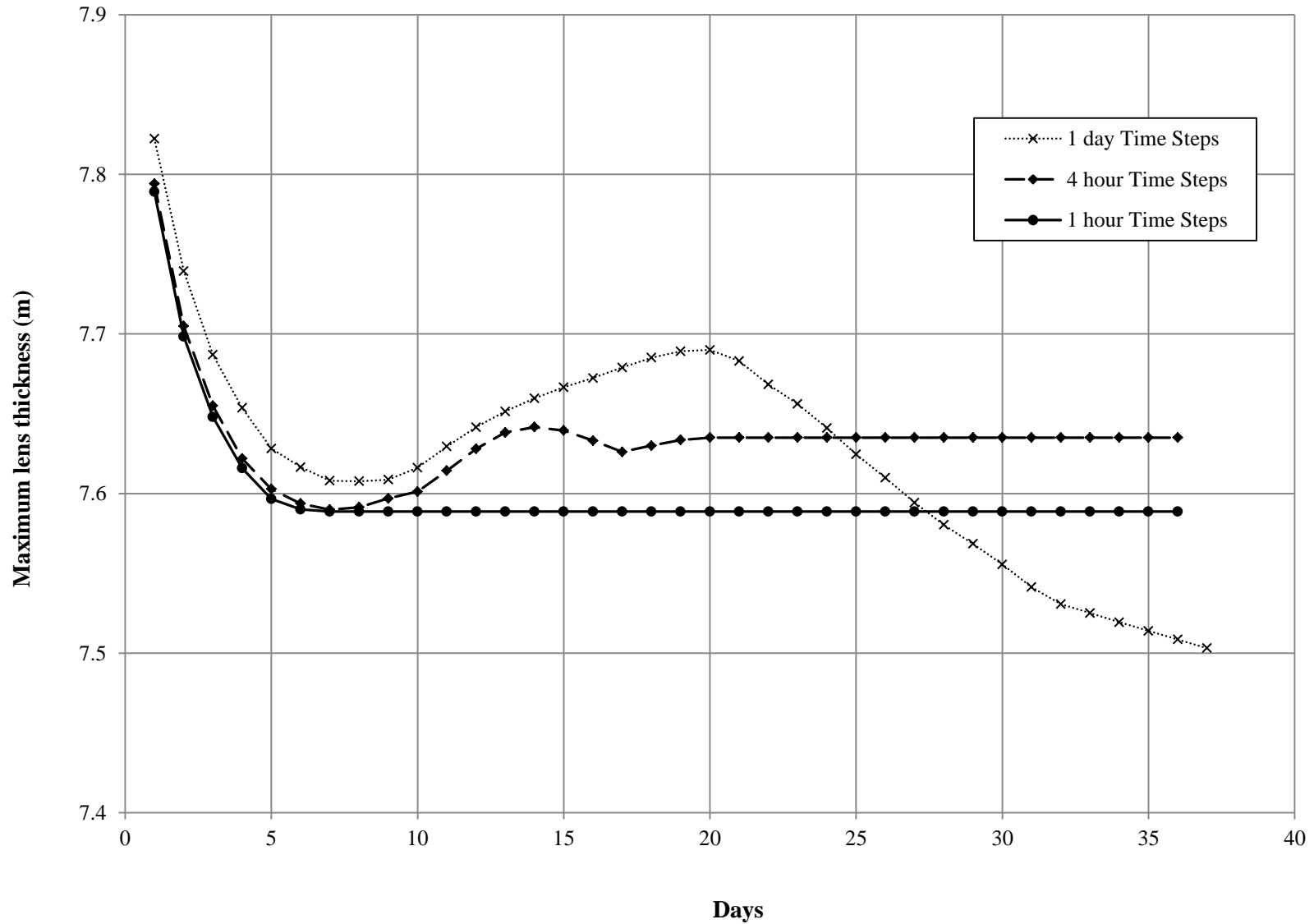
Dispensary	Dispensary	137.52	NA	NA	G	0%	NA	Concrete White plastic	20701 500	NA NA
Old satellite dispensary	Old satellite dispensary	42.34	NA	0%	G	0%	NA	Concrete	9477	0%
I15	House	139.86	20.46 18.66 28.68 6.00	53%	G		G G G G	Concrete Type A Type B MS	10944 2000 1884	100% 95% 100%
Community Catchment close to I15	Catchment	27.00	0.00	0%	F	0%	NA	Concrete	44376	0%
I6	House	15.75 14.50 NA 16.94	15.75 14.50 NA 16.94	100%	G	100% 100% 100% 100%	G G G G	Type B MS MS Type A	929 139 57 2000	100% 50% 100% 100%
I3	Catchment Cupboard Cupboard Catchment	10.85 6.60 3.23 4.60	10.85 6.60 3.23 4.60	100% 100% 100% 100%	G G F F	100% 100% 100% 100%	G G G G	Type A MS Type B Type C	2000 77 1884 1000	 100% NA NA
I5	House	98.90	28.37	29%	G	NA	G	Type B Type A	1884 2000	100% 100%

APPENDIX B – GROUNDWATER LENS THICKNESS PLOTS FROM CALIBRATED
ISLAND MODELS USING THREE TIME STEP CONDITIONS

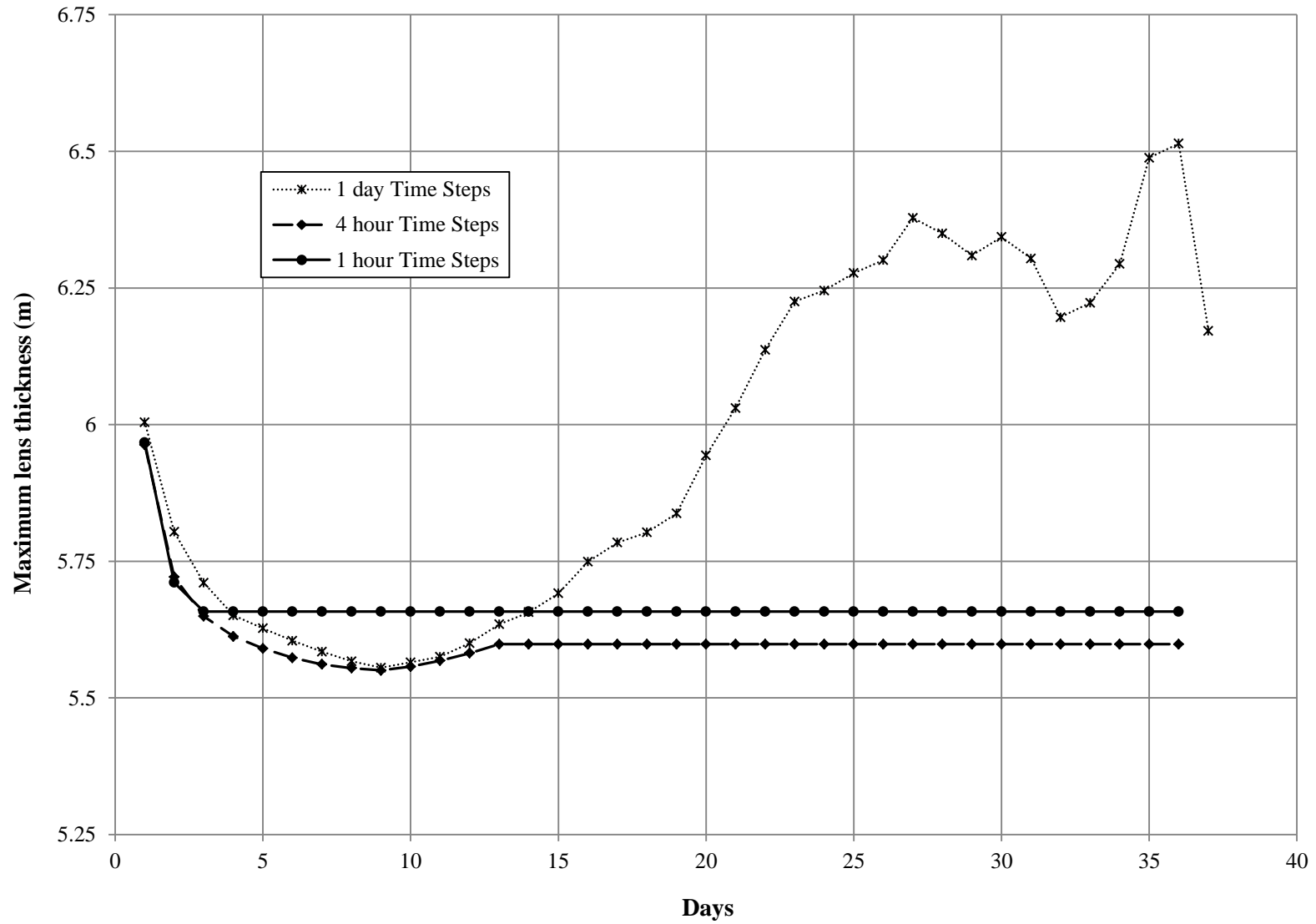
Eauripik Calibrated, Steady Rainfall Model



Falalop Calibrated, Steady Rainfall Model



Ifalik Calibrated, Steady Rainfall Model



Satawal - Calibrated, Steady Rainfall Model

